# Subsurface Technical Report

# Dynamic Reservoir Modelling of Wadden Fields for Subsidence. Meet&Regel 2015.

*Published May 2016*

**Static Model Extent**
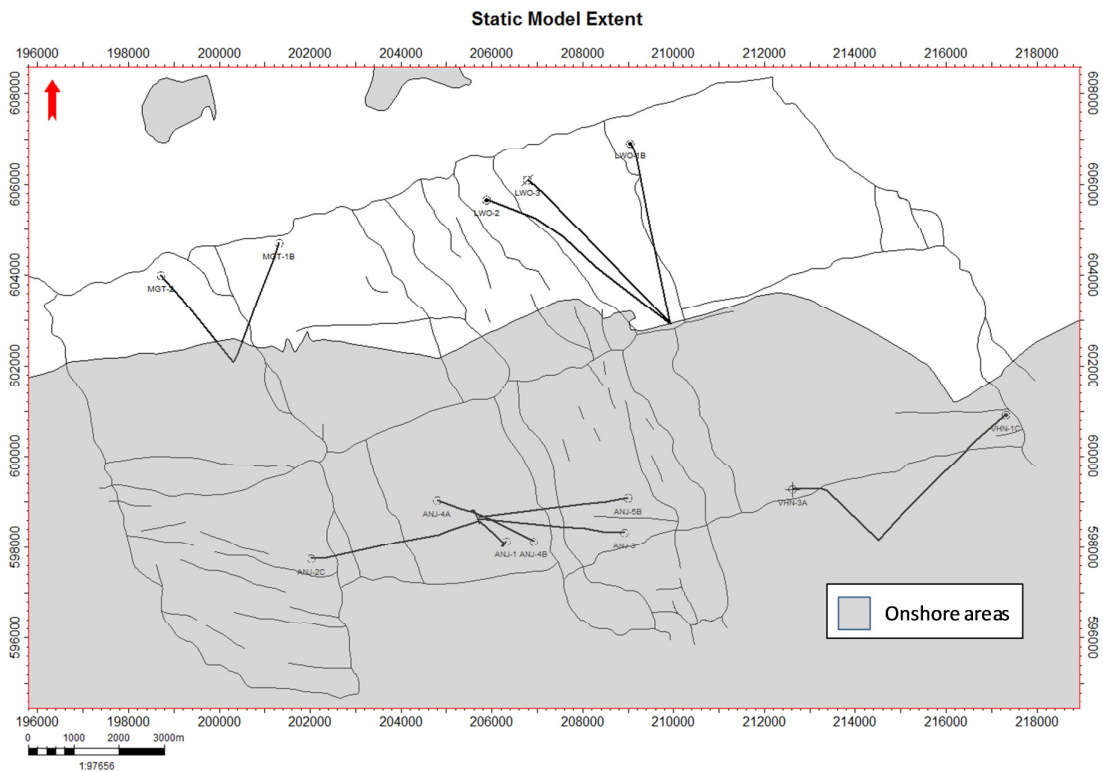


**Contributors:**

| | |
|---|---|
| Reservoir Engineering: | Alexander Tichler (author) |

| | |
|---|---|
| Geology: | Sahar Abdulla / Simon Haworth |
| Geomechanics: | Onno van der Wal |
| Geophysics: | Abdullah Hamood |
| Petrophysics: | Jan Seubring / Sarah Barber |

**Date:** January, 2016          **Document Number:** EP201605200121

**NEDERLANDSE AARDOLIE MAATSCHAPPIJ B.V. ASSEN**

**TABLE OF CONTENTS**

# 1 SUMMARY

## 1.1 Introduction

The Wadden dry gas fields are located in the environmentally sensitive Waddenzee area. To limit the environment impact, subsidence induced by gas production is closely monitored and modelled as part of the yearly *Meet&Regel* cycle. This document describes in detail the reservoir modelling performed as part of the *Meet&Regel 2015* cycle step 3: verify prognosis.

In previous years several models have been built for input in the Winningsplan and the *Meet&Regel* cycle to continuously improve the subsidence modelling. Top structure maps were updated in 2012 as a result of data acquired during drilling of MGT-3 infill well in the Nes field and updated time depth conversion in other fields. This update led to a reconstruction of the dynamic models for M&R2013. In the meantime, the fields Lauwersoog East and Moddergat have had a separate static model update in 2015, after new structural and property modelling was done. New production and pressure data were included in the updated models for M&R2014 and M&R2015. Outcomes of these models have been used to reassess subsidence predictions.

This document describes the workflow and details of the dynamic models updated for the Meet&Regel cycle of 2015 and also includes the comparison and changes compared to the Meet&Regel cycle of 2014.

## 1.2 Model objective and approach

The main objective of the modelling exercise is to generate an input for an expected case and a realistic low and high case subsidence scenario. This input consists of a pressure as function of location and time for each of the Wadden fields. Due to gas production, pressure in the reservoir will decline due course time and these models should capture a realistic range of pressure drop in the entire field.

In recent years, it has become evident that the depletion of laterally extensive water bearing layers has a large impact on subsidence of the surface. The mobility of aquifers is thus seen as primary uncertainty for subsidence throughout the fields. To make sure the entire range of possibilities is captured, the aquifer mobility has been varied to extreme cases: an (almost) fully immobile aquifer (low subsidence case) and fully mobile aquifer (high subsidence case). The truth is most likely somewhere in between: an aquifer that is impaired in mobility by the presence of (paleo-residual) gas in the water leg (base subsidence case).

In the M&R cycles of 2012 and 2013[1] the approach was as follows. Cases distinguished between a mobile aquifer and an immobile aquifer. For the fields Moddergat, Nes and Metslawier a high structure case was run, because the dynamic data indicated a higher GIIP than present in the static model. A stochastic approach was used for history matching. Models with a reasonable history match were scanned for high, low and base model GIIP case.

---

[1] M&R cycle 2012 (2013) refers to the work that was done during 2012 (2013) and was presented in Q1 2013 (2014).

After M&R 2013 it became clear that, in general, the mobility of the aquifer was of much bigger relevance to the subsidence than the variation of high, low and base case dynamic GIIP, since with more and more production data, the uncertainty in dynamic GIIP becomes less and less. It was therefore chosen not to use the dynamic GIIP uncertainty for M&R2014 and focus solely on two history matches: an immobile aquifer realisation and a mobile aquifer realisation. Recent data and understanding teaches us that the two history matches provided in M&R2014 did not sufficiently cover the base case subsidence scenario. Hence the M&R2015 approach now includes a new base case definition with an impaired aquifer (including presence of paleo-residual gas) described above.

For subsidence forecasting, the future yearly production as per Business Plan 2015 has been assumed. This differs from M&R2014 approach, where Winningsplan 2011 volumes were used. Since certain fields have by now reacted (slightly) differently than forecast in 2011, the more recent BP15 numbers are seen as more up-to-date, hence giving a better subsidence forecast.

*Table 1. Overview of dynamic realizations.*

|  | *Base structure* | *Immobile aquifer* | *Gas saturation below FWL* | *Mobile aquifer* | *Base dynamic GIIP* | *Business Plan 2015 profile* |
|---|---|---|---|---|---|---|
| *1 – Low pressure drop* | x | x |  |  | x | x |
| *2 – Base pressure drop* | x |  | x |  | x | x |
| *3 – High pressure drop* | x |  |  | x | x | x |

## 1.3  Main changes compared to M&R2014

The following changes have been implemented in the reservoir models.
- Three models have been built instead of two. Next to the immobile and mobile aquifer realisations, a third realisation has been constructed by modelling paleo-residual gas in the aquifer. See Table 1.
- An update in forecasting of the mobile aquifer has been made for the fields Anjum, Lauwersoog C and Lauwersoog West. The aquifer permeability multiplier was set to 0.1 last year and has been modified to 1.0 this year to align with the other models. This update has resulted in a higher average pressure drop for these fields for the high pressure drop realisation.
- The static models for Moddergat and Lauwersoog East have been revised. For Moddergat, the main change was a re-modelling of the permeability distribution, which caused a decrease in lateral connectivity in the field. This reduced the expected pressure drop (mainly in the water-bearing layers) towards the south.
- The intra-field fault for Lauwersoog-West, poorly visible on seismic, has been assumed non-baffling, causing a more even pressure distribution.
- For forecasting, the latest figures (Business Plan 2015) have been used. Previously the numbers of Winningsplan 2011 were used, which are now outdated. Base case forecasts for the most firm projects (Nes infill, Moddergat infill and Lauwersoog East infill) have been included. Changes are discussed in Section 5.2 .
- The Nes field, having an extra RFT measurement post-depletion (MGT-3 well), has a different approach to low-base-high models than depicted in Table 1. This is further described in Section 5.1.8.

## 1.4 M&R2015 Conclusion

Some general conclusions can be made from the modelling work done for M&R 2015.

The newly defined base case (gas below free water level) shows a somewhat higher average reservoir pressure drop than M&R2014's base case (where the aquifer was assumed to be immobile).

In general, the calculations of M&R2015 have caused an upward revision of the high case pressure drop realisations. This was mainly caused by the update of a permeability multiplier in a number of the fields.

The new low-case, with an immobile aquifer (aquifer permeability multiplied by a factor $10^{-4}$ compared with the gas-bearing reservoir), usually aligns with last year's base case, but sometimes has less pressure drop, where the aquifer has been tightened for a consistent aquifer model over all fields.

# 2 INTRODUCTION

The Wadden area consists of nine reservoirs on the shore face of northern Friesland. Anjum, Ezumazijl and Metslawier are the three fields not lying under the Waddenzee, which are used mainly for subsidence calibration. Lauwersoog Central, East and West, Moddergat, Nes are lying partly or entirely beneath the Waddenzee, of which gas production may cause subsidence to the Waddenzee. The fields are depicted in Figure 1.
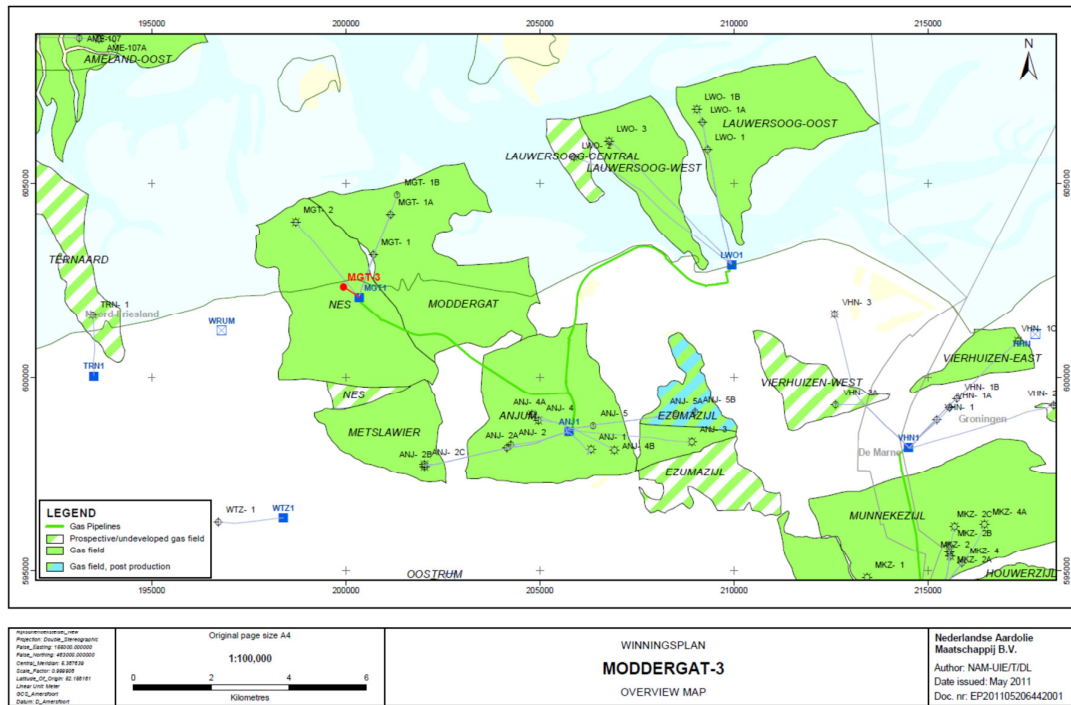


*Figure 1 Map of the Wadden area*

This document describes the workflow and details of the dynamic models updated for the Meet&Regel cycle of 2015 and also includes the comparison and changes compared to the Meet&Regel cycle of 2014. Chapter 3 describes the setup of the model. It includes the model input, the data upon which is history matched, the main uncertainty to subsidence: aquifer mobility, the way different realisations are defined and the forecasting method. Chapter 4 describes the main uncertainties and in what way they are taken into account. Chapter 5 discusses the individual dynamic models in greater detail and discusses the results and its implications.

# 3 MODEL DESCRIPTION & OVERVIEW

Dynamic reservoir models have been built in MoReS, which is a Shell proprietary reservoir simulation software. This software is able to do multiphase 3D simulations. This is particularly important to capture vertical and lateral heterogeneity, as well as two-phase behaviour .

## 3.1 Geological overview

### 3.1.1 Depositional model

Climate and creation of accommodation space are two factors that affect the distribution of sediments in the reservoirs of the northern Netherlands. Climatic changes were interpreted to range from extreme arid to humid conditions whilst the creation of accommodation space was dependent on subsidence and the rate of sedimentation. An increased rate in subsidence results in ephemeral (intermittent) ponds/lakes while a reduced rate in subsidence results in dryer more arid environments. A more variable control to deposition is the north-easterly aeolian processes that transport fine-grained sediments to the land and the south-westerly sourced wind which transports and deflates sand grains towards the ancient lake margins.

Super-imposed on the large-scale trends in reservoir quality are more local east to west trends in porosity. These trends are postulated to be a response to the presence of paleo-lows and paleo-highs. The Lauwerzee Trough marks a paleogeographic low with lower N/G and porosity values extending to the east due to preferential southward incursion of wetter, lacustrine facies. Furthermore, there is a slight reduction in porosity with depth. The fault boundary separating the Moddergat and Lauwersoog blocks marks a change in reservoir quality.

Unlike Ameland, trends in mineralogical composition between chlorite and kaolinite also don't vary across the Wadden fields. All wells are chlorite prone. The chlorite is a grain coating clay which helps to preserve reservoir quality by reducing compaction and preventing nucleation of other cements. Similar chlorite cements occur in the Rotliegend of northern Germany, interpreted as forming in a belt parallel to the shoreline of the desert lake, with Mg-rich fluids expelled from compacting basin shales forming chlorite from early precursor clays (Hillier et al., 1996). In the study area the chlorite is also interpreted as forming a belt parallel to the facies belts on the margin of the desert lake. Furthermore, a belt of anhydrite cementation can be traced from wells in Lauwersoog to Nes. The anhydrite is abundantly developed in certain stratigraphic layers significantly reducing porosity. The anhydrite is dominantly early and is interpreted as representing periods of sabkha development on the margins of the desert lake, with cementation from evaporitic groundwaters.

For modelling purposes, porosity distributions were designed to reflect influences on reservoir quality described above, that then link to permeability distribution. The realisations reflect changes in porosity from west to east although no hard trends have been included in the Petrel models perse. Where porosity reduction with depth is observed, these trends are included in the Petrel models.

### 3.1.2 Porosity, permeability and thickness trends

Overall, vertical heterogeneity of the Wadden reservoirs is greater than lateral variations of reservoir quality reflecting changes in the level of the water table with respect to the

depositional surface over time. Within the sand-rich intervals, evidence for high porosity and permeability streaks (HPS) is observed at the core level (typically 10-50cm thick). These are attributed to grainflow deposits that result in improved reservoir quality in aeolian dune settings. These features have 2-3 orders of magnitude of higher permeability than the background and can occur in ROSLU Unit's 1, 3, 4, and 6. Spatially, it was recognised that HPS have a wider spread in the east of Wadden. In this area thin high porosity/permeability streaks provide the major flow contribution during production. Although, only sometimes below log resolution, they require representation in the reservoir model to effectively capture key considerations that impact subsidence modelling such as differential depletion.

To capture the required heterogeneity due to interbedding and associated cementation (e.g. anhydrite), model layering is refined sufficiently but it balanced against the needs to reduce simulation time. The result is a more accurate representation of reservoir property distribution (e.g. porosity) and porosity ranges per unit.

Furthermore, the lack of resolution in porosity and permeability logs compared to in-situ corrected core data over the core interval results in an underestimation of the rock's heterogeneity. Even though the resolution at which the core plugs have been taken from the core is not much greater than the resolution of log porosity, they do not suffer from averaging effects that result from limited vertical resolution of a density tool. An approach chosen to accommodate for this was to upscale both core plug data and wireline data and replace wireline data where cored intervals existed. As most core was taken in key flowing units, a better approximation of magnitude of permeability contrast is achieved, compared to just averages calculated using a perm curve that varies in line with the porosity log; capture of high porosity/permeability streaks for differential depletion sensitivity.

### 3.1.3  Slochteren reservoir units

A change to wetter conditions, discussed above, can result in a widespread transgression of a playa lake margin across the area and an increase in water-lain sedimentation. These events result in barriers and baffles to flow represented by transgressive surfaces.

Cored intervals of Units 2, 4, 5, and 6 revealed correlatable shale horizons across the Wadden field (e.g. up to 10 km distances between wells). These transgressions were used as a sensitivity for vertical communication between units in the dynamic model, with Unit 5 further divided into 2 intra-units. Unit 2 shale is due to a regional "drowning" resulting in a development of a playa lake across the area (including Ameland) and a major barrier to flow. For example, LWO-3 encountered a ROSLU1 that was 1.9 bar lower in pressure than in ROSLU2-6 resulting in a different fluid contact. The most likely explanation is that ROSLU2 is sealing and ROSLU1 forms a separate accumulation within the majority of fields in the Wadden area. The other incursions are reflected by shale breaks between Unit 5A and 5B and Unit 5B and Unit 6 within the each field.

## 3.2 Model input

### 3.2.1  Rock compressibility

Rock compressibility has not changed since M&R2014.

Rock compressibility is a relatively minor energy term, but may have impact on the water influx. For the model rock compressibility was based on the compaction coefficients initially

provided by Geomechanics. The rock compressibility was calculated by dividing the compaction coefficient by the average porosity in the field. These are given in Table 2.

*Table 2 Rock compressibility per field*

| Field | $C_R$ ($10^{-5}$ bar$^{-1}$) |
|---|---|
| Anjum | 6.5 |
| Ezumazijl | 6.5 |
| Lauwersoog-Central | 7.6 |
| Lauwersoog-East | 6.6 |
| Lauwersoog-West | 7.1 |
| Metslawier | 6.7 |
| Moddergat | 6.9 |
| Nes | 7.0 |
| Vierhuizen | 5.7 |

### 3.2.2  Hydrocarbon volumes in place

Since the M&R2014 model cycle, the static models have not changed for the majority of the fields. However a few fields now have new GIIPs resulting from a new depth map based on the new seismic reprocessing that became available in Q3 2015.

The structure of the reservoir of the Wadden and Anjum fields was last fully updated in 2012, following the MGT-3 drilling results, where the top reservoir came in deeper than expected by 22m TVDNAP. This led to changes in (static) volumes in place. For Anjum, the static GIIP was updated based on the dynamic volume seen.

However, since then some separate updates have been made:
1. Lauwersoog-Oost: A new depth map was used. There is no significant GIIP change, although the popups in the east of the field are excluded, to give a better comparison with dynamic GIIPs.
2. Moddergat: Depth map was updated in preparation from the Moddergat (south) infill opportunity, decreasing GIIP significantly. Furthermore, the MGT-SE blocks are excluded, and the NES-North block included conform what is currently believed to be in connection with the MGT-1B well.

In addition to the changes in the structure, a few Petrophysical iterations were performed around using porosity depth trend. This was implemented only in Lauwersoog East and Moddergat during their separate model updates.

*Table 3 Static gas initially in place (GIIP)*

| Field | Base Case GIIP M&R2014 (BNCM) | Base Case GIIP M&R2015 (BNCM) | Main reason for change |
|---|---|---|---|
| Anjum | 16.6 | 16.6 | |
| Ezumazijl | 2.1 | 2.1 | |
| Lauwersoog-Central | 1.2 | 1.2 | |
| Lauwersoog-East | 7.8 | 5.1 | Exclusion of eastern popups from GIIP calculation |
| Lauwersoog-West | 3.4 | 3.4 | |
| Metslawier | 5.2 | 5.2 | |
| Moddergat | 8.2 | 6.8 | Exclusion of MGT-SE blocks, inclusion of Nes-North block. |
| Nes | 18.9 | 18.9 | |

### 3.2.3  Absolute Permeability

Modifications have been made to the permeability model for Moddergat and Lauwersoog East. For Moddergat and Lauwersoog an updated permeability log was created based on flow zone indicators. For Moddergat, the FZI log was used in combination with the actual stress corrected core porosities and permeabilities to populate the interwell space. Specifically, the interwell space was co-kriged with porosity as a the guiding secondary variable to control the permeability distribution based on the core data. This had a significant impact by reducing connectivity across the field. For Lauwersoog-East, a similar modelling approach was followed however the core data was not used directly. The effect was marginal. For M&R2016, it will be investigated whether also other fields require permeability updates.

Furthermore, permeability multipliers may have changed on a field-by-field basis, specified in Section 5.1 .

Permeability is largely based on the porosity-permeability correlation established in 2004 (Ref 1). After the drilling and coring of MGT-3 updates were made on the porosity-permeability correlations for some fields. Horizontal and vertical permeability are used as a matching parameter in the history matching process.

The permeability of the aquifer is used as a separate parameter in order to capture the uncertainty in the depletion of the water bearing layers. Core data show that the permeability in the water leg can be a factor 2-4 smaller than those in the gas leg (Ref 1) or even a factor 10 smaller (Figure 2, Ref 2). See also Section 3.4 .

### 3.2.4  Capillary pressure

Capillary pressure is calculated from the saturation height function as described in the petrophysical study from 2004 (Ref 1).

Some modifications have been made for Moddergat and Lauwersoog East fields:

    o  Moddergat[2]. Saturation Height functions have been re-generated for the Modergat and Nes Fields. The new functions are Lambda-functions, based on log derived gas saturations. The reason for generating new functions is was a slight mismatch between log derived saturations and SHF saturations in Unit 1 in the Upper Slochteren reservoir. To improve the match, the irreducible water saturation (B) was increased from 0.05 to 0.075. This increase in B resulted in a GIIP reduction of 0.5 BCM. The irreducible water saturation in the lower units in the Upper Slochteren, remained unchanged at 0.1, and as such did not attribute to the GIIP reduction.

    o  Lauwersoog fields[3]. Saturation Height functions have been assessed for the three Lauwersoog Fields. The new functions are simple Lambda-functions, based on log derived gas saturations. Reason for generating new functions was a slight mismatch between log derived saturations and SHF saturations, in Unit 1 in the Upper Slochteren reservoir. To improve this fit, the irreducible water saturation (B) was increased from 0.05 to 0.075. In the lower units of the Upper Slochteren, the irreducible water saturation remained unchanged at 0.1. This increase in B in Unit 1, resulted in a GIIP reduction of approximately 0.2 BCM in each of the three LWO fields.

### 3.2.5  PVT properties

The PVT model has not changed since M&R2014.

For gas fields, the PVT property model exists of viscosity and expansion factor. Expansion factors per field differ depending on pressure, temperature,  and gas composition. The correlations used in the simulator are established from PVT reports on gas samples. Viscosity is usually not measured, but correlations from literature predict gas viscosity well. Here, Lee and Gonzalez correlation was used.

For dry gas fields, their dynamic behaviour is rather insensitive to PVT parameters, hence no uncertainty ranges are specified: their properties are fixed.

### 3.2.6  Initialisation

The initialisation process has not changed since M&R2014.
All fields were hydrostatically initialised with initial pressure at datum depth. All other pressures and saturations are calculated by the simulator from the given FWL and capillary pressure curves.

### 3.2.7  Wells

The well trajectories are imported from the static reservoir model (Petrel). Perforation intervals are obtained from the corporate database (Discovery/DREAM). Using recompletion tables, the perforations can be opened and closed at specific times during their history. Lift tables are generated with Prosper software and assigned to their respective wells. These are

---

[2] This modification will also be applied to future models or Nes. For now, only applied in the model update of Moddergat.
[3] This modification has only been applied to Lauwersoog East in M&R2015. In future models, this change will be applied to all Lauwersoog fields.

also included in the history matching run in order to check the well inflow performance over time.

The well trajectories of existing producers have not changed since M&R2014. However, for Moddergat and Lauwersoog East fields, the most up-to-date infill well placing has been used, to incorporate production potentially coming from these wells (LWO-EE and MGT-S). See also Section 5.2 .

Furthermore, the lift table of VHN-1C is now included in the model, enabling the possibility of history matching to tubing-head pressure for the Vierhuizen East field as well (see Section 3.3.6).

## 3.3 History matching data

Historical data used to history match the reservoir behaviour are summarized below and comments are provided on their importance for history matching.

### 3.3.1  Historical production

Historical production for the M&R2015 models have included monthly production from until and including October 2015. Two methods for implementing production data were used.

*Anjum, Metslawier, Vierhuizen East:*
For these fields, the model is constrained by historical production with monthly time steps. This means that short shutdowns are not captured; only long shutdowns are accurately represented. This means that the BHP cannot always be used to history match the closed-in pressure measurements. For history matching, a permeability averaged reservoir pressure is calculated. This calculates the equivalent shut-in pressure (for fixed shut-in times) while the well is flowing, by averaging reservoir pressures over grid cells depending on the permeability that is connected. This means that adding or closing in perforations can have significant impact on the pressure observed. This is also observed in reality, for example ANJ-3. A permeability averaged pressure is considered to give a good representation of the pressure that would be measured by a pressure gauge in the well.

*Ezumazijl, Lauwersoog Central, - West, - East, Nes, Moddergat*
A slightly more accurate approach is used for these fields, by refining the historical production time steps around pressure points, taking shut-in times to nearest day into account. In this case, the BHP is more reliable. This is especially needed for fields with large permeability contrasts.

Effectively, both simulated reservoir pressures and simulated BHP are plotted together with the historical pressure points to observe the history match adequately.

### 3.3.2  Bottom-hole pressure measurements

This is the main source of data used for history matching, since it is most reliable. One way of obtaining the data is via static pressure gradients (SPG) by lowering a pressure gauge in a well until perforations during a shut-in period. SPGs are normalised to datum depth. In all wells, SPGs are taken at regular intervals. The following measurements were made since M&R2014.

| Well | Field | Date | Pressure at datum |
|------|-------|------|-------------------|
| LWO-2 | Lauwersoog C | 22/4/2015 | 188 bara |
| LWO-1B | Lauwersoog East | 23/4/2015 | 187 bara |
| LWO-3 | Lauwersoog West | 24/4/2015 | 154 bara |
| MGT-1B | Moddergat | 22/4/2015 | 205 bara |
| MGT-3 | Nes | 27/4/2015 | 260 bara |

Another way of obtaining BHP data is by taking a closed in tubing head pressure measurement, which is then correlated to a BHP. This is somewhat less accurate, but still can give appropriate results for history matching.

| Well | Field | Date | Pressure at datum |
|------|-------|------|-------------------|
| ANJ-4B | Anjum | 5/6/2015 | 54 bara |
| ANJ-3 | Ezumazijl | 18/6/2015 | 97 bara |
| MGT-2 | Nes | 2/5/2015 | 263 bara |

### 3.3.3  Production logging data

In some wells production logging tools have been run. These tools are lowered in a flowing well and measure the inflow rate as function of depth. PLTs are used to get a match on permeability contrasts in the field. No new measurements were done since M&R2014.

### 3.3.4  Pulsed neutron log data

Pulsed neutron logs are used to determine water saturation changes in the reservoir and can hence monitor aquifer encroachment. These were not run in this area and therefore are not used for history matching.

### 3.3.5  Water production

Liquid production is only accurately measured and reconciled at system level. Individual well water gas ratios have been estimated from WaCo tank level changes and changes in the amount of liquid produced historically. As the only reliable way to look at the water production is at system level, the uncertainties are relatively large. This data is therefore not strictly used for history matching, but may sometimes act as a guide to observe the order of magnitude of water production in the model compared to reality.

The main parameters that impact the water production are the residual gas and water relative permeability end point. The first determines the timing of water break through, while the latter mainly impacts the amount of water produced at all times.

Two new WGR estimates were provided in M&R2014, by observing liquid-to-gas ratio and subtracting the expected CGR:

| Well | Field | Date | LGR (sm3/E6Nm3) | WGR (sm3/E6Nm3) |
|------|-------|------|-----------------|-----------------|
| ANJ-4B | Anjum | 1/9/2015 | 87 | 65 |
| ANJ-3 | Ezumazijl | 1/9/2015 | 70 | 58 |

Furthermore, at 1-9-2015 a consolidated MGT-LWO LGR was found to be 21 sm3/E6Nm3. With CGR around 8, this makes a WGR of 13 sm3/E6Nm3. Since this figure cannot be back-allocated to a well, it is not included in the data. However it does show that in 2015, the WGR of the large producers MGT-1, -2, -3 cannot exceed this figure by a great amount.

Water production is usually a combination of *condensed* water and *formation* water. Only the latter is modelled in the MoReS simulator. Using the Wehe-McKetta correlation, an estimate of the condensed water to gas ratio can be given, depending on reservoir temperature, pressure and salinity. The salinity used for all fields is 300000 ppm. The condensed WGR number (pressure, hence time dependent) is added to the formation WGR to give a total WGR, which is matched to the data points.

### 3.3.6  Tubing head pressure data

During the history matching process, gas rates are used as a constraint. In order to assess the well inflow performance, the tubing head pressure data is used. When the inflow and lift table are correct, one would expect to reproduce the tubing head pressure. Near wellbore effects and water influx may however cause deviations. Therefore, THP data is generally matched qualitatively, but is considered of secondary importance compared to downhole pressure measurements.

Tubing head pressures are continuously measured. The pressures have been updated until 31/10/2015 for M&R2015.

## 3.4 Aquifer mobility

The main uncertainty for subsidence modelling is the depletion of water bearing sections of the reservoir. Depletion of the water bearing layers cannot be accurately determined from material balance analysis, due to water's low compressibility.

There is a strong belief that the aquifer is less permeable than the gas leg. The theory for this is twofold: firstly, the permeability of the water zone can be lower due to clay particles existing in the waterleg (see Figure 2). Secondly, there is evidence for existing trapped gas below the free-water-level, which negatively impacts effective permeability of the water and will sustain a higher pressure in the waterleg (Ref 2). The MGT-3 RFT measurements showed that the aquifer was at 100 bar higher pressure than the gas bearing layers above, backing the understanding described above[4]. Also the subsidence behaviour due south of the Ameland field (due north of Nes field) suggests a slow aquifer response, implying a less permeable aquifer.

---

[4] Although there are also other reasons for this pressure lag: mainly the 'unit 2 shale', causing a pressure differential between the gas-bearing and water-bearing zone.
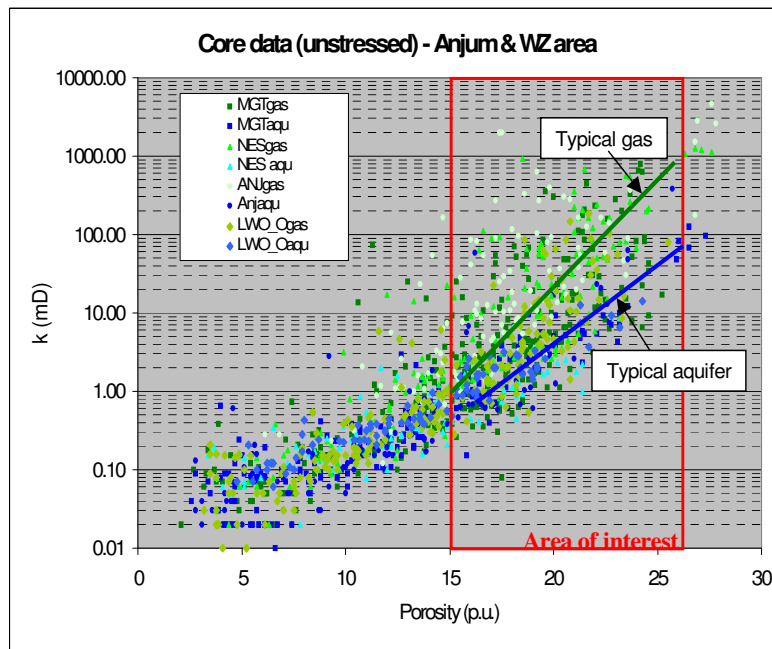
*Figure 2 Core plug permeability data for gas and aquifer leg.*

In M&R2015, the distinct cases have been defined somewhat differently compared to M&R2014. Previously, two cases were run, one with a low aquifer mobility (aquifer permeability varying between $10^{-3}$ and $10^{-4}$ times the gas permeability) and one with a high aquifer mobility (aquifer permeability equalling that of the gas leg).

This year, three cases have been generated: the low pressure drop realisation (all aquifer permeabilities $10^{-4}$ times the gas permeability), the base pressure drop realisation (with paleo-residual gas modelled in the aquifer and only a small reduction of absolute permeability in the waterleg) and the high aquifer mobility (aquifer permeability equalling that of the gas leg).

For the base aquifer mobility models, trapped paleo-gas is modelled as follows. The saturation height functions are cut off on the trapped gas saturation; such that at a capillary pressure of 0, there is a constant trapped gas saturation (see also Ref 3). The expected gas saturations below FWL are depicted in Table 4.

*Table 4: Average of gas saturation measurements in aquifer and the weighted average resulting in expected field averages for residual gas saturation below FWL (encircled in green). This saturation was used as a starting point and was only modified if an insufficient history match could be made.*

| Well | Average Gas bFWL | Weights for averaging | | | | | | | | |
|---|---|---|---|---|---|---|---|---|---|---|
| | | Anjum | Ezumazijl | Metslawier | Lauwersoog E | Lauwersoog C | Lauwersoog W | Moddergat | Nes | Vierhuizen |
| ANJ- 2C | 0.061 | 2 | | 3 | | | | | 1 | |
| ANJ- 3 | 0.1743 | 1 | 3 | | | | | | | |
| ANJ- 5B | 0.1698 | 1 | 1 | | | | | | | |
| LWO- 1B | 0.2313 | | | | 3 | | 1 | | | 1 |
| LWO- 2 | 0.2808 | | | | | 3 | 1 | 1 | | |
| LWO- 3 | 0.19 | | | | 1 | 1 | 2 | | | |
| MGT- 1B | 0.1895 | | | | | 1 | | 2 | 1 | |
| MGT- 2 | 0.1738 | | | | | | | 1 | 2 | |
| MGT- 3 | 0.1875 | | | 1 | | | | 1 | 2 | |
| VHN- 1C | 0.137 | | | | 1 | | | | | 3 |
| VHN- 3A | 0.1511 | | | | 1 | | 1 | | | 3 |
| Res Gas bFWL | | **0.12** | **0.17** | **0.09** | **0.20** | **0.24** | **0.21** | **0.20** | **0.16** | **0.16** |
| High | | 0.28 | 0.28 | 0.28 | 0.28 | 0.28 | 0.28 | 0.28 | 0.28 | 0.28 |
| Low | | 0.06 | 0.06 | 0.06 | 0.06 | 0.06 | 0.06 | 0.06 | 0.06 | 0.06 |

These numbers used for Residual Gas bFWL models, unless otherwise stated.

Some precaution is required when examining these models, since by doing this, trapped gas is existent throughout the entire aquifer, changing the GIIPs, which are then no longer comparable to P/Z and static GIIP. Model GIIP numbers presented in this document refer to GIIP *above the FWL*. This ensures that a comparison is possible between model GIIPs and static or P/Z GIIPs.

## 3.5 Upscaling

The model is upscaled one-to-one. Vertical permeability is set at 0.1 from the horizontal permeability by default, which resembles the microscopic permeability contrast between flow along and across the bedding. The history matching sensitivity parameter on the vertical permeability is used as an additional modification of vertical permeability, to account for extra macroscopic vertical flow barriers.

## 3.6 Defining subsurface realisations

### 3.6.1 Pre-M&R2014 method

Since history matching is an inverse problem, often many realisations can give a reasonable history match. Before M&R2014, multiple scenarios were taken using a probabilistic method. A low, base and high case scenario would be extracted from a cloud of realisations with an acceptable root-mean-square (rms) error. A P90, P50 and P10 dynamic GIIP realisation would then be constructed. This exercise would be done for a mobile aquifer and an immobile aquifer case (as described in Section 3.2.3), giving six realisations. Since the immobile aquifer cases generally gave the better pressure history match, as well as the better subsidence match, the P50 immobile aquifer case would be seen as the deterministic base case used for other reservoir engineering purposes. This model would generally also be further optimised to create a perfect working model. The other five models we mere probabilistic scenarios to capture the uncertainty range, but were insufficiently correct for a deterministic case.

*Table 5. Overview of dynamic realizations. Cases 1-6 apply to all fields. The high structure cases were applied to Moddergat and Nes only.*

|    | Base structure | High structure | Immobile aquifer | Mobile aquifer | Low dynamic GIIP | Base dynamic GIIP | High dynamic GIIP |
|----|----------------|----------------|------------------|----------------|------------------|-------------------|-------------------|
| 1  | x              |                | x                |                | x                |                   |                   |
| 2  | x              |                | x                |                |                  | x                 |                   |
| 3  | x              |                | x                |                |                  |                   | X                 |
| 4  | x              |                |                  | x              | x                |                   |                   |
| 5  | x              |                |                  | x              |                  | x                 |                   |
| 6  | x              |                |                  | x              |                  |                   | X                 |
| 7  |                | x              | x                |                | x                |                   |                   |
| 8  |                | x              | x                |                |                  | x                 |                   |
| 9  |                | x              | x                |                |                  |                   | x                 |
| 10 |                | x              |                  | x              | x                |                   |                   |
| 11 |                | x              |                  | x              |                  | x                 |                   |
| 12 |                | x              |                  | x              |                  |                   | x                 |

## 3.6.2  M&R 2014 method.

As of M&R2014, it has become clear that the uncertainty with the largest impact on modelling subsidence is the mobility of the aquifer. The other uncertainties are of lesser significance and generally give a similar result for subsidence. It was therefore decided to eliminate the uncertainty of the other parameters and focus solely on the difference between immobile and mobile aquifer cases, see Table 6.

*Table 6. Overview of dynamic realizations. Cases 1-2 apply to all fields. The high structure cases were applied to Moddergat and Nes only.*

|   | Base structure | High structure | Immobile aquifer | Mobile aquifer | Base dynamic GIIP |
|---|----------------|----------------|------------------|----------------|-------------------|
| 1 | x              |                | x                |                | x                 |
| 2 | x              |                |                  | x              | x                 |
| 3 |                | x              | x                |                | x                 |
| 4 |                | x              |                  | x              | x                 |

Since the amount of realisations is smaller, there can be more focus on getting a usable deterministic mobile aquifer case. By default the old base case dynamic GIIP realisations are used where the match is acceptable. The immobile aquifer case were generally in optimum shape and needed little revision. For the mobile aquifer case, which is seen as a sensitivity and a high subsidence case, it was attempted to, except for the aquifer permeability, change the immobile (base case) model as little as possible for optimum transparency of the two cases. Where possible, an attempt was also made to increase the transmissibility of existing faults as much as possible, since this will maximise the subsidence.

Although high structure realisations were made, they were eventually not used in the calculations for the eventual subsidence realisations, with the other realisation giving sufficient range of subsidence uncertainty.

## 3.6.3  M&R 2015 method.

After RFT measurements in the waterleg in MGT-3 and especially after observing late subsidence above an aquifer due south of the Ameland field, it has become more and more evident that the expectation case should be somewhere in between the extreme cases of Table 6. This intermediate solution was modelled by placing residual gas in the aquifer (as described in Section 3.4 Moreover, since the high structure realisations were not used during M&R2015, as well as that these models no longer resemble reality considering the dynamic

data observed, the high structure models were dropped. An overview of the different realisations is given in Table 7.

*Table 7. Overview of dynamic realizations during M&R 2015 for all Waddenzee fields except Nes and Vierhuizen.*

|  | Base structure | Immobile aquifer | Paleo-residual gas below FWL | Mobile aquifer | Base dynamic GIIP |
|---|---|---|---|---|---|
| *1 – Low pressure drop* | x | x |  |  | x |
| *2 – Base pressure drop* | x |  | x |  | x |
| *3 – High pressure drop* | x |  |  | x | x |

For Vierhuizen, the immobile aquifer realisation is discarded (Table 8), which is further discussed in Section 5.1.9.1.

*Table 8. Overview of dynamic realizations during M&R 2015 for Vierhuizen*

|  | Base structure | Immobile aquifer | Paleo-residual gas below FWL | Mobile aquifer | Base dynamic GIIP |
|---|---|---|---|---|---|
| *1 – Base pressure drop* | x |  | x |  | x |
| *2 – High pressure drop* | x |  |  | x | x |

The Nes field has a somewhat different approach, where GIIP and unit 2 transmissibility are varied (Table 9). The reasoning behind this is described further in Section 5.1.8.2.

*Table 9 Overview of dynamic realizations during M&R 2015 for Nes.*

|  | Base structure | Residual gas below FWL | Semi-Mobile aquifer | GIIP [BNCM] above FWL | Transmissibility unit 2 |
|---|---|---|---|---|---|
| *1 – Low pressure drop* | x | x |  | 21.7 | sealing |
| *2 – Base pressure drop* | x | x |  | 19.4 | large baffle |
| *3 – High pressure drop* | x | x |  | 17.2 | small baffle |

# 3.7 Forecasting

Pre-M&R2015, multiple forecasting scenarios were constructed: a base profile and an accelerated profile. The former was based on the production as given in the Winningsplan Wadden 2011, in the latter these yearly production figures were increased by 20% until the UR was reached, after which the forecast stopped. This to ensure that the total bandwidth given in the Winningsplan (+/- 20%) is accounted for.

In M&R2015, a different approach was taken. The main reason for this is that the Winningsplan 2011 numbers by now are outdated. Therefore, in 2015, only the Business Plan 2015 forecasts are taken. These are the sum of the no-further-activity (NFA) profiles and some expected forecasts from firm infill opportunities (Nes Infill wells, Moddergat infill well, Lauwersoog East infill well).

After the history matches are obtained, the model is ready for forecasting. The production profiles from Business Plan 2015 are taken and imposed on the wells.

Since some dynamic models have changed since Business Plan 2015, minor changes have been implemented for some fields. This will be covered on a field-by-field basis in Chapter 5

## 3.8 Translation into subsidence realisations

The Anjum, Ezumazijl and Metslawier fields (or *Anjum fields)* are mature fields and their subsidence has been thoroughly monitored. These fields therefore act as a calibration for the compaction coefficients of the neighbouring *Wadden fields*: Nes, Moddergat, the Lauwersoog fields and Vierhuizen.

An immobile aquifer results in higher aquifer pressures than is the case for a depleting aquifer. In order to match the observed subsidence, compaction coefficients will be higher for an immobile aquifer than for a depleting aquifer. It is the combination of different reservoir realisations for the Anjum fields versus the Wadden fields that form a deterministic subsidence scenario.

The results of the reservoir modelling work are combined with geomechanical parameters and calibrated to actual subsidence data. The way the separate reservoir model realisations are implemented in subsidence scenarios is described in Section 5.2.3.

# 4 UNCERTAINTY MANAGEMENT

Many parameters that act as input for the dynamic model have their uncertainty. This section describes what uncertainties have been considered and how they have been implemented in the different realisations.

As described in Section 3.6.3, aquifer mobility has been used as the main uncertainty parameter, defining the low, mid and high subsidence cases for each field. However, there are more dynamic properties with uncertainty ranges. The three distinct cases often had to optimised to create a good history match. This was done by modifying the parameters described in Section 4.1 .

Uncertainty ranges have not been modified for M&R2014, except for relative permeability, described in Section 4.1.3.

## 4.1 Uncertainties

### 4.1.1 GIIP

Statically, the main uncertainty parameters to test are GIIP and permeability. GIIP Different static parameters (Top structure, FWL, Net-over-gross, porosity and water saturation) determine the gas initially in place (GIIP). All these parameters have their uncertainties in their mean values and their distributions around the reservoir, especially away from the wells. Since the amount of wells in the Wadden area is rather limited, uncertainties can be very significant. Taking all these into account separately is a laborious exercise and will not give a great deal of insight. It is therefore chosen to capture the GIIP uncertainty as a whole by changing only the net pore volume (NPV), by a factor 0.9-1.1 from base case, and the free water level (range dependent on field by field). When modifying the NPV by a large amount, the GIIP distribution might be distorted too much. Therefore a high-structure case was also captured for the Nes and Moddergat fields to observe whether these matches were more plausible than the base-structure realisation.

### 4.1.2 Absolute Permeability

Permeability is distributed by applying a porosity-permeability relation that applies to well or field. A large number of wells in the Wadden area have been cored and analysed. The porosity and permeability relation around the wells are therefore well established (Ref 1). But uncertainties, especially away from the wells, can be large.

Field-wide horizontal and vertical permeability multipliers have been used as sensitivity parameters. These sensitivity parameters are defined logarithmically, because of their exponential impact on flow. When applying this to assisted history matching (see Section 4.2 ) it makes the proxy more efficient. Uncertainty range generally varies between -0.5 and 0.5 in the log domain (or between a factor 0.3 and 3.0 of the multiplier).

### 4.1.3 Relative permeability

The relative permeability ranges that are used have been slightly changed since M&R2014, (see Ref 4).

| | Meet&Regel 2014 | | | Meet&Regel 2015 | | |
|---|---|---|---|---|---|---|
| **Quantity** | **Low** | **Base** | **High** | **Low** | **Base** | **High** |
| **krw @ Sgr** | 0.01 | 0.1 | 0.2 | 0.01 | 0.1 | 0.3 |
| **ResGas = $S_{gr}/(1-S_{wc})$** | 0.10-0.25 | 0.30 | 0.45 | 0.15 | 0.30 | 0.45 |
| **krg @ Swc** | | 0.84 | | 0.84 | 0.84 | 0.84 |
| **Swc** | | *from capcurves – porosity dependent .* | | | *from capcurves – porosity dependent .* | |
| **Corey water** | 2 | 3 | 4 | 3 | 4.0 | 6 |
| **Corey gas** | 1 | 1.5 | 2 | 1 | 2.0 | 5 |

The specific values used may differ for every field (or realisation), specified in Section 5.1 .

Relative permeability has a significant impact on the water influx. The two most important parameters are residual gas and the water endpoint permeability. The first determines the point of water breakthrough, because when it is larger the water will more quickly bypass the gas towards the well. The latter mainly determines the rate of water production and influx. Core experiments on ANJ-1 are available (Ref 5) and show that (Figure 3) the residual gas is a function of the initial water saturation. This was taken along in defining the relative permeability model. The core experiments also show that (Figure 4) the water relative permeability endpoint is between 0.3 and 0.01.

The gas relative permeability end point is not varied, since modifying the absolute permeability has a similar effect.

Base case values for relative permeability are used as a starting point. The values are typical matching parameters: they are modified so as to ensure an optimum match, but are not seen as the key uncertainty to subsidence modelling.
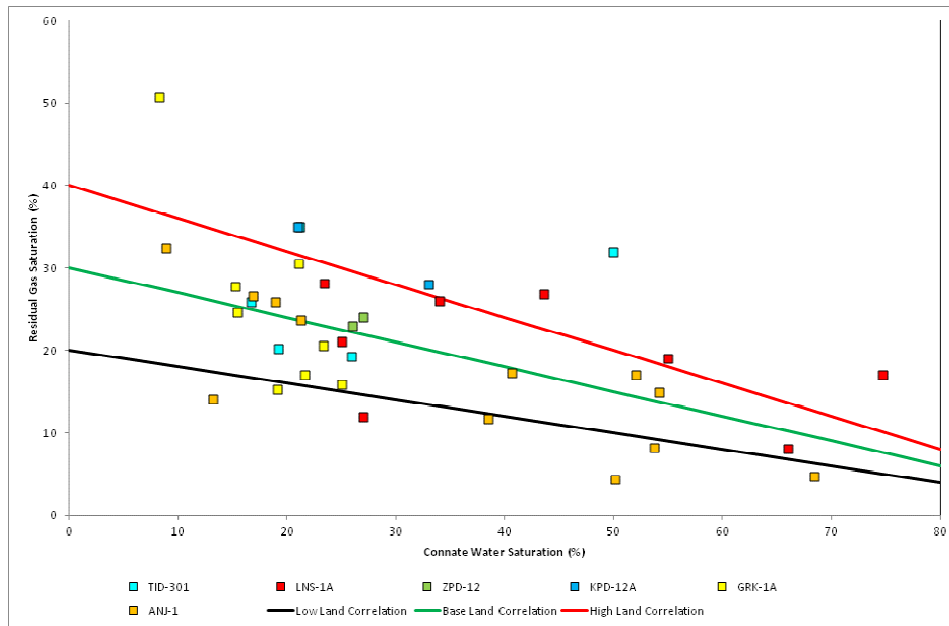
*Figure 3 Residual gas saturation as a function of the connate water saturation*
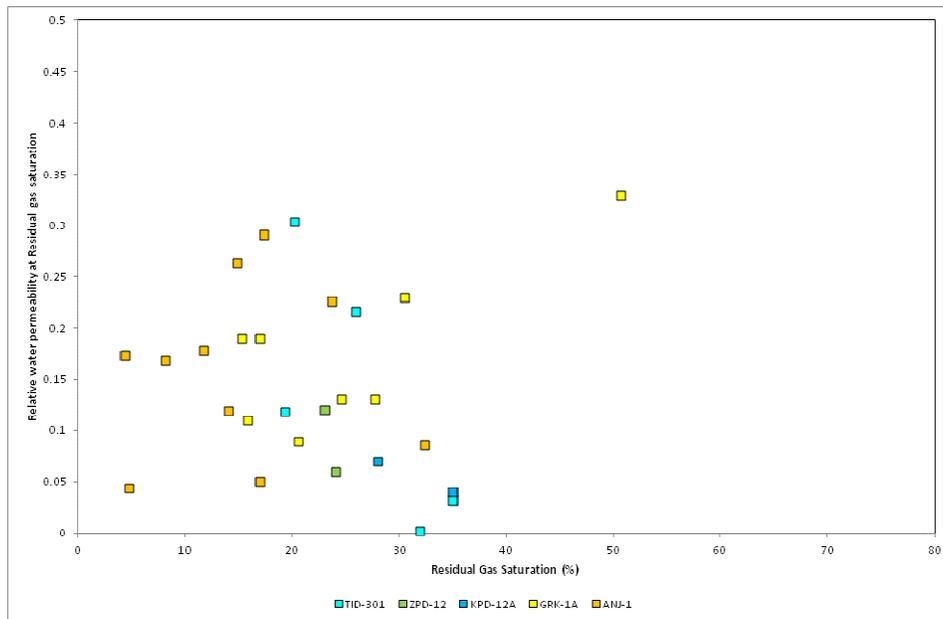


*Figure 4 Relative water permeability at residual gas saturation as a function of the residual gas saturation.*

### 4.1.4  Vertical permeability

Vertical permeability is an often poorly known quantity in these fields and is often very much dependent on vertical grid refinement, especially in vertically heterogeneous reservoirs. During the import of the static models to the dynamic simulator, as mentioned in Section 3.5 , by default the vertical permeability $k_v$ is set to 0.1 times the value of the horizontal permeability $k_h$. This represents a first guess for the "microscopic" $k_v/k_h$ ratio, observed in core plugs. However, considering that vertical layers in the dynamic models (~1m) are much larger than core plugs (~5 cm), heterogeneities of the scale between these two dimensions are not captured. To overcome this, an extra $k_v$-multiplier is used, of which the value is poorly known beforehand and hence is used as matching parameter. Typical values range from maximum 1 to minimum ~$10^{-3}$.

### 4.1.5  Vertical heterogeneities

High porosity sand streaks have been observed. Because of their size, these are difficult to detect and model. These layers can have high impact on inflow performance and water inflow. Only for Lauwersoog East and Lauwersoog West this uncertainty has been added, by having the freedom of multipliers on the low and high perm zones separately.

### 4.1.6  Faulting

Few intra-field faults have been observed. Only in Ezumazijl and Moddergat and faults are identified that have large sealing potential. The fault seal multiplier is, similar to the permeability multiplier, applied as a logarithmic sensitivity parameter. In M&R2014 Lauwersoog-West had a fault drawn in, which was poorly visible on seismic, since this gave a better match to the dynamic data. Although a possibility, N-S faults being abundant in the area, it was chosen not to use this fault baffle to limit the risk of underestimating subsidence behind it (due east).

### 4.1.7  Water encroachment behaviour

The parameters that have most impact on this behaviour apart from the static uncertainties in dip, free-water level and high permeable streaks, are residual gas and water relative permeability end point.  These have been used as dynamic uncertainty parameters.

Residual gas has an important effect on water behaviour: first, by increasing the residual gas, more gas can be bypassed by the water resulting in water breakthrough. Second, residual gas expands which results in an extra drive on the water by keeping the pressure relatively high.

## 4.2 Assisted history matching workflow

In order to assess the uncertainties with respect to the fields, a history matching workflow is set-up in SUM++. This workflow is used to assist in assessing the impact of uncertainties on the history match. Since M&R2014, the results of this workflow are not directly implemented as a final history matched realisation, but simply used as a tool to quicken history matching and gain model insight.

SUM++ is a Shell propriety assisted history matching tool that manages the in- and output of several runs in order to create a polynomial approximation (the so-called 'proxy') of the input-output relation. This proxy is then used to explore the uncertainty parameter space.

The number of uncertainty parameters and the number of matching points determines the complexity of the proxy. Often this does not improve the predictive quality of the proxy. This is because most parameters counterbalance, and therefore the proxy behaviour is dominated by the most sensitive parameters. The best matches that are obtained from the assisted history matching workflow are therefore only meaningful for these most sensitive parameters.

Runs can be exported to Spotfire software, in order to explore cross-correlations by filtering the data. From the remaining subset of data, an insight can be given on whereto the solution converges.

# 5  DYNAMIC MODELLING

In this chapter, the history matches and production/pressure forecasts are discussed on a field-by-field basis.

## 5.1  Field models and history matching

The history matching results, uncertainties and opportunities are discussed per field. Also, a comparison is made between the models used for M&R2014 and M&R2015. For each field, a table is given with the most important variable values used each model. Therein, the colours indicate which columns are used for comparison between 2014 and 2015.

### 5.1.1  Anjum

The Anjum field is located in the central onshore part of the Noord Friesland Concession (Lauwerszee Trough, NE-Netherlands). It was discovered in 1992 by ANJ-1, finding (virgin) pressure at 563 bara, which is strongly overpressured at a datum depth of 3850mTVNAP. In 1996-97 ANJ-4 was drilled as a horizontal production well. Both wells were drilled from the Anjum location and are producing since 1997 to the on-site Anjum facilities. At the time of drafting the report, more than 85% recovery has been obtained from the field with respect to the static GIIP.

The Rotliegend formation in the Anjum field consists of the Ten Boer Claystone Member (ROCLT), the Upper Slochteren Sandstone Member (ROSLU), the Ameland Claystone Member (ROCLA) and the Lower Slochteren Sandstone Member (ROSLL). Only the ROSLU and the ROSLL contain sandstone of reservoir quality. They consist of aeolian and fluvial/lacustrine sediments deposited in a desert environment. The thickness of the ROSLU in ANJ-1 is 106.0 m. The Anjum gas field consists of two fault blocks. The main block is situated in the East, and the small block in the West contains only about 1% of the total GIIP. Detailed geology is described in the Geology section above.

The Anjum field (Figure 5) contains two wells, ANJ-1 and ANJ-4B. Dynamic data suggests that they are draining the same volume (Figure 6).
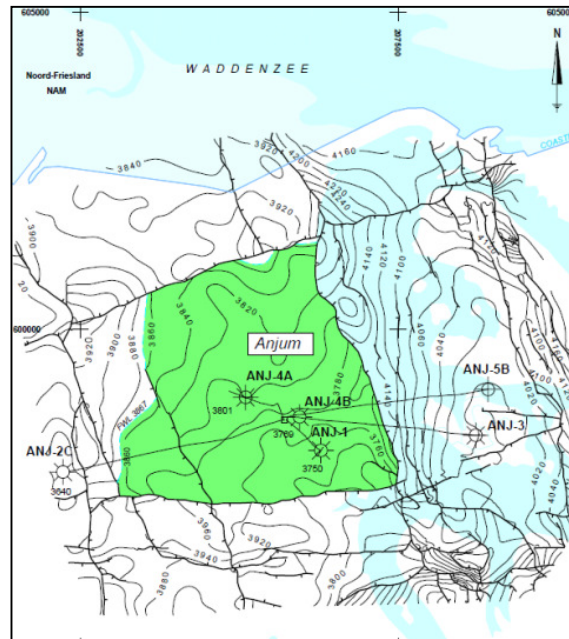
*Figure 5 ARPR top ROSL map of Anjum field*
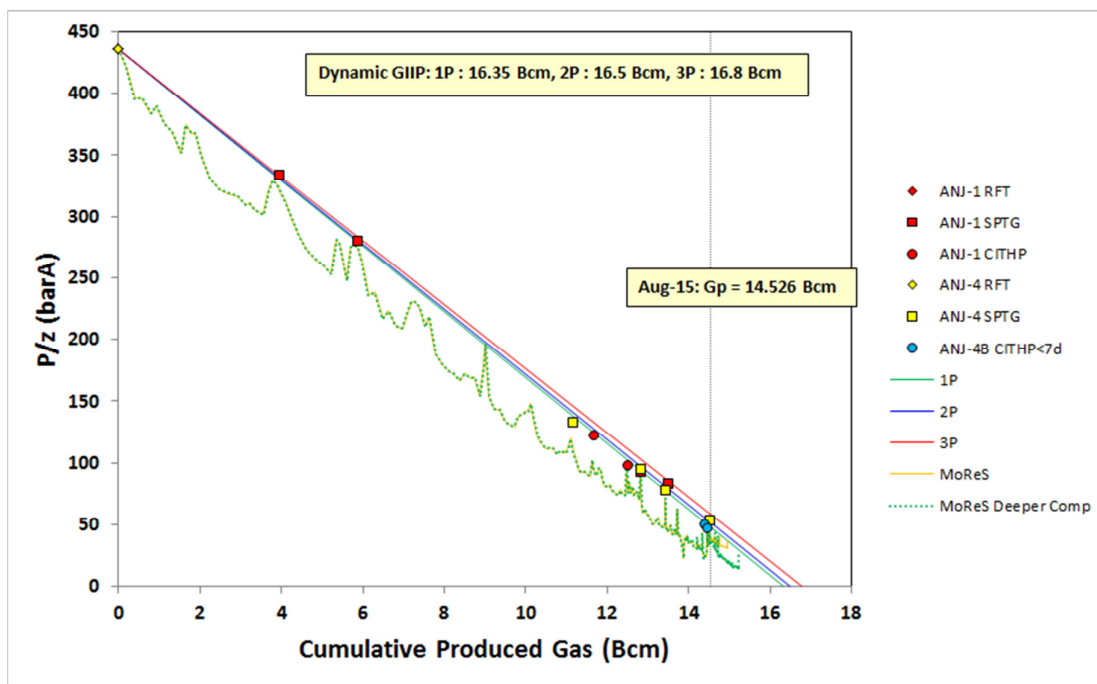


*Figure 6 P/z plot Anjum-1 and Anjum-4 combined*

ANJ-1 is more or less vertical and has ceased production in 2012 to a high hold-up depth (HUD). The high HUD is most likely related to sand production from Unit 2[5], that has been perforated in 2006. Unit 2 has high porosity/permeability streaks embedded in shale layers. Restoring the well with a straddle over the high porosity units and a workover to replace the tubing was deemed not economic, since the other well, ANJ-4 is situated in the same hydraulic unit.

---

[5] Unit 2 is a shale layer within the Rotliegend Upper Slochteren (ROSLU) that is deemed laterally extensive throughout the entire Wadden area. Flow is known to be significantly baffled if not sealing between the Unit 1 on top of it and Unit 3-6 below.

ANJ-4B is a more or less horizontal well, which is currently the only producer of the Anjum field. Unit 2 has not been perforated in this well.

### 5.1.1.1   **Reservoir model**

As is shown in Figure 7 and Figure 8, a good history match was achieved on downhole pressure.
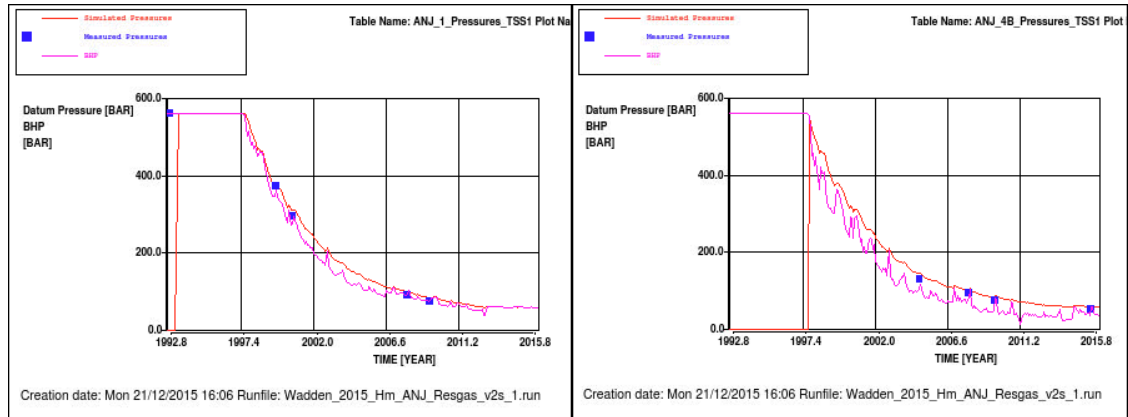


*Figure 7 Simulated pressure (red line), simulated BHP (violet line) and measured down hole pressure (blue squares) for base case. Left: ANJ-1, Right: ANJ-4B.*
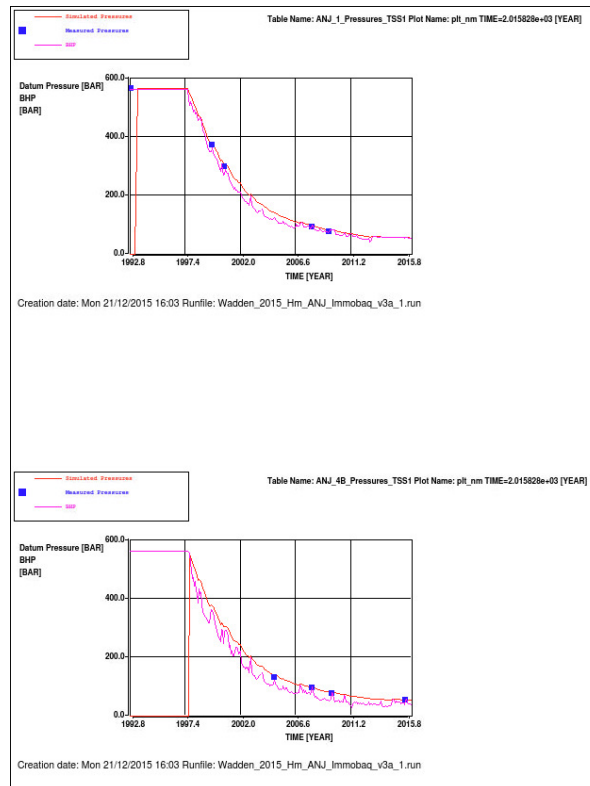
*Figure 8 Simulated pressure (red line), simulated BHP (violet line) and measured down hole pressure (blue squares) for low case. Left: ANJ-1, Right: ANJ-4B.*
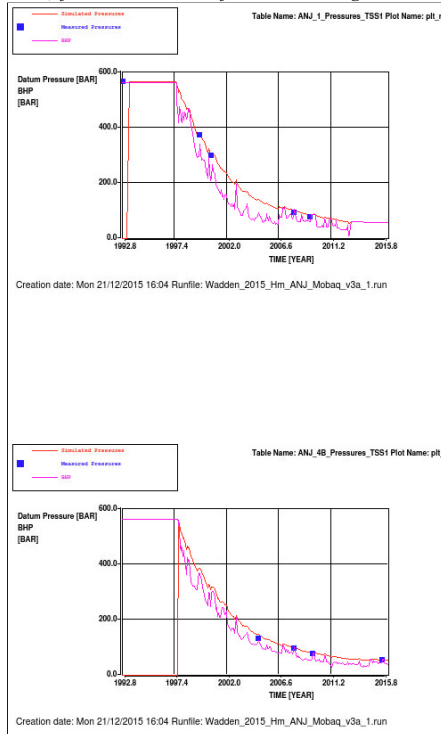


*Figure 9 Simulated pressure (red line), simulated BHP (violet line) and measured down hole pressure (blue squares) for high case. Left: ANJ-1, Right: ANJ-4B.*

The match on tubing-head pressures in ANJ-4B is shown in Figure 10. It is clear that the historical inflow performance is well matched.
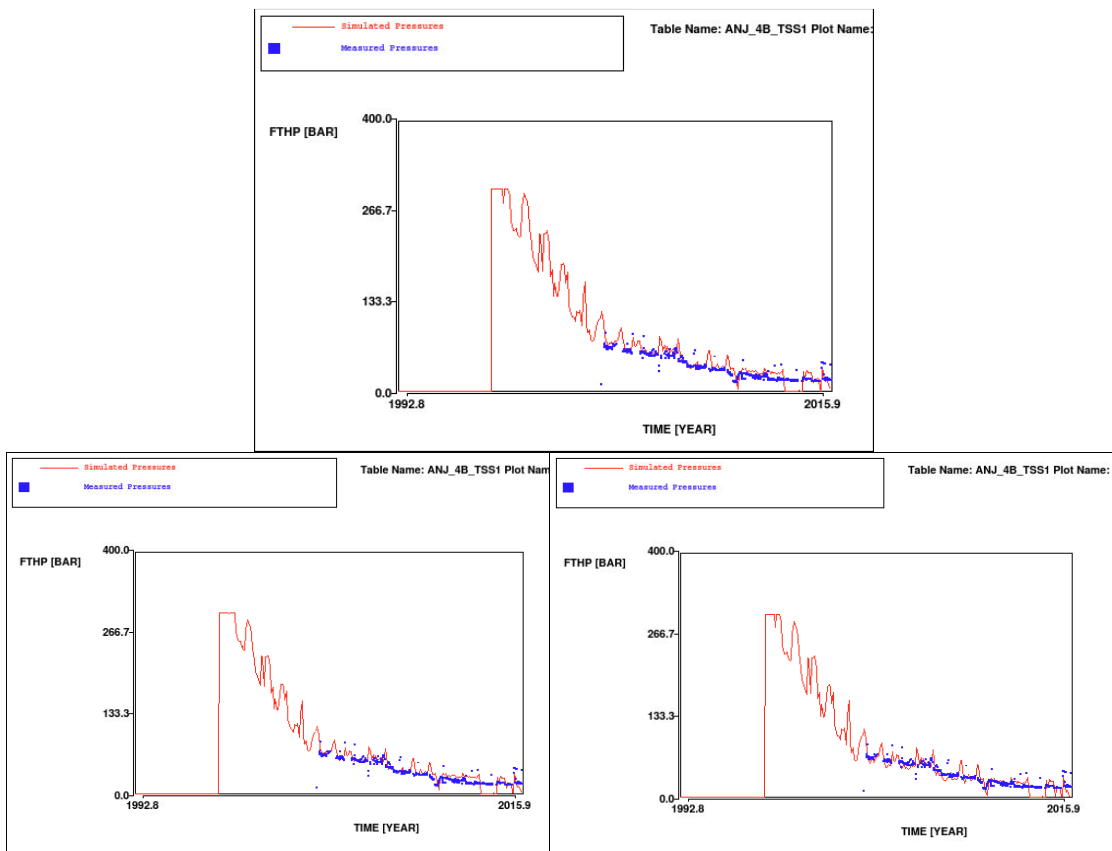
*Figure 10 Simulated (red line) and measured (blue squares) FTHP data in ANJ-4B. Top: base case. Left: low case. Right: high case.*

In ANJ-1, a PLT has been run in 1997 and the match is shown in Figure 11. A decent match was obtained. It indicates that in the bottom a high permeable layer has not been fully captured. Considering that the inflow performance in ANJ-4B has been captured well, this is not considered an issue.
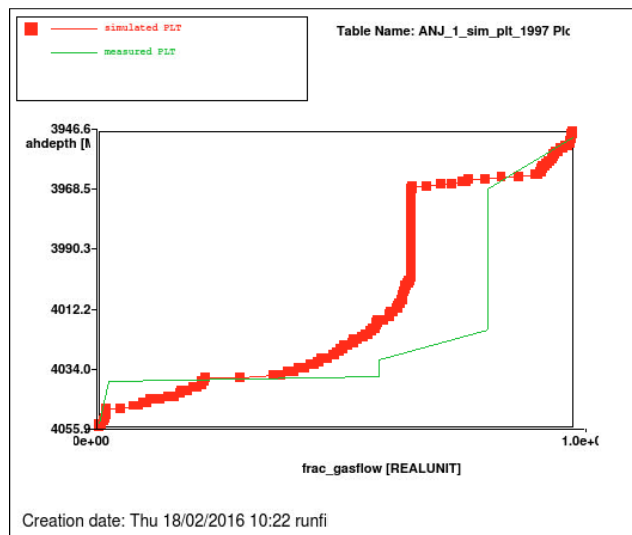


*Figure 11 Simulated (red line + squares) and measured (green line) PLT in ANJ-1. Base case model.*

The Anjum field has a good history match. The history matching parameters used are shown in Table 10.

*Table 10 History matching parameters used for the Meet & Regel cycle for Anjum.*

| Parameter | Static base | Low M&R2015[6] | Mid M&R2015[6] | High M&R2015[6] | Immob M&R2014[7] | Mob M&R2014[7] |
|---|---|---|---|---|---|---|
| Residual gas sat. below FWL | 0.12 | **0** | **0.06** | **0** | **0** | **0** |
| GBV multiplier | 1.0 | **0.98** | **0.96** | **0.97** | **0.96** | **0.95** |
| $k_h$ multiplier | 1 | **0.49** | **0.56** | **0.13** | **0.62** | **0.16** |
| $k_v$ multiplier | NA | **0.032** | **0.014** | **0.20** | **0.03** | **0.20** |
| FWL (m TVNAP) | 3867 | **3870** | **3870** | **3870** | **3870** | **3870** |
| $k_h$ multiplier aquifer | 1 | **$1. 10^{-4}$** | **0.1** | **1** | **$1. 10^{-4}$** | **1** |
| $k_v$ multiplier aquifer | 1 | **$1. 10^{-4}$** | **0.1** | **1** | **$1. 10^{-4}$** | **1** |
| Fault I_2 transm. | N/A | **0.1** | **0.1** | **0.91** | **0.10** | **0.91** |
| Residual gas | 0.30 | **0.30** | **0.15** | **0.1** | **0.30** | **0.2** |
| $k_w@S_{rg}$ | 0.1 | **0.1** | **0.08** | **0.1** | **0.1** | **0.1** |

Overall, the values of the dynamic modelling parameters are well within the expected uncertainty range. A permeability multiplier of between 0.13 and 0.56 is acceptable, accounting for heterogeneities within gridblocks. Although the mid case, with the permeability multiplier closest to unity, has the preference. The FWL is modelled marginally deeper than expected.

The new mid-case model was based on the immobile aquifer (low subsidence case) model. Inserting the expected value of 12% residual gas below free water level hugely overestimated the pressure support from the aquifer. Adjusting relative permeability parameters did not have the desired effect. Hence the value has been decreased to 6%. This figure is not unreasonable: the aquifer of Anjum has not been logged, hence the estimate was based on analogue wells. One important analogue well, ANJ2C in the Metslawier field, measured only 6% gas saturation below FWL.

Because of the aquifer model, residual gas and kw end-point had to be lowered to limit water production. Also the permeability was increased to limit drawdown caused by this water production. Since there is (late) pressure support coming from the aquifer, the GBV was reduced. Kv was also slightly lowered for an optimal match. Furthermore, the Corey exponents adjusted to latest figures (not reflected in the table).

The intra-field fault, running in N-S direction, appears not to be sealing. A slight baffle (0.1) is modelled in the base case (immobile aquifer) model, but this is not substantial. The static GIIP has already been updated (increased) due to dynamic input. A sealing fault will imply an even higher GIIP, which appears unlikely.

### 5.1.1.2  **Meet & Regel cycle 2014 vs 2015 model comparison**

The two models of M&R2014, that were carried over to M&R2015's low and high case, have not changed significantly as can be seen in Table 10. The mobile aquifer realisation had a multiplier of 0.1, which is updated to 1.0 to align with high case models of other fields.

---

[6] Input deck: Wadden_2015_ANJ_MRN_v2.INP
[7] Input deck: Wadden_2015_ANJ_MRN_v1.inp.

### 5.1.1.3  **Water production**

Water production for the base case realisation has been reasonable matched (Figure 12). It slightly overestimates water production, but values are in the right order of magnitude.
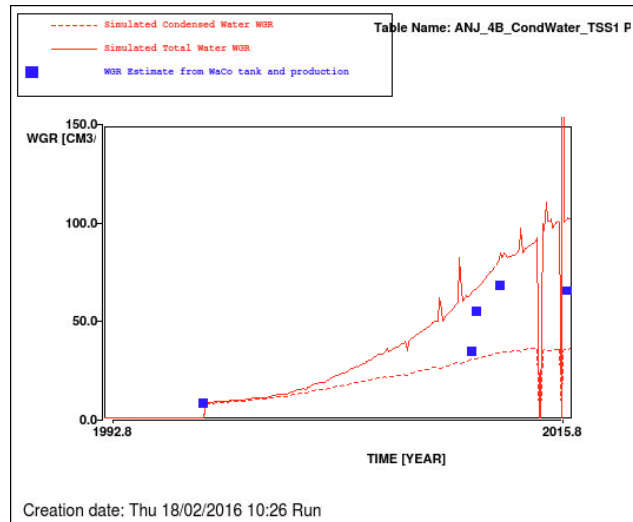


*Figure 12 Simulated total WGR (red solid line), simulated condensed WGR (red dashed line) and estimated WGR from production and WaCo tank observations (blue squares) for ANJ-4B. Base case realization.*

## 5.1.2  Ezumazijl

The Ezumazijl field forms part of the deepest graben trend in the Lauwerszee Trough. . It was discovered by ANJ-3 in 1998, finding virgin pressures at 493 bara. Ezumazijl was brought on-stream in February 1999, with ANJ-3 hooked-up to the on-site Anjum facilities. The field is fully covered by a 3D Pre-SDM seismic dataset.

Ezumazijl is a down thrown Rotliegend fault block. ANJ-3 encountered approximately 121 m of gas bearing sandstone in the Rotliegend Upper Slochteren, which consists of aeolian and fluvial/lacustrine sediments deposited in a desert environment.

The field consists of the Ezumazijl main block and a smaller block to the Southeast. Two faults run to the south and to the north of the well ANJ-3 and separate the main field into a northern, a central and a southern lobe. A material balance analysis indicates the faults act as a seal or at least a baffle to gas flow, however some uncertainty remains and will be addressed through material balance analysis after prolonged production.

Ezumazijl field (Figure 13) contains three wells, ANJ-3, ANJ-5B and ANJ-6, of which only ANJ-3 is producing. Its P/z plot can be found in Figure 14. ANJ-5B was drilled in the northern flank of the field and found initial pressures. Due to the small and low saturation gas column, it was decided to abandon ANJ-5 (Ref 6). In 2014, the southern block was drilled by the ANJ-6 wells and found a mere 20m of gas column, with poorer reservoir quality than expected. The pressure acquired was around 480 bara, which is almost virgin, indicating poor connectivity between the ANJ-6 well and the producing ANJ-3.

The Ezumazijl field is relatively tight: slow pressure build-ups have been observed. Flow is dominated by unit 2 that has the highest permeability.
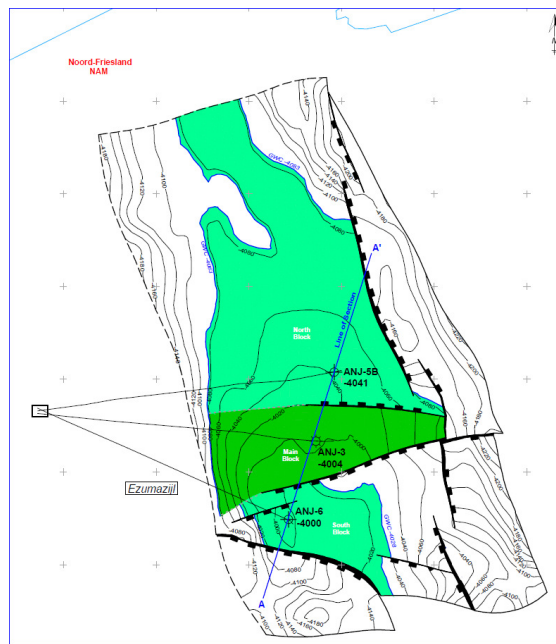
*Figure 13 Ezumazijl ARPR top ROSL map*
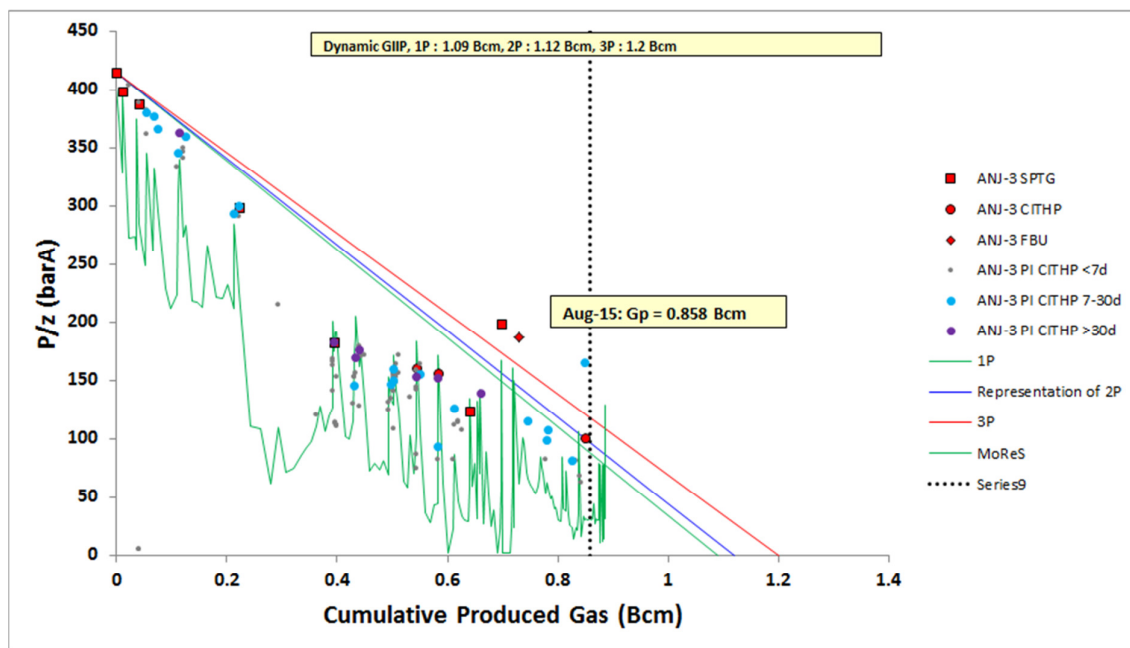

*Figure 14 P/z plot ANJ-3*

### 5.1.2.1  Reservoir model

Downhole pressures in Ezumazijl are matched as shown in Figure 15. In 2009, pressures in Ezumazijl went up 100 bar, while the production dropped. This is most likely due to a collapse of the high permeable unit 2. This is similar to the issue observed in ANJ-1. After reperforating this high permeable unit, pressures went down and rates went back up. In order to accommodate this behaviour, the perforations in unit 2 are switched off in the recompletion table.

In order to achieve a match, both the fault between ANJ-3 and ANJ-5B, and the fault south of ANJ-3 needed to be practically closed. The high initial pressure of ANJ-6 (south of ANJ-3)

backs this observation. The other history matching parameters used for the different models are shown in Table 11.

Since the drilling of Anjum-6 in 2014, there has not been a static model update. However, since the faults were closed-in anyway, no changes were needed to get a correct model representation.
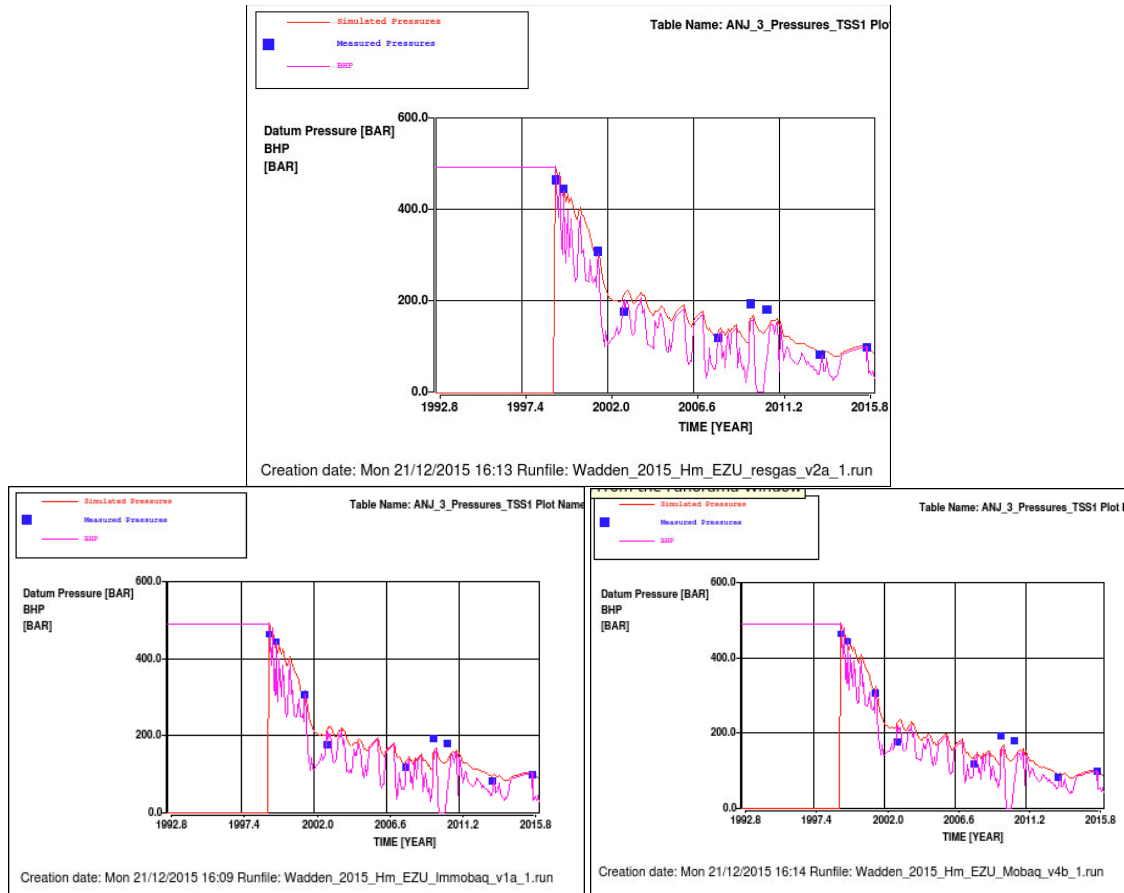


*Figure 15 Simulated pressure (red line ), simulated BHP (violet line) and measured (blue squares) downhole pressure data in ANJ-3. Top: base case. Left: low case. Right: high case.*

The historic pressures show that around 2009, higher pressures were seen than before. It is currently believed that the higher pressures observed in the well are related to more tight layers in the reservoir. Due to sand production from the high permeable streaks, part of the high permeability perforations were closed off. That resulted in pressures in the well to be dominated by more tight, higher pressure layers. After clean-out and reperforation of high permeable layers, pressures returned to original trend.

Historical well performance has been decently matched as is shown in Figure 16. The most recent points show deviations, which could be due to the scaling issues or the formation water produced. This leads to larger pressure drop over the formation or in the well and hence lower FTHP.
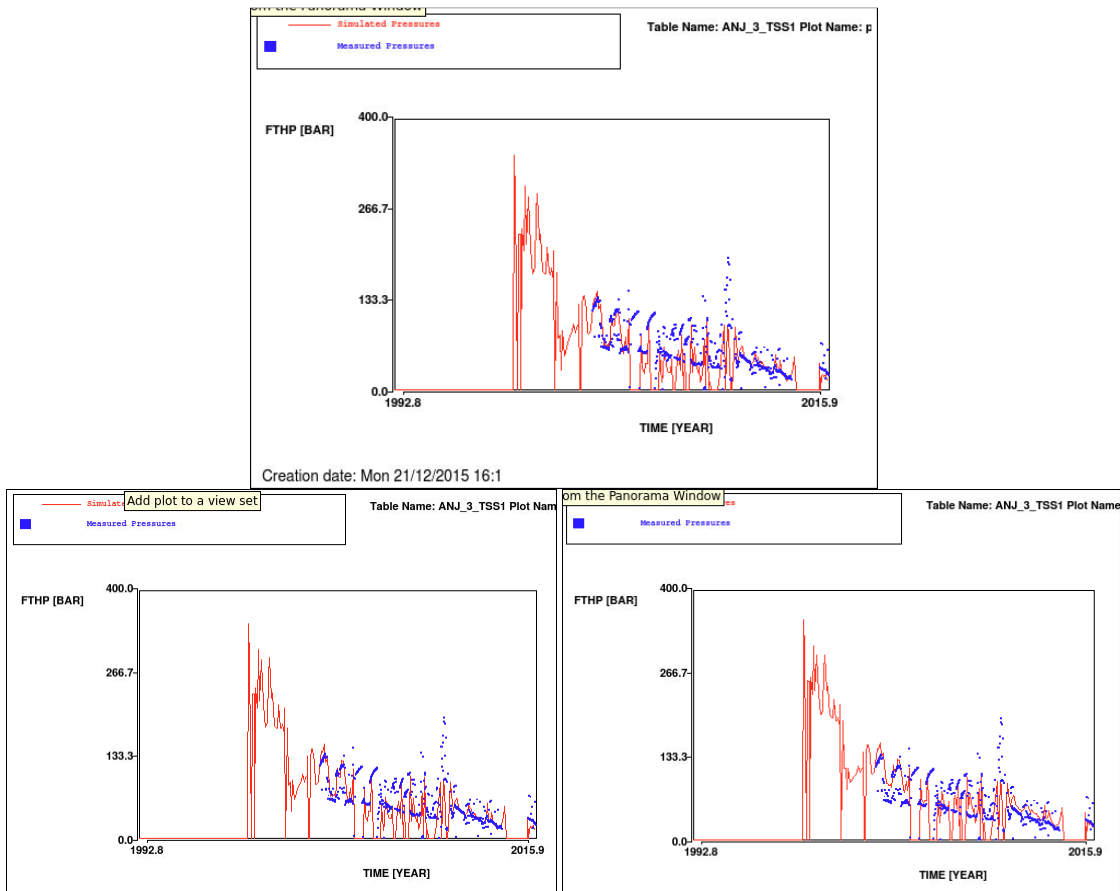
*Figure 16 Simulated (red line) and measured (blue squares) flowing tubing head pressures in ANJ-3. Top: Base case. Left: Low case. Right: High case.*

The reservoir has quite some permeability contrast, but this is well matched as is shown by the PLT match in Figure 17.
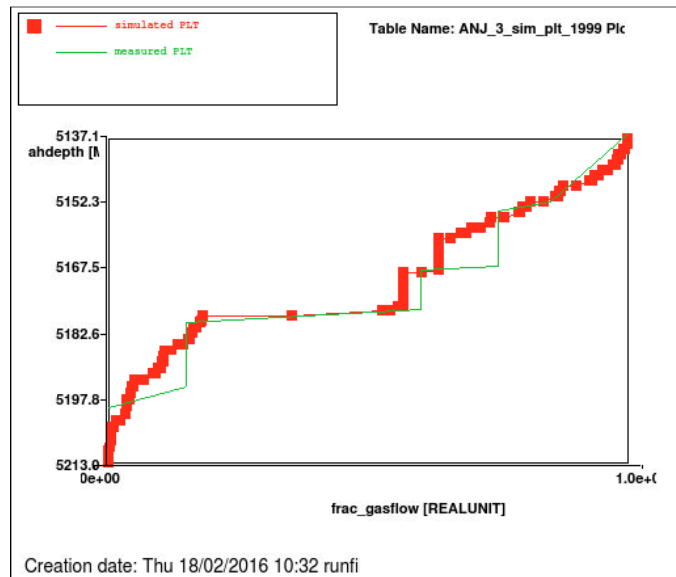


*Figure 17 Simulated (red line + squares) and measured (green line) PLT in ANJ-3*

*Table 11 History matching parameters used for the Meet & Regel cycle for Ezumazijl.*

| Parameter | Static | Low M&R2015[8] | Base M&R2015[8] | High M&R2015[8] | Immob Base M&R 2014[9] | Mob Base M&R2014[9] |
|---|---|---|---|---|---|---|
| Residual gas below FWL | 0.17 | **0** | **0.17** | **0** | 0 | 0 |
| GBV multiplier | 1.0 | **0.93** | **0.85** | **0.85** | 0.93 | 0.90 |
| $k_h$ multiplier | 1 | **0.40** | **0.40** | **0.40** | 0.32 | 0.38 |
| $k_v$ multiplier | N/A | **$1.0\ 10^{-3}$** | **$1.0\ 10^{-3}$** | **$1.0\ 10^{-3}$** | $1.02\ 10^{-3}$ | $1.91\ 10^{-4}$ |
| GWC (m TVNAP) | 4083 | **4080** | **4080** | **4080** | 4080 | 4080 |
| Fault Seal N | N/A | $10^{-7}$ | $10^{-7}$ | $10^{-7}$ | $10^{-7}$ | $10^{-7}$ |
| Fault Seal S | N/A | $10^{-6}$ | $10^{-6}$ | $10^{-6}$ | $10^{-6}$ | $10^{-6}$ |
| $k_h$ multiplier aquifer | N/A | **$1.2\ 10^{-4}$** | **0.1** | **1** | $1.20\ 10^{-4}$ | 1 |
| $k_v$ multiplier aquifer | N/A | **$1.8\ 10^{-4}$** | **0.1** | **1** | $6.46\ 10^{-4}$ | 1 |
| Residual gas | 0.30 | **0.43** | **0.20** | **0.20** | 0.43 | 0.30 |
| $k_w @ S_{rg}$ | 0.1 | **0.1** | **0.1** | **0.1** | 0.1 | 0.1 |

Since faults have been closed and the aquifer of Ezumazijl is not laterally extensive, vertical permeability has a large impact on the subsidence cases, but since the vertical perm was already set to a minimum ($10^{-3}$), the GBV multiplier was altered to ensure a good pressure response for the base and high case models.

All in all, average pressure drop and the induced subsidence for Ezumazijl is minimal.

### 5.1.2.2  Meet & Regel cycle 2014 vs 2015 model comparison

The low (immobile aquifer) case has remained largely unchanged, with a slight modification of permeability to match the latest THP measurments. The high (mobile) aquifer case was modified to ensure consistency with the other two models. The GBV was reduced to 0.85, so that the pressure drop exceeded that of the base case.

### 5.1.2.3  Water production
Water production has not been specifically matched on, but the match is good.  In ANJ-3 the salt scaling suggest that indeed formation water is being produced. The estimated WGR and modelled WGR are shown in Figure 18.

---

[8] Input deck: Wadden_2015_EZU_MRN_v2.INP
[9] Input deck: Wadden_2015_EZU_MRN_v1.inp.
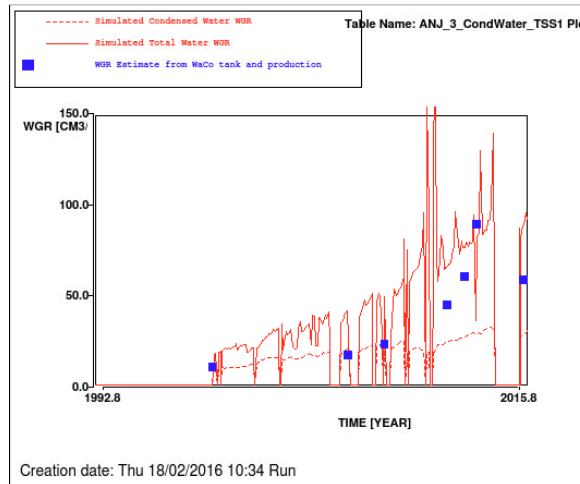
*Figure 18. Simulated total WGR (red solid line), simulated condensed WGR (red dashed line) and estimated WGR from production and WaCo tank observations (blue squares) for ANJ-3. Base case realisation.*

### 5.1.3 Lauwersoog Central

Lauwersoog-Central is the most western Lauwersoog block (Figure 19). It was discovered in 1997 by the well LWO-2 and found virgin pressures at 500 bara. LWO-2 was brought on stream in 2012. The well is drilled on the low side of the structure.

Its P/z plot can be found in Figure 20. LWO-2 is currently producing intermittently: producing for 8 hours and closed in for 16 hours every day.
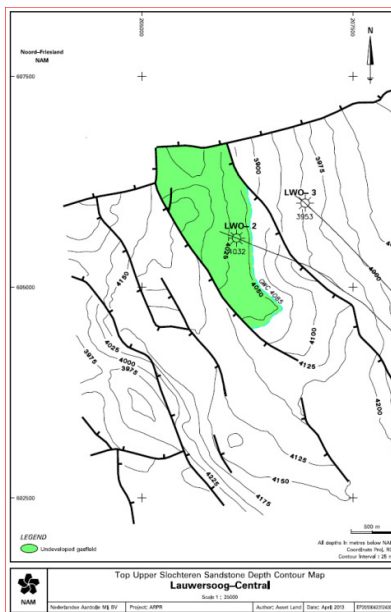


*Figure 19 Lauwersoog-Central ARPR top ROSL map*
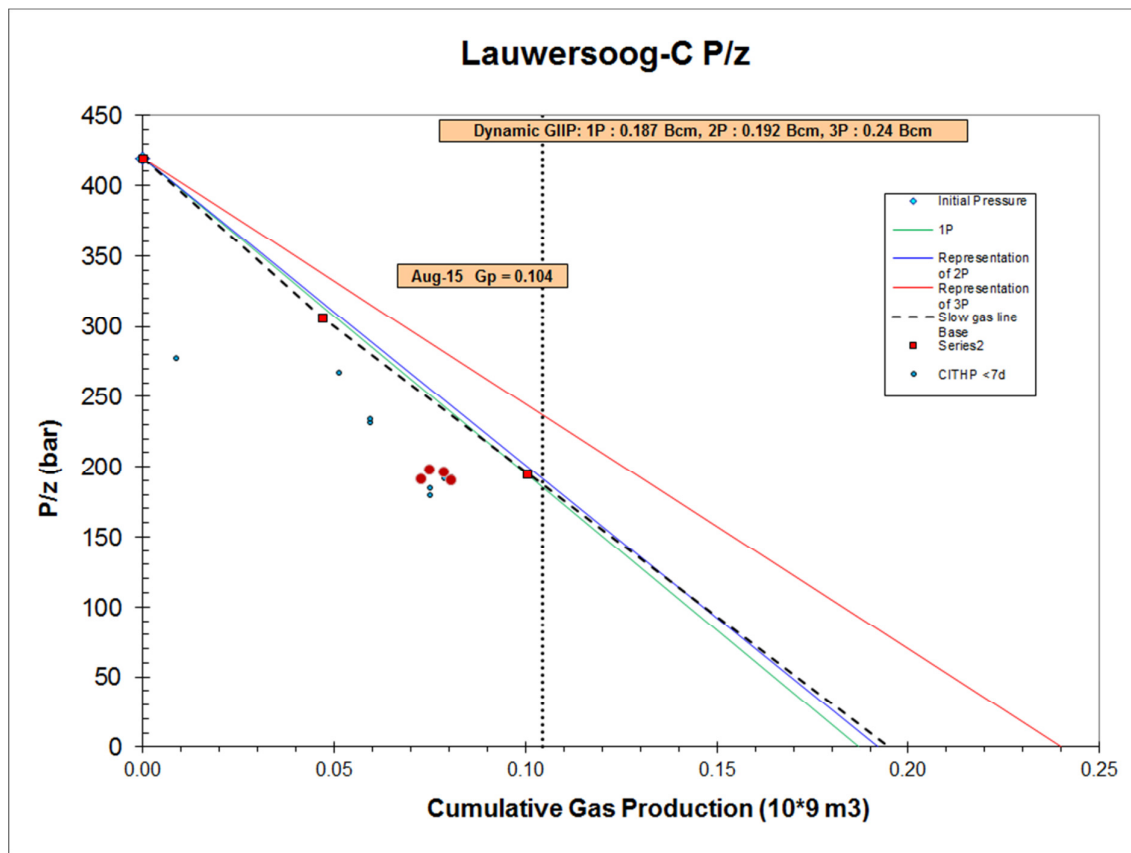
*Figure 20 P/z plot for LWO-2.*

### 5.1.3.1   Reservoir model

For the Lauwersoog-Central –East and –West field, as described in Section 3.3.1, the shutins are modelled to the nearest day, and therefore BHP can be used for history matching. Since initial production, a fish has been stuck in the well. Due to this, the well model might not reflect the true pressure drop over the well. Therefore, the flowing THP match is not strictly matched upon. Moereover, the intermittent production of this well causes near-well behaviour and water production to be difficult to model.
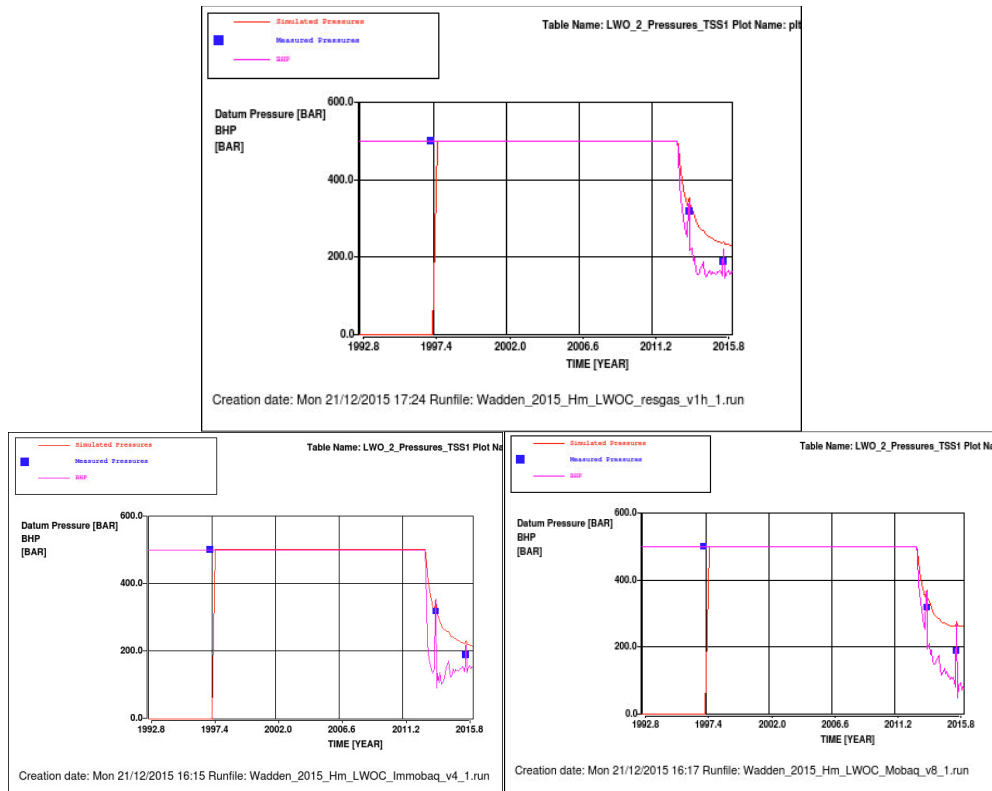
*Figure 21 Simulated pressure (red line ), simulated BHP (violet line) and measured (blue squares) downhole pressure data in LWO-2. Top: base case. Left: low case. Right: high case.*
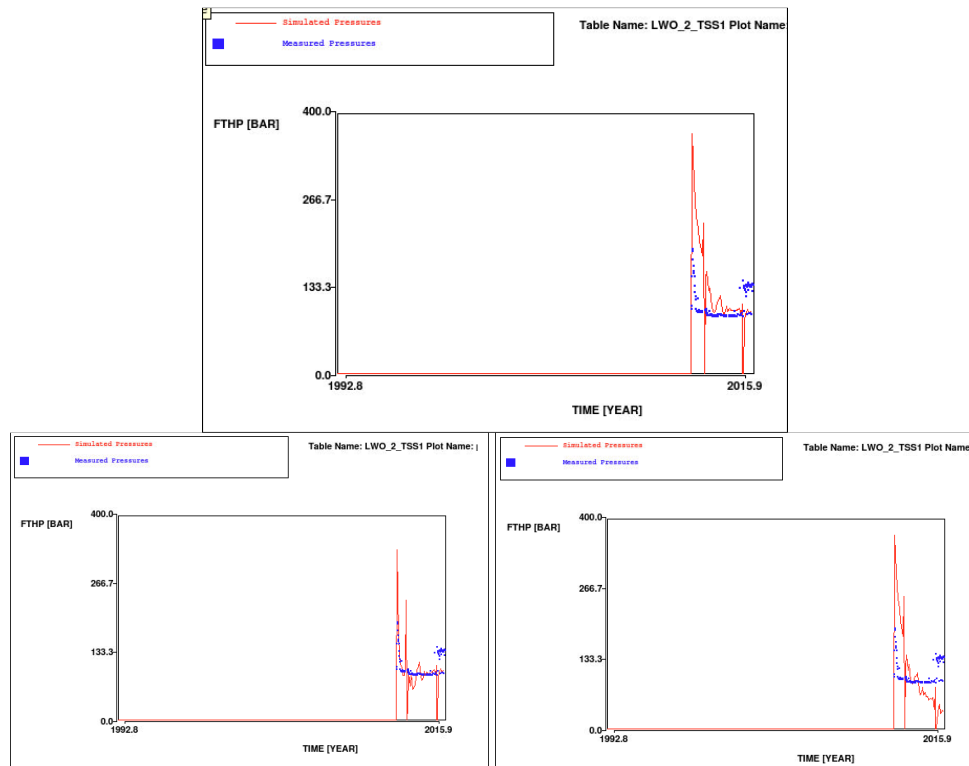
*Figure 22 Simulated (red line) and measured (blue squares) flowing tubing head pressures in LWO-2. Top: base case. Left: low case. Right: high case.*

From Figure 21 and Figure 22, it can be seen that history match of this field is not ideal. The left pictures, the immobile aquifer realisation and the residual gas saturation realisation give a better match than the mobile aquifer realisation. The mobility of the aquifer mainly causes water encroachment, affecting the relative permeability around the wellbore. To keep an acceptable BHP match, the absolute permeability must increase for the mobile aquifer realisation, which takes its toll on the THP match. This is a good example of a field where dynamic data suggests that the aquifer cannot be as mobile as the gas leg.

In Table 12, the parameter settings are shown that are used to get a match for the field. To get a reasonable match, the GIIP is lowered significantly. Moreover, the $k_h$ is significantly lower than expected, although, probably due to the contrasts in permeability that have not been entirely captured. Also, the FWL is deeper to keep out formation water.

*Table 12 History matching parameters used for the Meet & Regel cycle for Lauwersoog C.*

| Parameter | Static | Low M&R 2015[10] | Base M&R2015[11] | High M&R2015[10] | Immob Base M&R 2014[12] | Mob Base M&R 2014[12] |
|---|---|---|---|---|---|---|
| Residual gas below FWL | 0.24 | **0** | **0.24** | **0** | 0 | 0 |
| GBV multiplier | 1 | **0.86** | **0.90** | **0.86** | 0.86 | 0.86 |
| $k_h$ multiplier | 1 | **0.18** | **1** | **0.56** | 0.18 | 0.56 |
| $k_v$ multiplier | N/A | **1.6 10$^{-4}$** | **1.5 10$^{-4}$** | 1.6 10$^{-4}$ | 1.6 10$^{-4}$ | 1.6 10$^{-4}$ |
| FWL (m TVNAP) | 4074 | **4079** | **4067** | 4079 | 4079 | 4079 |
| $k_h$ multiplier aquifer | N/A | **1.0 10$^{-4}$** | **0.1** | 1 | 1.0 10$^{-4}$ | 1 |
| $k_v$ multiplier aquifer | N/A | **1.0 10$^{-4}$** | **0.1** | 1 | 1.0 10$^{-4}$ | 1 |
| Residual gas | 0.3 | **0.25** | **0.27** | 0.25 | 0.25 | 0.25 |
| $k_w @ S_{rg}$ | 0.1 | **0.1** | **0.09** | 0.1 | 0.1 | 0.1 |

The new base case model, using residual gas below FWL, was not trivial to match. A lot of problems occurred with water approaching the well, hence creating large relative permeability effects not visible in the THP data. Therefore, a shallow contact was assumed, as to keep the water out. Considering the small pressure drop in this field (on average only a depletion of under 40 bar for the high case after forecasting) it was decided to keep this realisation, even though the match is not ideal. Indeed this base case was situated between the low and high case after forecasting (Section 5.2.2.2 ).

### 5.1.3.2   Meet & Regel cycle 2014 vs 2015 model comparison
No changes have been made between M&R2014's two models and the current low and high case model.

### 5.1.3.3   Water production
Lauwersoog-Central has only been producing since 2012. Due to the short history and the relatively low rates, it is difficult to detect formation water. Hence, the water-gas-ratios estimated from the change in WaCo tank level as given in Figure 23, have large uncertainties. However, the proximity of the well to the water because of its downdip position, does give a large risk of water breakthrough. This is also suggested by dynamic simulation.

---

[10] Input deck: Wadden_2015_LWOC_MRN_v2.INP
[11] Input deck: Wadden_2015_LWOC_MRN_v3.INP
[12] Input deck: Wadden_2015_LWOC_MRN_v1.inp
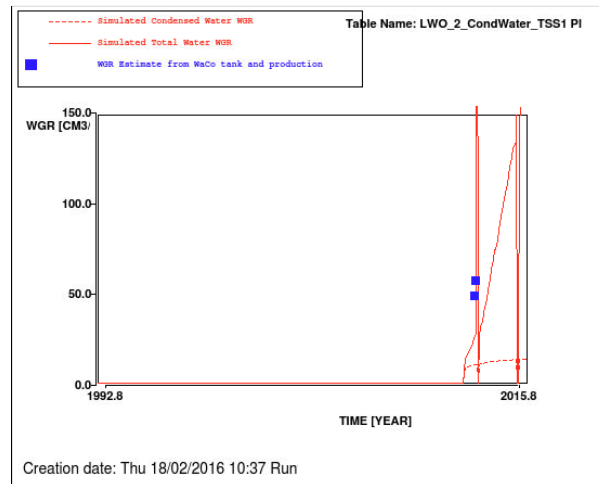
*Figure 23 Simulated total WGR (red solid line), simulated condensed WGR (red dashed line) and estimated WGR from production and WaCo tank observations (blue squares) for LWO-2. Base case realisation.*

### 5.1.4  Lauwersoog-East

The Lauwersoog-Oost field (Figure 24) lies beneath the Waddenzee at the eastern end of the Noord Friesland concession. It was discovered in 1996 by the well LWO-1 and brought online in November 2008. It found virgin pressures at 481 bara. The gas is evacuated to the Anjum facilities. Its P/z plot can be found in Figure 25.

The Lauwersoog Oost gas field is a fault / dip closed structure at Base Zechstein level on the Vierhuizen-Munnekezijl trend. LWO-1 well encountered approximately 78 m of gas bearing Rotliegend Upper Slochteren (ROSLU) reservoir, which consists of aeolian and fluvial/lacustrine sediments deposited in a desert environment. The thickness of the ROSLU in LWO-2 is 113 mTV (gross).

Seismic indicates a saddle structure with the most crestal points on the edges of the structure, although – with only well in the structure – this has not been confirmed by well penetration. The free water level has been found in the lower units of the structure. It is unknown whether the shallower ROSLU1 layer is sharing its FWL.
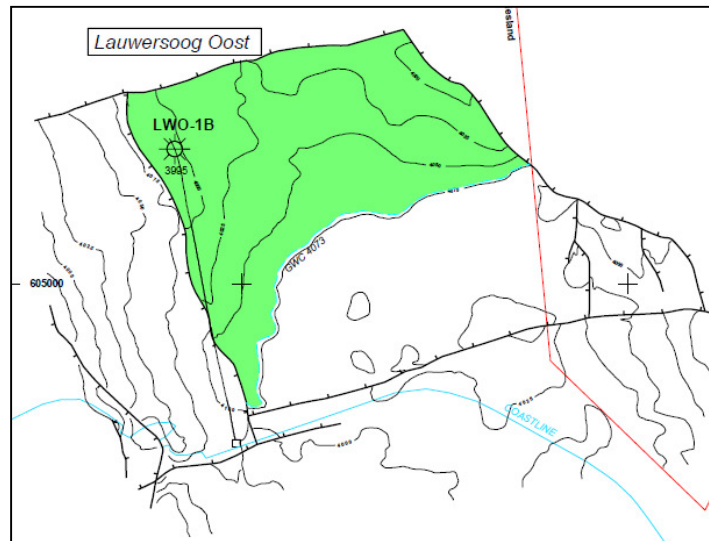
*Figure 24 Lauwersoog-East ARPR top ROSL map*
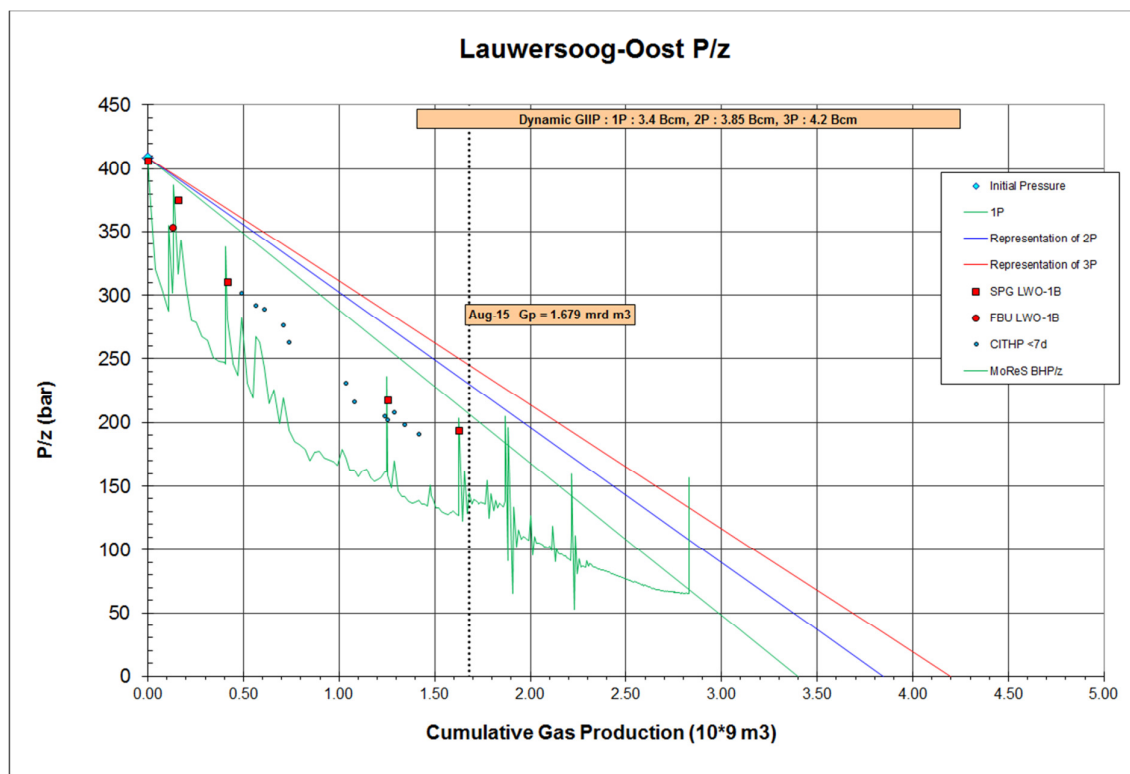


*Figure 25 P/z plot for LWO-1B*

### 5.1.4.1  **Reservoir model**

The material balance for Lauwersoog-East indicates that not the entire static volumes are seen. However, dynamic 3D simulation volumes are in line with static volumes since no GBV multiplier was needed to match the data (Table 13). Permeability for this field is not infinite and considering the lateral extent of the field, with only one producer, it is believed that an amount of gas on the eastern flank of the structure is effectively not being drained. Model permeability is in line with static properties. The sensitivity on vertical permeability to the history match indicates that the permeability contrasts are important.

A PLT was done in 1997 (Figure 26), which indicated that the top layers contribute most to the flow. In order to obtain a match in the model, the permeability of the top 14 layers is increased by a factor 5 with respect to the other layers. This is most likely due to a number of high permeable streaks that have not been fully captured. The PLT was repeated in 2014, showing that vertical flow distribution of the model is still reasonably in line with measurements. The portion of production from the lower units is increasing over time, pointing towards differential depletion between the top and bottom units.
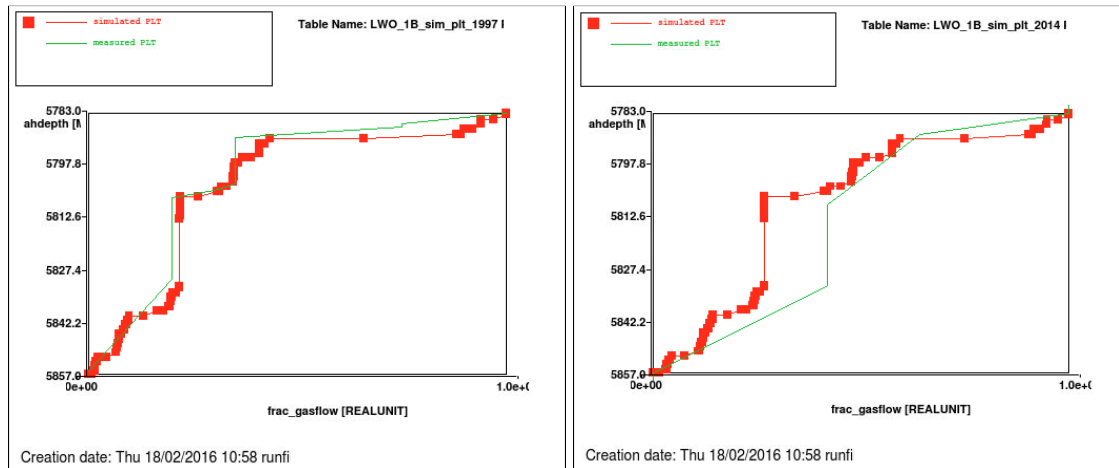


*Figure 26 Simulated (red line + squares) and measured (green line) PLT in LWO-1B. Left: 1997, pre-production. Right: 2014.Base case realisation.*

The static model was recreated in 2015, during the maturation of the Lauwersoog East infill project. Although properties were updated, the resulting model was marginally different from previous models. Therefore, similar history matches could be created. As part of the update, the popups due east of the field were excluded. Last year it was evident that, even with fully open faults and a mobile aquifer, the pressure decline was negligible.

The model was matched on FTHP and SPG data as can be seen in Figure 28 & Figure 27.
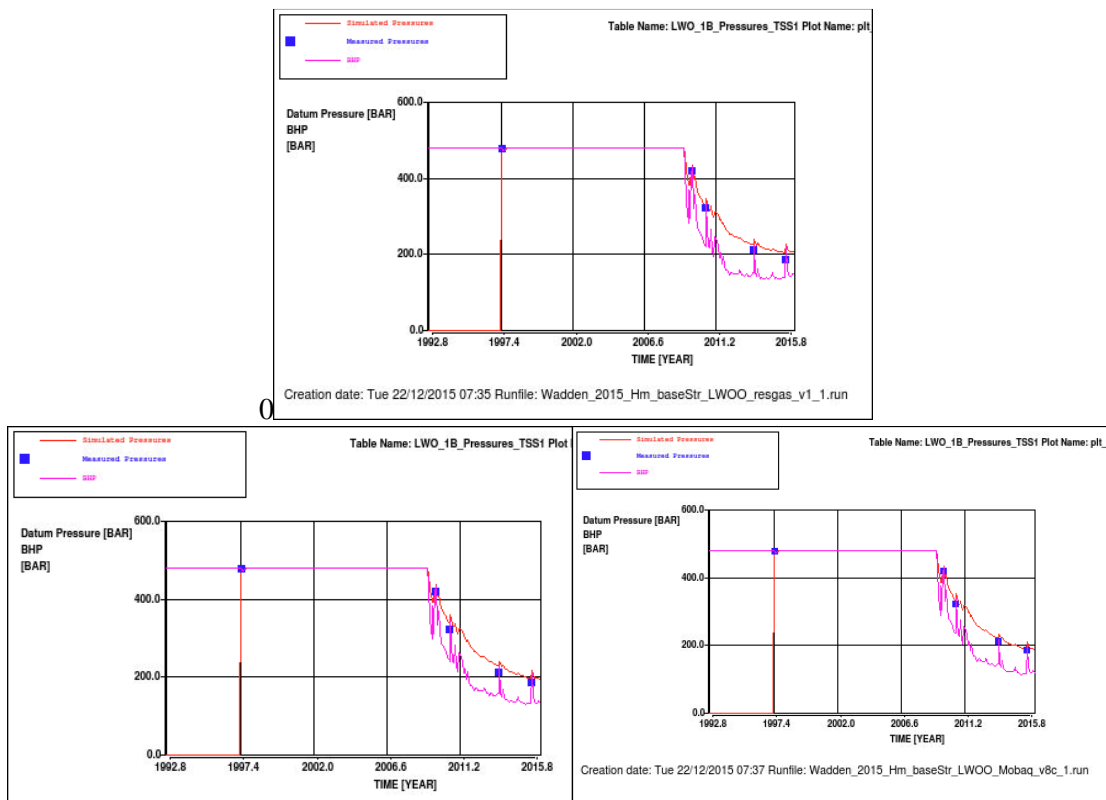
*Figure 27 Simulated reservoir pressure (red line), flowing bottom hole pressure (violet line) and measured (blue squares) downhole pressure data in LWO-1B. Top: base case. Left: low case. Right: high case.*
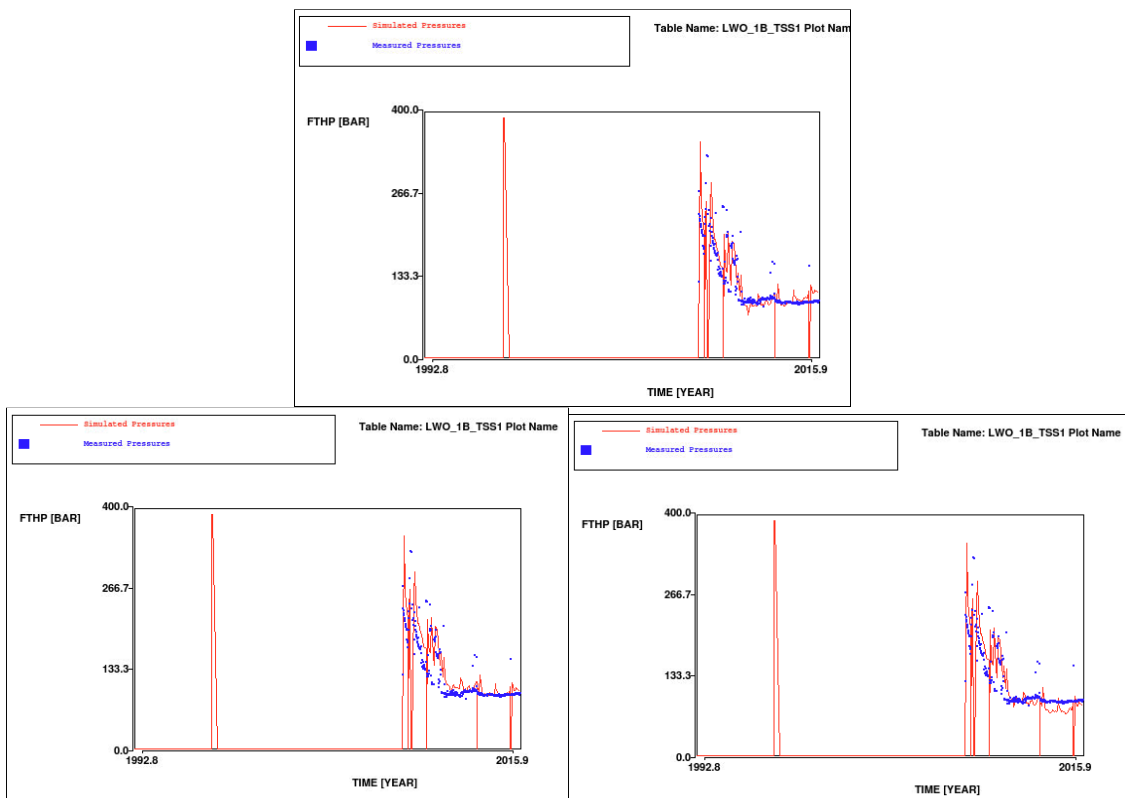


*Figure 28 Simulated (red line) and measured (blue squares) flowing tubing head pressures in LWO-1B. Top: base case. Left: low case. Right: high case.*

Table 13 shows the parameters used for M&R2015 models. Since the (new) model was modelled first with residual gas in the aquifer (base case), the other two cases have been based on this model. Very little needed to be done the models to keep the fit with dynamic data. For the low case, kv was increased to counteract some missing pressure support from the (residual gas in the) aquifer. For the high case, the residual gas saturation was slightly lowered to counteract water encroachment that is not seen in the well. This field is a textbook example of a large uncertainty in aquifer pressure, where its behaviour cannot be deduced from measurements around the well.

*Table 13 History matching parameters used for the Meet & Regel cycle for Lauwersoog East.*

| Parameter | Static | **Low M&R2015**[13] | **Base M&R2015**[13] | **High M&R2015**[13] | Immob. M&R 2014[14] | Mob M&R2014[14] |
|---|---|---|---|---|---|---|
| Residual gas sat. below FWL | 0.20 | **0** | **0.23** | **0** | 0 | 0 |
| GBV multiplier | 1.0 | **1.0** | **1.0** | **1.0** | 0.96 | 0.98 |
| $k_h$ multiplier low perms | 1 | **1.4** | **1.4** | **1.4** | 0.32 | 0.45 |
| $k_h$ multiplier high perms | 1 | **4.0** | **4.0** | **4.0** | ? | ? |
| $k_v$ multiplier | N/A | **0.10** | **0.010** | **0.010** | 0.67 | $1.7\ 10^{-4}$ |
| FWL (m TVNAP) | 4073 | **4073** | **4073** | **4073** | 4078 | 4078 |
| $k_h$ multiplier aquifer | N/A | **$1.0\ 10^{-4}$** | **0.1** | **1.0** | $1\ 10^{-4}$ | 1 |
| $k_v$ multiplier aquifer | N/A | **$1.0\ 10^{-4}$** | **0.1** | **1.0** | $1\ 10^{-4}$ | 1 |
| Residual gas | 0.3 | **0.25** | **0.25** | **0.20** | 0.44 | 0.4 |
| $k_w@S_{rg}$ | 0.1 | **0.1** | **0.1** | **0.1** | 0.1 | 0.02 |

### 5.1.4.2  **Meet & Regel cycle 2014 vs 2015 model comparison**

As described in the previous subsection, three new realisations were made due to the static model update. One difference is that no extremely low $k_v$ was needed to match the models. This does however remain an uncertainty to this field. Also the kw end point is now the base value for all realisations. The FWL has been set to its base value as opposed to 5 metres deeper last year.

### 5.1.4.3  **Water production**

The well LWO-1B has been in production since 2008. The well has not been shut-in on its own and therefore water-gas-ratios determined from WaCo tank level changes are not very accurate (Figure 29) and hence are not matched upon. The model does not expect water breakthrough here yet, but depending on the aquifer behaviour, this might occur in the future.

---

[13] Input deck: Wadden_2015_LWOO_MRN_v2.INP
[14] Input deck: Wadden_2015_LWOO_MRN_v1.inp.
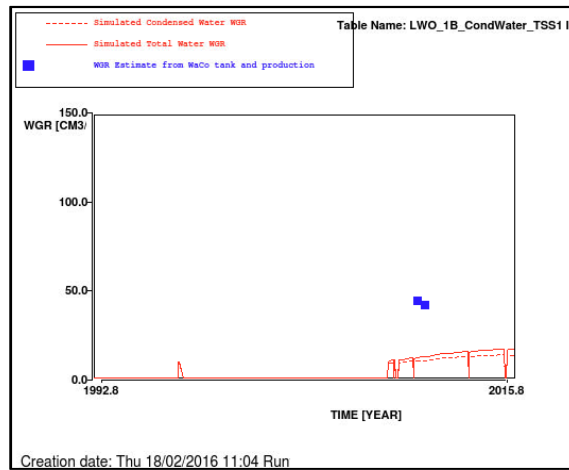
*Figure 29 Simulated total WGR (red solid line), simulated condensed WGR (red dashed line) and estimated WGR from production and WaCo tank observations (blue squares) for LWO-1. Left: Immobile aquifer. Right: Mobile aquifer.*

### 5.1.5  Lauwersoog West

The Rotliegend (ROSLU) Lauwersoog-West field was discovered by the well LWO-3 in 1998, drilled from the Lauwersoog location. It found virgin pressures at 484 bara. It is situated in the Eastern part of the Noord Friesland Concession. The field is bounded to the West and East by the Lauwersoog-C and Lauwersoog-Oost gas fields respectively.

The LWO-3 well was perforated in the Upper Slochteren zones and brought on-stream in November 2008, and is evacuated to the Anjum facilities. Its P/z plot can be found in Figure 31.

An RFT was taken for this field and showed a 2 bar pressure difference between the gradient of the top unit and the gradient of the units below. No nearby fields were in production at that time and a (lengthy) production test of LWO-1B (investigated during Lauwersoog East infill work) is assumed not to have been able to cause this depletion. Hence the ROSLU2 shale has a good chance of being fully sealing. The FWL could not be accurately determined because it is located in the Ameland shale layer, but based on saturation and spill point it was estimated at 4055 m TVNAP. With the ROSLU1 having a different pressure gradient, its FWL may well be slightly different.
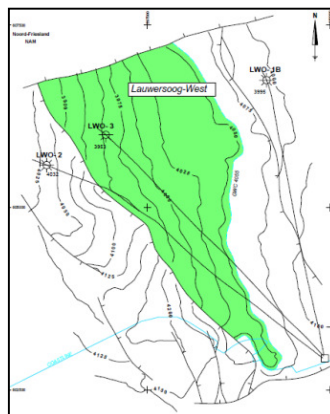


*Figure 30 Lauwersoog-West ARPR top ROSL map*
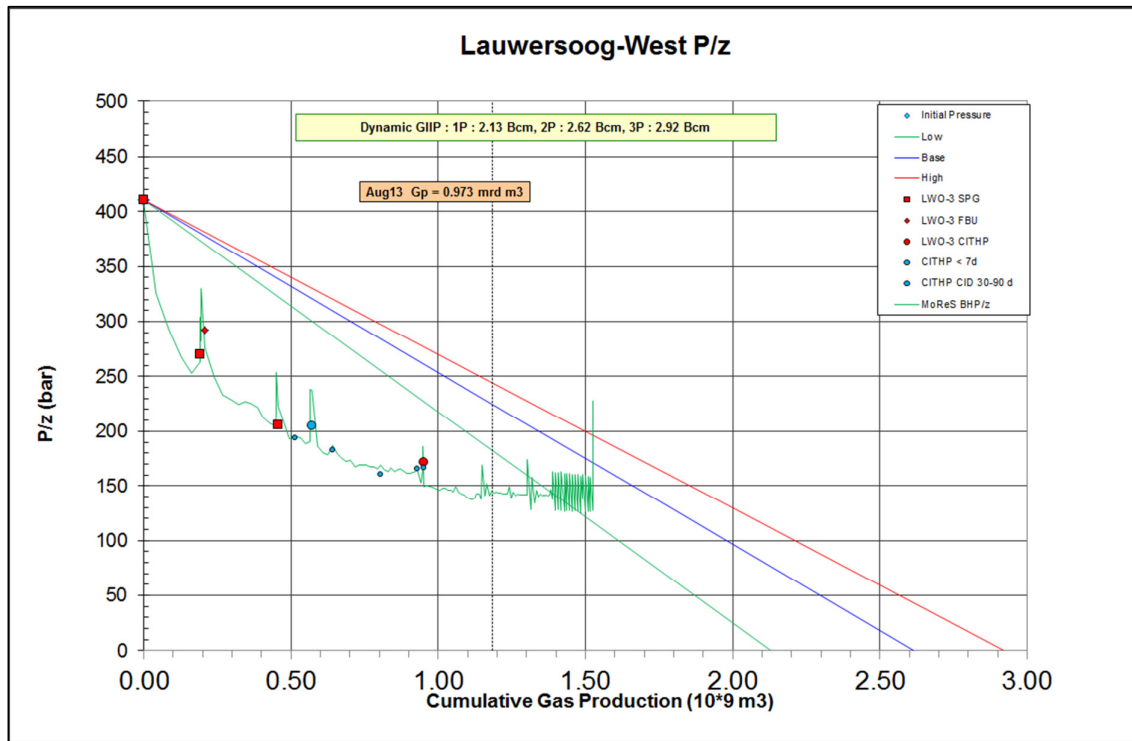
*Figure 31 P/z plot LWO-3*

### 5.1.5.1  **Reservoir model**

Even though the RFT shows two bar pressure differential, this has not been taken into account in initialization. The field has been initialized on a single pressure and FWL as is shown in Figure 32.
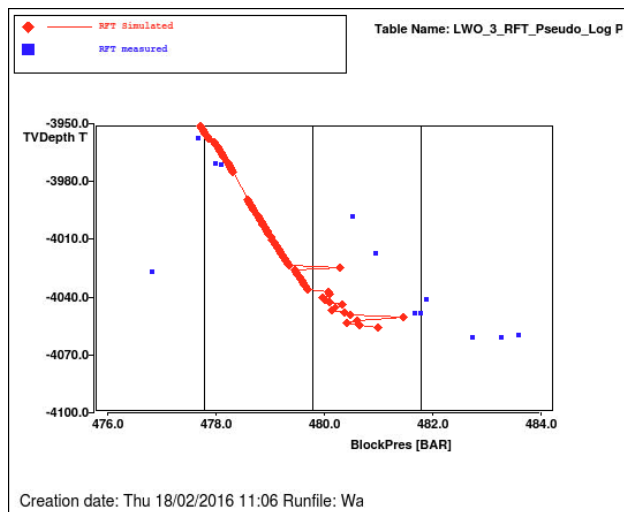


*Figure 32 Simulated (red line and squares) and measured RFT pressure data (blue squares) for LWO-3.*

The permeability contrast has been captured with a PLT, which has been well matched as can be seen in Figure 33.
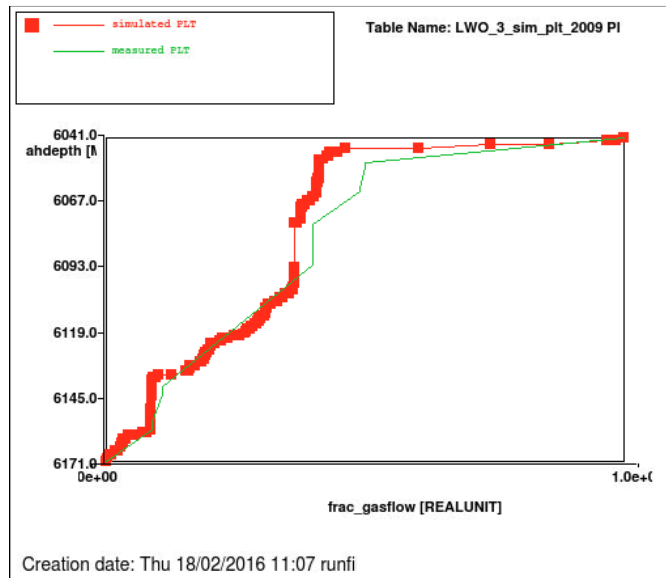
*Figure 33 Simulated (red line + squares) and measured (green line) PLT in LWO-3. Base case realisation.*

For the Lauwersoog-Central –East and –West field, as described in Section 3.3.1, the shutins are modelled to the nearest day, and therefore BHP is used for history matching.
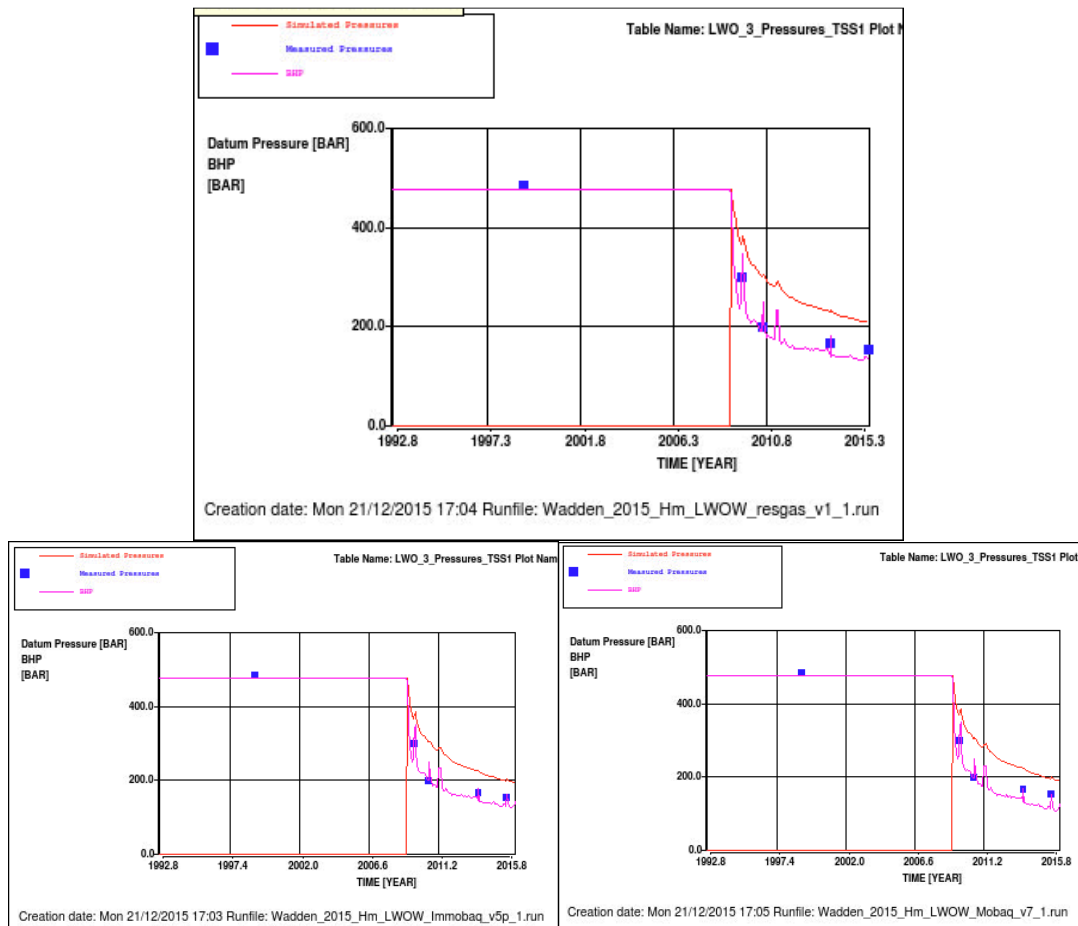


*Figure 34 Simulated reservoir pressure (red line), flowing bottom hole pressure (violet line) and measured (blue squares) downhole pressure data in LWO-3. Top: Base case Left: low case. Right: high case.*

A north-south fault that is somewhat visible on seismic is included east of LWO-3 to give the model extra flexibility in mimicking slow gas behaviour (Figure 35). North-South faults are abundant in the area and have proven to be sealing or baffling in some cases. However, for M&R2015 it was decided to ignore any baffling potention of this fault, since this could underestimate pressure drop and hence subsidence behind the fault.
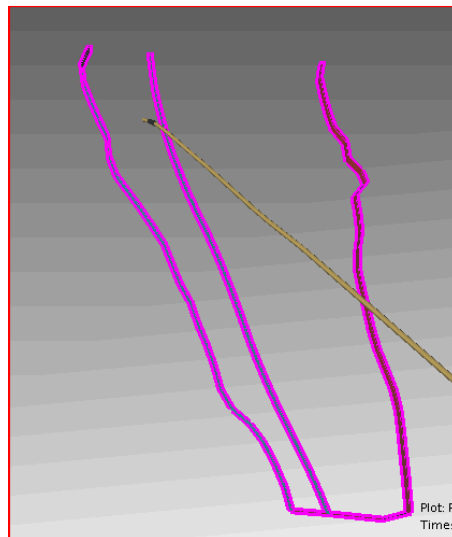
*Figure 35 Faults in the MoReS simulation model.*
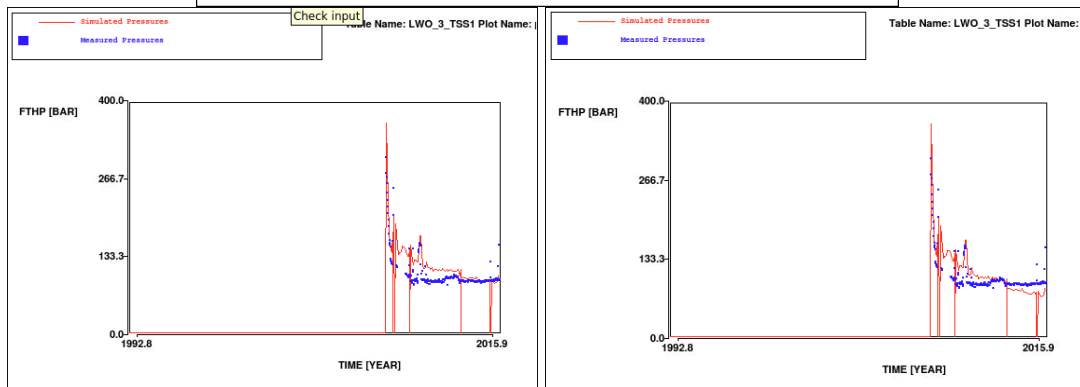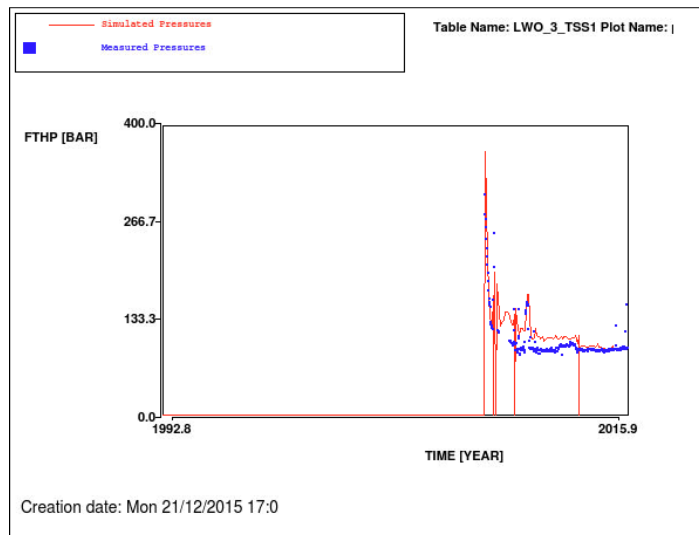


*Figure 36 Simulated (red line) and measured (blue squares) flowing tubing head pressures in LWO-3. Top: base case. Left: low case. Right: high case.*

Figure 36 shows the THP match with the well. Although the match is not bad, the response indicates that slightly more late pressure support exists than modelled for all three cases. This might indicate that some intra-field (fault) baffling might be taking place. However, with (the sealingness) of this fault not proved, it chosen to be slightly conservative and assume full connectivity.

For Lauwersoog-West, the main uncertainties are the existence of vertical pressure differentials, depletion of the water bearing layers, the FWL and (slow gas) volumes.

The parameters that are used for matching are shown in Table 14 below. In the Lauwersoog area there is quite some uncertainty around the FWL. But since the mobility of the aquifer is the dominant uncertainty for subsidence, the uncertainty of the free water level is not considered an issue and is kept constant. To model vertical pressure differentials, it is chosen to distinguish between low (<1mD) and high (>1mD) permeability zones when applying permeability multipliers. This is a key ingredient to the slow gas behaviour seen in this well.

*Table 14 History matching parameters used for the Meet & Regel cycle for Lauwersoog West*

| Parameter | Static | Low M&R2015[15] | Base M&R2015[15] | High M&R2015[15] | Immob Base M&R2014[16] | Mob Base M&R2014[16] |
|---|---|---|---|---|---|---|
| Residual gas sat, below FWL | 0.21 | **0** | **0.21** | **0** | 0 | 0 |
| GBV multiplier[17] | 1 | **1** | **1** | **1** | 1.52 / 0.34 | 1.52 / 0.34 |
| $k_h$ multiplier, high k zones | 1 | **0.28** | **0.28** | **0.28** | 0.45 | 0.45 |
| $k_h$ multiplier, low k zones | 1 | **0.035** | **0.035** | **0.035** | 0.060 | 0.060 |
| $k_v$ multiplier | N/A | **$3.4\ 10^{-3}$** | **$3.4\ 10^{-3}$** | **$3.4\ 10^{-3}$** | $3.4\ 10^{-3}$ | $3.4\ 10^{-3}$ |
| N-S fault | N/A | **1** | **1** | **1** | $3.0\ 10^{-3}$ | $3.0\ 10^{-3}$ |
| GWC (m TVNAP) | 4055 | **4055** | **4055** | **4055** | 4035 | 4035 |
| $k_h$ multiplier aquifer | N/A | **$1\ 10^{-4}$** | **0.32** | **1** | $5.9\ 10^{-3}$ | 1 |
| $k_v$ multiplier aquifer | N/A | **$1\ 10^{-4}$** | **0.32** | **1** | $3.4\ 10^{-5}$ | 1 |
| Residual gas | 0.3 | **0.25** | **0.25** | **0.25** | 0.25 | 0.25 |
| $k_w@S_{rg}$ | 0.1 | **0.1** | **0.1** | **0.1** | 0.1 | 0.1 |

This field is a clear example of the aquifer having little impact on the pressure response at the well, but a large impact on average reservoir pressure. Only aquifer properties have been varied between the three cases, but the impact is large as will become apparent in Section 5.2.2.

### 5.1.5.2   **Meet & Regel cycle 2014 vs 2015 model comparison**
During M&R2014, it was already recommended that this model needed a some reinvestigation. This has indeed been done and it resulted in modifications of the models of M&R2014. The main difference, is the transmissibility of the intra-field fault. By equalling this to 1, it has resulted in a much more gradual pressure gradient, instead of a discontinuous pressure drop. The latter was an unwanted situation, since especially for the high case a pressure drop in the entire field should be as high as realistically possible. Hence without a fault baffle that elevates all pressures behind it (if the dynamic data allows this).

---

[15] Input deck: Wadden_2015_LWOW_MRN_v4.INP
[16] Input deck: Wadden_2015_LWOW_MRN_v2.inp.
[17] In M&R2014, a disctinction was made between GBV for high and low permeability zones.

Second of all, the FWL has been moved to the base case value of 4055 mTVNAP. With the aquifer mobility being the dominant uncertainty, it was not needed to vary FWL as well.

And lastly, a distinction was mad between GBV multipliers of high (>1mD) and low (<1mD) zones. The values of these parameters wer deemed too far from reality. With the uncertainty space being so large, an attempt was made to stick with a GBV of 1. Acceptable matches were possible without modifying this number.

### 5.1.5.3   Water production

LWO-3 has been producing since 2008. No specific stops were done on the well that allow for a reliable water-gas-ratio from the WaCo tank levels as can be seen in Figure 37. With the lowering of the FWL in this year's model, formation water production is marginal. There are currently no indications of excessive water production from this well, although with the structure dipping into the water, there is always a risk of future water breakthrough.
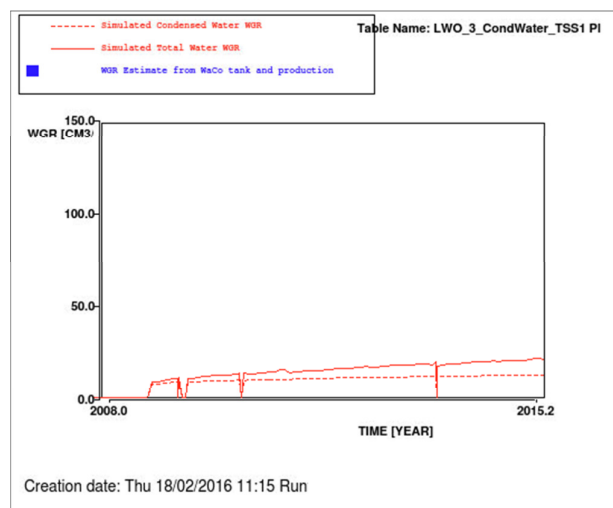


*Figure 37 Simulated total WGR (red solid line), simulated condensed WGR (red dashed line) and estimated WGR from production and WaCo tank observations (blue squares) for LWO-3. Base case realisation.*

## 5.1.6  Metslawier

The Metslawier field (Figure 38) is located in the central onshore part of the Noord Friesland Concession (Lauwerszee Trough, NE-Netherlands), adjacent to the Hantum fault zone. It was discovered in 1994 by ANJ-2, drilled from the Anjum surface location into a crestal position. The field started production in 1997 through the Anjum facilities. Its P/z plot can be found in Figure 39.

The Rotliegend formation in the Metslawier field consists of the Ten Boer Claystone Member (ROCLT), the Upper Slochteren Sandstone Member (ROSLU), the Ameland Claystone Member (ROCLA) and the Lower Slochteren Sandstone Member (ROSLL). Only the ROSLU was evaluated as being gas bearing. It consists of aeolian and fluvial/pond sediments deposited in a desert environment. The thickness of the ROSLU in ANJ-2 is 111 m, of which approximately 88 m TV (gross) is gas bearing.

The ANJ-2C well has been sidetracked 3 times due to lost drill strings that could not be fished. The well was production tested in 1994, but suspended awaiting a workover with Cr-13 tubing. The workover was done in 1997, but during the workover, the original perforations from 1994 were seriously damaged. This is observed in PLT in 1999, which lead to

reperforation of the initial perforations in 1999. The well was taken into production in 1997. In water samples in 2005, it was found that formation water was being produced. In 2006, the well was produced with foam and in 2009 the well died at 350 000 Nm3/d, well above its liquid loading rate for condensed water. Several activities have been done in order to restore the well; the well was perforated in unit 2 in 2011, which had not been perforated before. This did not restore the well (even after nitrogen lifting).
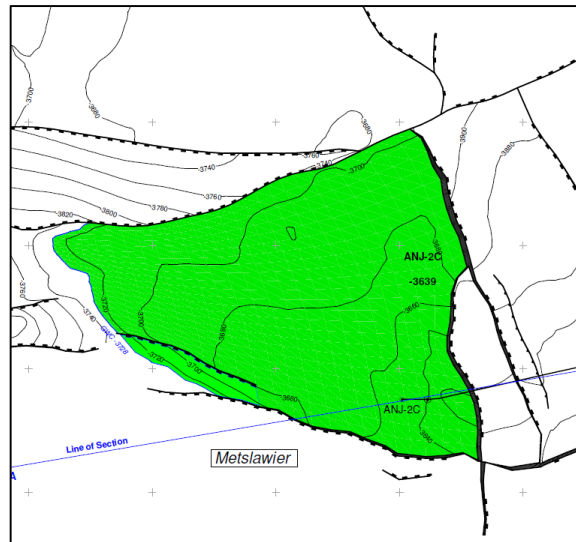


*Figure 38 Metslawier ARPR top ROSL map*
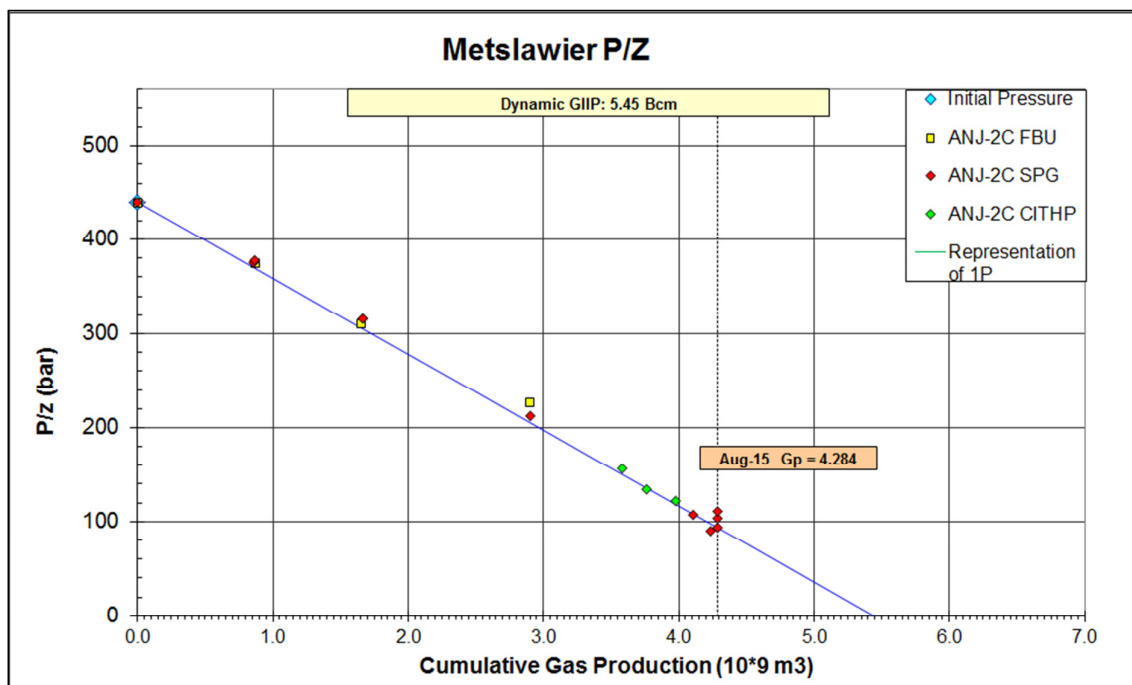


*Figure 39 P/z plot for ANJ-2C.*

The reservoir pressure measured in downhole pressure measurements has been steadily increasing since 2007, as well as the liquid level in the well. In is believed that formation water has been flowing in from the lower perforations and cross-flowing into the upper layers, creating a water-invaded zone around the well that causes the well not to be able to produce anymore. In a gamma-ray log done in 2012, salt scaling was identified over the

perforations that supports the hypothesis of crossflow. Activities to restore well production were not successful and end 2012 it was decided to stop these activities. The project to drill a sidetrack was too risky and was cancelled.

Also in 2015, an attempt was made to reopen the well. A plug was set in the ROSLU2 (shale). The well produced briefly into test equipment (surface pressure 3 bara), but flow did not sustain. The WGR observed was ~1000 m3 per mln Nm3 – a factor 3 lower than before setting the plug. Also this observation supports the hypothesis described in the previous paragraph.

### 5.1.6.1 **Reservoir model**

The Metslawier field has been studied in the previous years in detail for the maturation of the mentioned sidetrack of ANJ-2. The field has been matched in the previous Wadden model of 2010 and reproduced in the current model. In order to reproduce the model, the permeability in unit 1 (see Figure 44), was increased by a factor 2 (1994 perforations in unit 1) – 30 (1997 perforations in unit 1). This was done in order to model the high permeable layers that were included in the previous model and in line with PLT (Figure 40 and Figure 41) and FBU data (Table 15). These high permeable streaks in unit 1 are also observed in MGT-2 PLT, LWO-3 PLT (Figure 33) and ANJ-1 PLT (Figure 11).

| Perforation | Perforated | kh model | Modified | FBU 24/11/1994 | FBU 3/8/1999 | FBU 21/8/2000 | FBU 9/8/2002 |
|---|---|---|---|---|---|---|---|
| | | mD m | mD m | mD m | mD m | mD m | mD m |
| P1 | 1997 | 3 | 90 | | 600 | 1152 | 1152 |
| P2 | 1997 | 14 | 420 | | | | |
| P3 | 1994/1999 | 135 | 270 | 578 | | | |
| P4 | 2011 | 870 | 128 | | | | |
| P5 | 1994/1999 | 1511 | 220 | | | | |
| P6 | 1997 | 28 | | | | | |
| P7 | 1999 | 11 | | | | | |
| P8 | 1999 | 32 | | | | | |

*Table 15 Permeability thickness and modifications compared to permeability thickness obtained from FBU data. Black squares indicate that these zones did not participate in the kh of the FBU.*
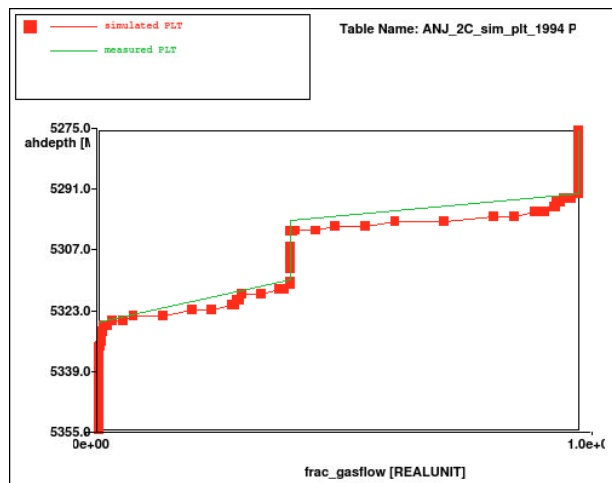


*Figure 40 Simulated (red line + squares) and measured (green line) PLT in ANJ-2C with original perforations in 1994. Base case realisation.*

The second PLT in 1999 (Figure 41) could only be matched if the original perforations from 1994 were closed, indicating that the original perforations were indeed damaged during the workover as was stated, although the match is still not ideal.
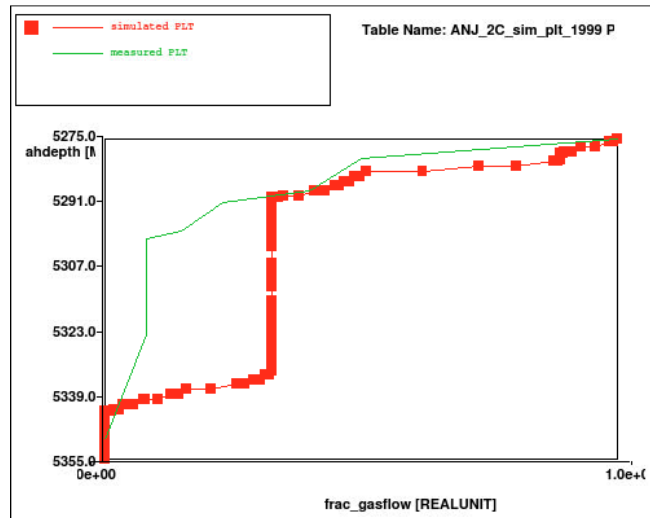


*Figure 41 Simulated (red line + squares) and measured (green line) PLT in ANJ-2C in 1999 with original perforations from 1994 closed and new perforations from 1997 added. Base case realisation.*

On top of these modifications, high permeable layers in the bottom units were modelled as 1m thick and were therefore reduced in magnitude by a factor 10 as is indicated in Table 15. This is well in line with the historical well performance as is shown in Figure 42. The permeability modifications seem to represent the historical well production well.
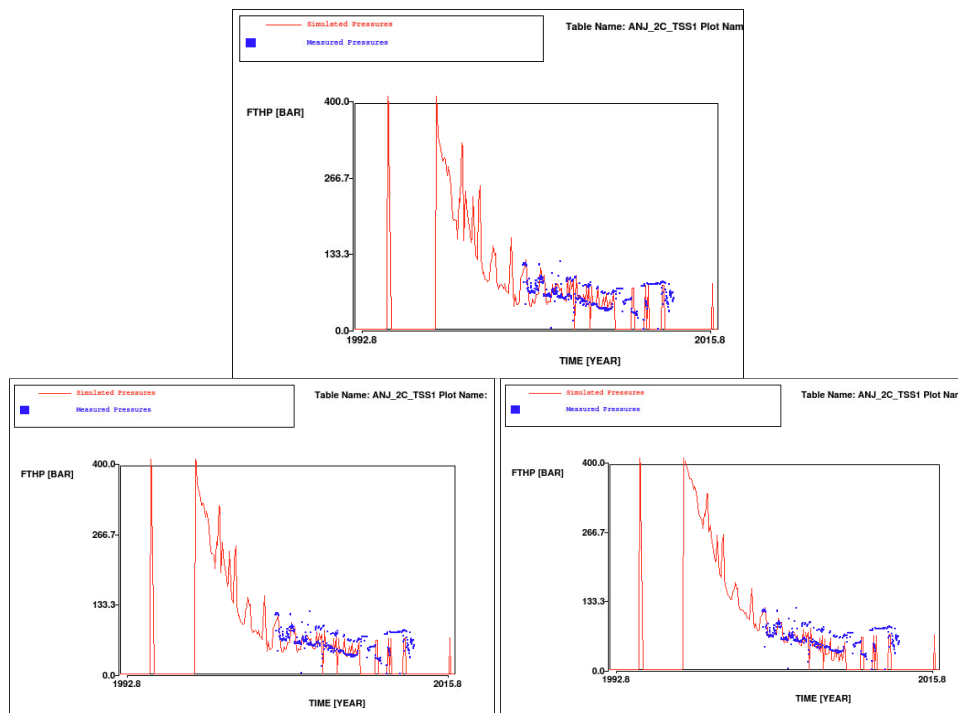


*Figure 42 Simulated (red line) and measured (blue squares) flowing tubing head pressures in ANJ-2C. Top: base case. Left: low case. Right: high case.*

The downhole pressure match is shown in Figure 43. The cause of the pressure build-up in the recent years is believed to be the aquifer influx.
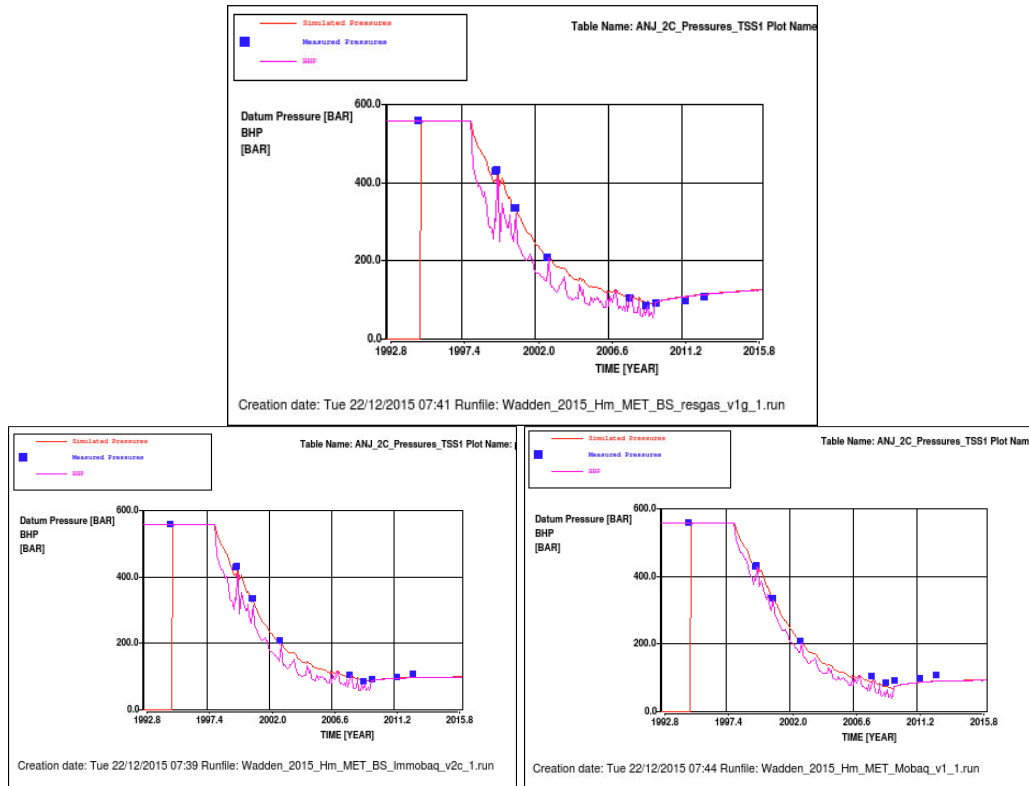
*Figure 43 Simulated reservoir pressure (red line) and measured (blue squares) downhole pressure data in ANJ-2C. Top: base case. Left: low case. Right: high case.*

Like Anjum, Metslawier is a mature field that can be used for calibrating compaction coefficients. Little depletion of the aquifer results in higher compaction coefficients and vice versa. Core measurements suggest high compaction coefficients for this area. To match with subsidence measurements, aquifer depletion is expected to be limited. This residual gas below FWL reservoir realisation supports this subsidence model, where aquifer depletion is hampered by gas in the water leg.

The parameters used for history matching for field development and for the M&R cycle are shown in Table 16. The base case (residual gas below FWL) model has been based on the immobile aquifer model, with a modified aquifer. This model makes water influx more natural, since the aquifer expands more when depletion. Where an immobile aquifer requires a relatively high water relative permeability end-point (0.2), the base case value can be used (0.1) when assuming gas below FWL.

*Table 16 History matching parameters used for the Meet & Regel cycle for Metslawier.*

| Parameter | Static | Low M&R2015[18] | Base M&R2015[18] | High M&R2015[18] | Immob M&R2014[19] | Mob M&R2014[20] |
|---|---|---|---|---|---|---|
| Residual gas below FWL | 0.09 | **0** | **0.08** | **0** | | |
| GBV multiplier | 1 | **1.07** | **1.07** | **1.00** | 1.07 | 1.00 |
| $k_h$ multiplier | 1 | **0.85** | **0.85** | **1.0** | 0.85 | 1 |
| $k_v$ multiplier | N/A | **$8.5\ 10^{-3}$** | **$8.5\ 10^{-3}$** | **0.010** | $8.5\ 10^{-3}$ | 0.010 |
| GWC (m TVNAP) | 3728 | **3728** | **3728** | **3728** | 3728 | 3728 |
| $k_h$ multiplier aquifer | N/A | **$1\ 10^{-4}$** | **0.10** | **1** | 0.001 | 1 |
| $k_v$ multiplier aquifer | N/A | **$1\ 10^{-4}$** | **0.10** | **1** | 0.001 | 1 |
| Residual gas | 0.3 | **0.30** | **0.20** | **0.25** | 0.3 | 0.25 |
| $k_w@S_{rg}$ | 0.1 | **0.20** | **0.10** | **0.1** | 0.2 | 0.1 |

### 5.1.6.2   **Meet & Regel cycle 2014 vs 2015 model comparison**

A minor change was implemented to the immobile aquifer model (low case), where the aquifer permeability was decreased by an order of magnitude ($10^{-3}$ to $10^{-4}$) to align with the other low case aquifer models. It has negligible difference to the match with well data.

The high structure model, in last year's documentation already described as unrealistic, has been discarded.

### 5.1.6.3   **Water production**

The well ANJ-2C has observed water breakthrough. This is seen in the salinity of water samples in 2005, the foam lifting required since 2006, the liquid rise in the well bore and the salt scaling over the perforations (Figure 44). Water movement was extensively modelled in 2013 and 2014 and was concluded to be encroaching from the west, where the structure dips into the water. The water is thought to have entered the well via high permeable streaks (Figure 45) and subsequently have cross-flowed into the top reservoir units (Figure 46).

---

[18] Input deck: Wadden_2015_MET_MRN_v3
[19] Input deck: Wadden_2015_MET_MRN_v2
[20] Input deck: Wadden_2015_MET_MRN_v1
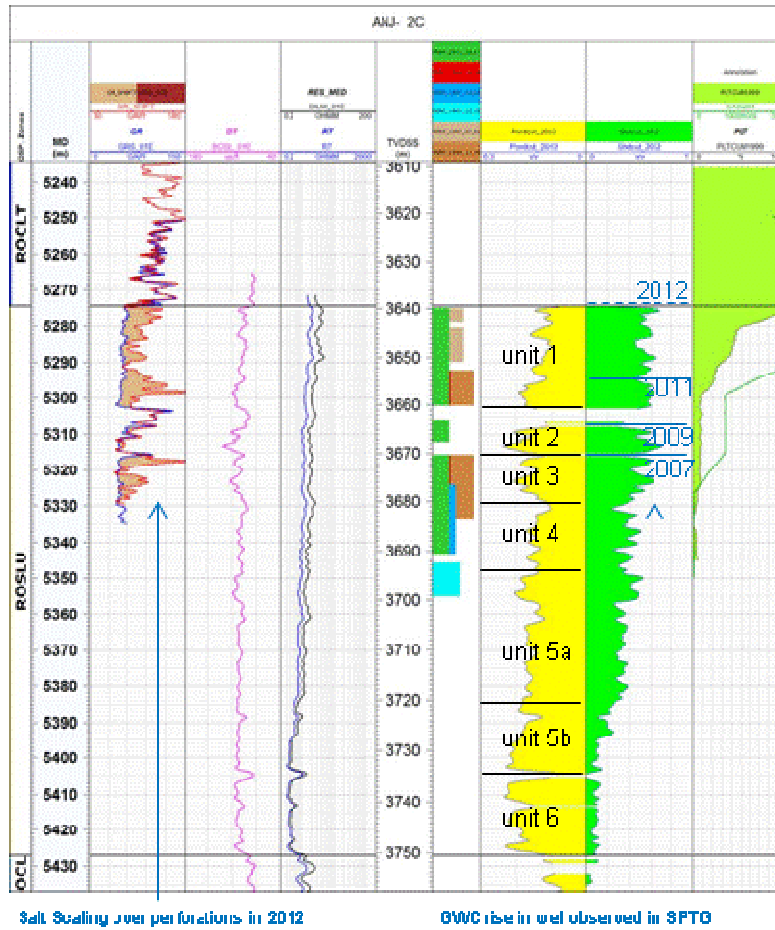
Figure 44 Log of ANJ-2C showing the salt scaling with the gamma ray log in the left panel and the liquid rise from SPTG in the right panel.

| Date | Density (kg/L) | Cl (mg/L) |
|---|---|---|
| 11/07/2005 | 1.18 | 161000 |
| 12/07/2005 | 1.17 | 149000 |
| 13/07/2005 | 1.15 | 131000 |
| 14/07/2005 | 1.14 | 126000 |

Table 17 Water sample data from ANJ-2C in 2005
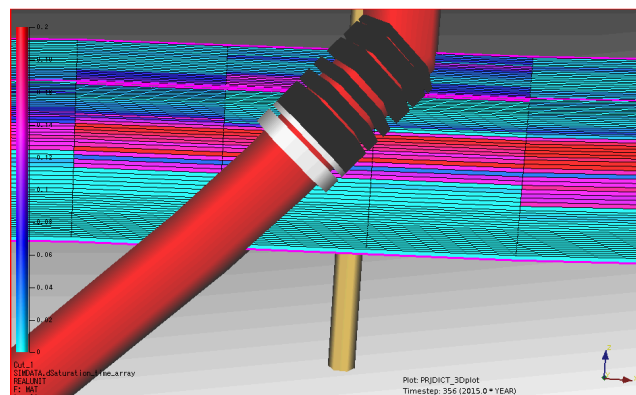


Figure 45 Cross section of the water saturation change around ANJ-2C with in red the water entering via high permeable streaks and cross flowing at the top (blue is no change in saturation).
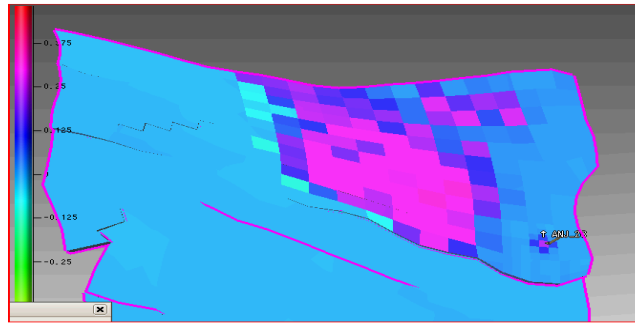
*Figure 46 Water saturation change in unit 1, with in red the water encroaching from the west (blue is no change in saturation), and around the well the cross-flow.*

Based on this model, the limited water production data has been matched (Figure 47). This seems to be in line with the estimated WGR from WaCo tank level observations.
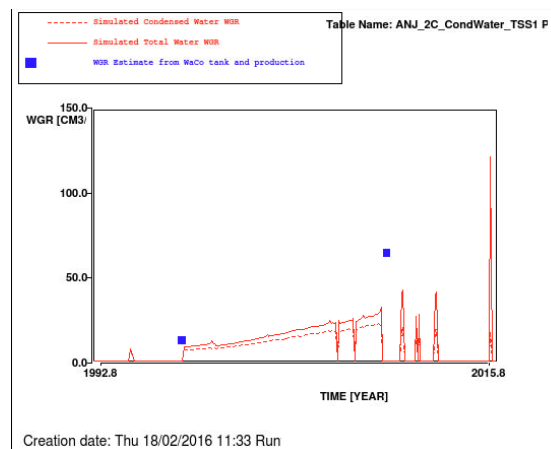


*Figure 47 Simulated total WGR (red solid line), simulated condensed WGR (red dashed line) and estimated WGR from production and WaCo tank observations (blue squares) for ANJ-2C*

### 5.1.7  Moddergat

The Moddergat field (Figure 48)  is located in the eastern Waddenzee section of the Noord Friesland Concession (NE-Netherlands). It was discovered by the well MGT-1B in 1995 and found virgin pressures at 567 bar, which is significantly overpressured (datum level equals 3860mTVDNAP). Wet gas is evacuated to the Anjum plant facilities as of February 2007. Its P/z plot is shown in Figure 49.

The Moddergat field is contained in the Upper Slochteren Sandstone Member (ROSLU) of the Rotliegend Formation. It consists of aeolian and fluvial/lacustrine sediments deposited in a desert environment. The thickness of the ROSLU in MGT-1 is 108 m, of which approximately 78 mTV (gross) is gas bearing. The Moddergat gas field is mainly a fault closed structure at Base Zechstein (Rotliegend) level.

Seismic indicates a fault in the E-W direction that separates the field in a northern and a southern part. The single well only sees the northern section. It is difficult to judge whether this fault is (partly) sealing. The small fault block, named Nes North, is likely in communication with the field and is included in the modelling.
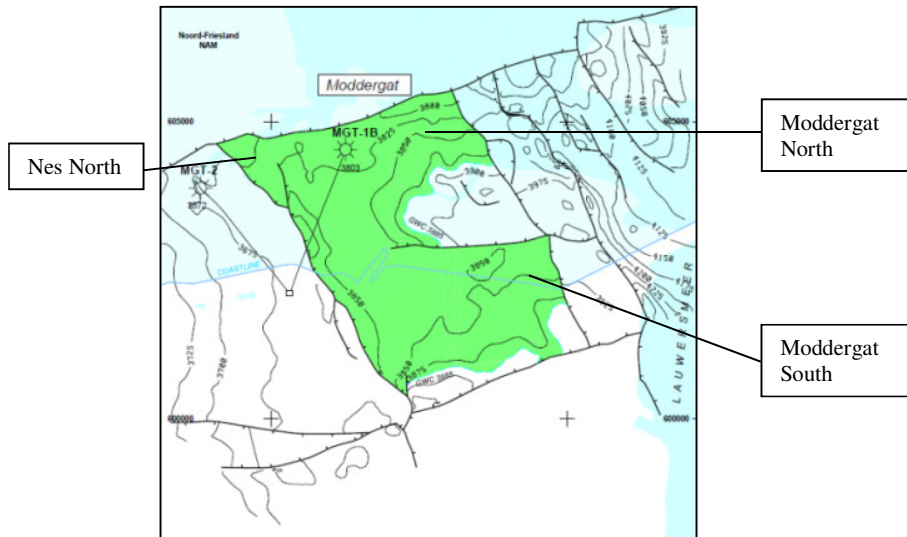
*Figure 48 Moddergat ARPR top ROSL map*
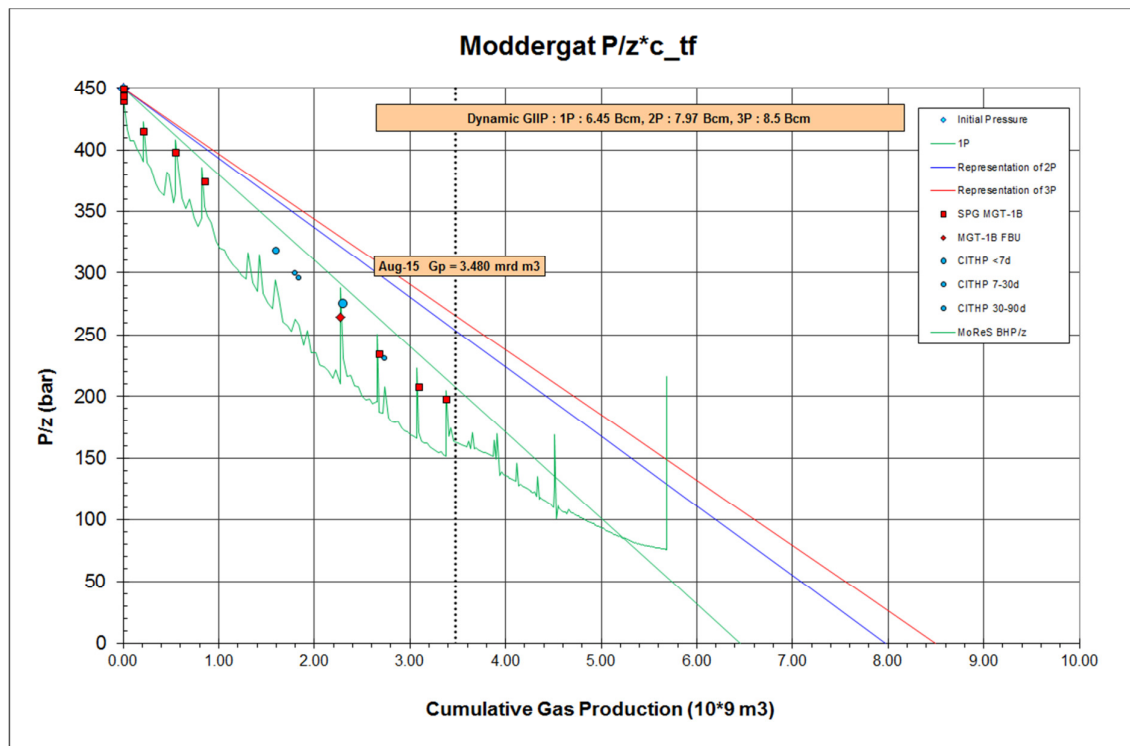


*Figure 49 P/z plot for MGT-1B.*
*Due to its high initial pressures, P/z has been corrected for rock compressibility ($c_{tf}$).*

### 5.1.7.1   **Reservoir model**

This field was extensively modelled in 2015, in preparation of a potential infill well targeting the southern block of the field. A critical look at the permeability model, backed by core data from MGT-1B, suggested that connectivity throughout the field is probably poorer than previously thought. It hence seems likely that, irrespective of fault sealing behaviour, pressures in the southern half of the field are lagging the reservoir pressure around MGT-1B (see Figure 50).
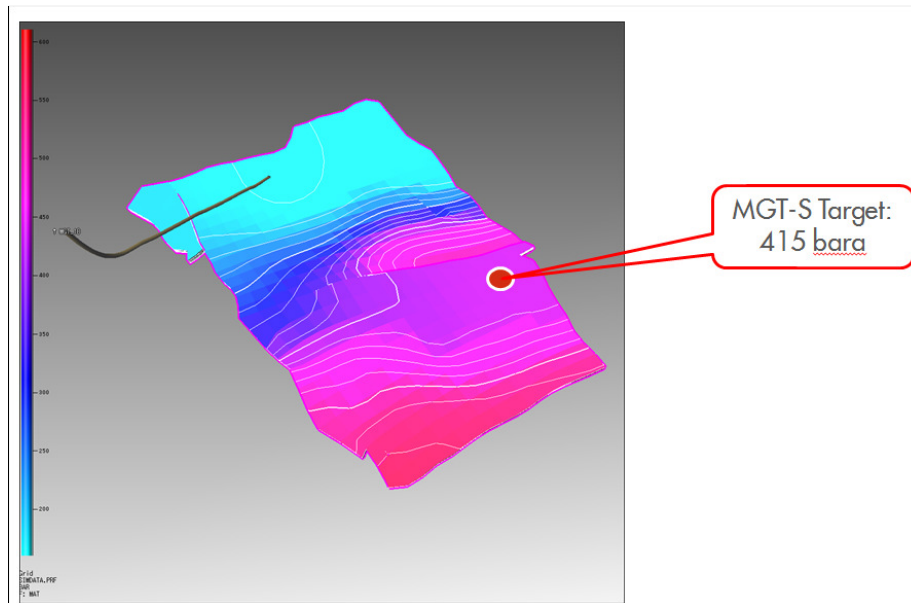
*Figure 50 Base case pressure profile in the Moddergat field in 2015.*

The history match on downhole pressure is shown in Figure 51 and the flowing THP match is shown in Figure 52. Although the matches are good, history matching has proved a challenge. The two-phase model predicts water encroachment to MGT-1B, impacting relative permeability and hence expecting that lower FTHPs are needed to fit production rates. Currently this is overcome with a very low $k_{rw}$ end point (not outside the $k_{rw}$ uncertainty range described in Section 4.1.3, but on the low end).

Furthermore, modelling has revealed that, with the given static model, some extra pressure support must exist to fit the base case GIIP with dynamic data. Residual gas below FWL can actually give this pressure support and this is precisely what happened in the base case model.

Alternatively, the model can be matched with a much higher GIIP and with a radiating southern half the field through a baffling fault. But to follow the base case GIIP as much as possible, and to avoid underestimating subsidence due south of the east-west intra-field fault and pressure drop in general, the former option with a base case GIIP was preferred for the base case subsidence match (Table 18). For the low and high case subsidence models, where residual gas below FWL is absent, this higher GIIP and baffling fault combination *has* been used.

The initial PLT was well matched indicating that the modelled permeability contrasts are in line with the well performance (Figure 53).
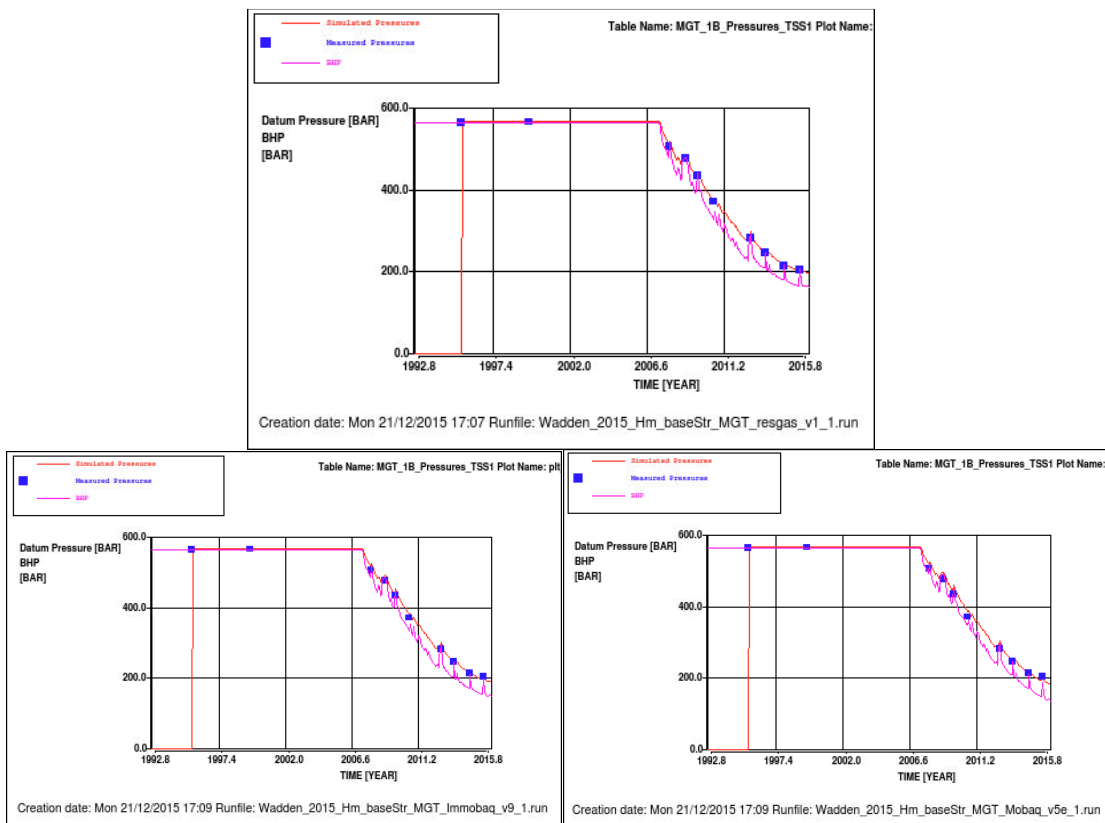
*Figure 51 Simulated reservoir pressure (red line), simulated BHP (violet line) and measured (blue squares) downhole pressure data in MGT-1B. Top: base case. Left: low case. Right: high case.*
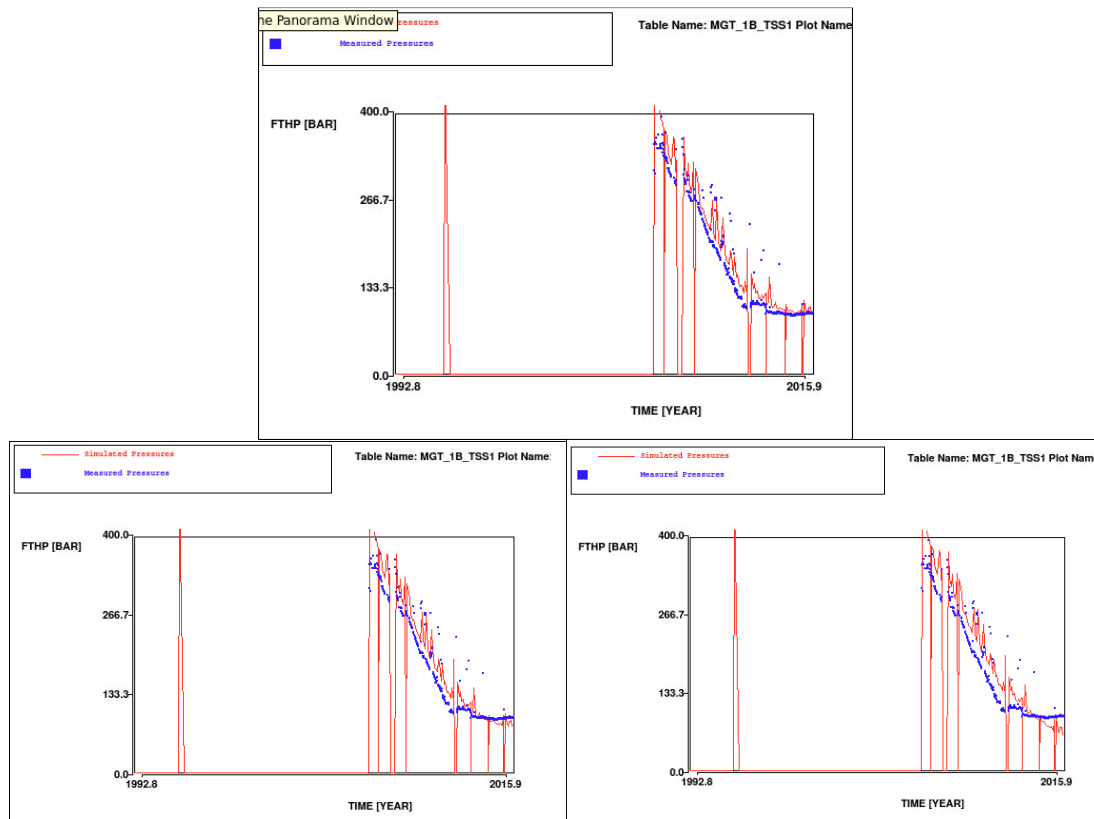


*Figure 52 Simulated (red line) and measured (blue squares) flowing tubing head pressures in MGT-1B. Top: base case. Left: low case. Right: high case.*
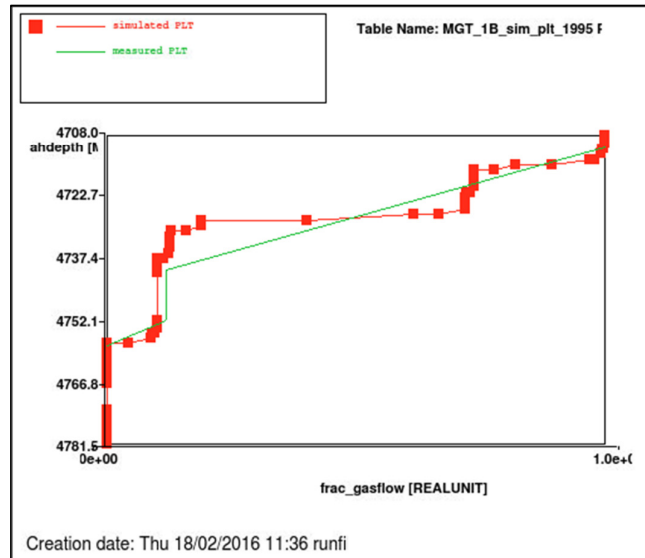
*Figure 53 Simulated (red line + squares) and measured (green line) PLT in MGT-1B in 1995*

*Table 18 History matching parameters used for the Meet & Regel cycle for Moddergat*

| Parameter | Static | Low M&R2015[21] | Base M&R2015[21] | High M&R2015[22] | Immob M&R2014[23] | Mob M&R2014[23] |
|---|---|---|---|---|---|---|
| Residual gas sat. below FWL | 0.20 | **0** | **0.20** | **0** | 0 | 0 |
| GBV multiplier | 1.0 | **1.3** | **1.0** | **1.2** | 0.99 | 0.99 |
| GIIP (BNCM) above FWL. | 6.8 | **8.9** | **6.8** | **8.2** | 9.6 | 9.6 |
| E-W Fault Seal (east) | N/A | **0.01** | **1** | **0.01** | $10^{-10}$ | 0.001 |
| E-W Fault Seal (west) | N/A | **0.01** | **1** | **0.01** | $5.1\ 10^{-3}$ | $5.1\ 10^{-3}$ |
| $k_h$ multiplier[24] | 1 | **2.0** | **2.0** | **2.0** | 1 | 1 |
| $k_v$ multiplier[24] | N/A | **0.10** | **0.10** | **0.10** | 0.19 | 0.19 |
| GWC (m TVNAP) | 3885 | **3885** | **3885** | **3885** | 3885 | 3885 |
| $k_h$ multiplier aquifer | N/A | **$1\ 10^{-4}$** | **0.32** | **1** | 0.001 | 1 |
| $k_v$ multiplier aquifer | N/A | **$1\ 10^{-4}$** | **0.32** | **1** | 0.001 | 1 |
| Residual gas | 0.3 | **0.25** | **0.23** | **0.15** | 0.3 | 0.3 |
| $k_w@S_{rg}$ | 0.1 | **0.01** | **0.01** | **0.01** | 0.1 | 0.1 |

---

[21] Input deck: Wadden_2015_MGT_MRN_v2
[22] Input deck: Wadden_2015_MGT_MRN_v3
[23] Input deck: Wadden_2015_MGT_BS_MRN_v1.INP
[24] Due to the (absolute) permeability model update, the two M&R cycles are incomparable.

### 5.1.7.2   Meet & Regel cycle 2014 vs 2015 model comparison

For M&R 2014, a switch was made back to the old model, pre MGT-3 well results. This was done to get a more reasonable realisation from a permeability multiplier and GBV multiplier point of view. This model had a static GIIP of 9.6 BCM.

In 2015, full static remodelling was done. With MGT-3 well results, the GIIP was assumed significantly lower: 6.8 BNCM. This included the Nes North fault block. With the dynamic GIIP almost equalling this number, it seemed that the MGT-1B was simply draining the entire block.

But also a second update was made: the permeability was revised and this resulted into much lower perms, in the southern half of the field; in some cases even multiple orders of magnitude. This resulted in poorer general connectivity of the field. So the permeability multiplier of 2.0 imposed on all three realisations of M&R2015 (Table 18) are still much lower than the permeabilities of M&R2015, where no multiplier was needed.

### 5.1.7.3   Water production

The water production for MGT-1B is given in Figure 54. The WGR measurements have quite some uncertainty, although with MGT-1B being a significant well in the system we know that it cannot be an excessive water producer. In Nes, water influx was related to perforations in the highly permeable unit 3. In MGT-1B this unit and below has also been perforated, however, the gas column in the lower layers is much larger. Also the distance between bottom perforations and GWC is larger. Nevertheless, the gas column and distance to the GWC in Metslawier is similar. Therefore, it is possible that larger water breakthrough will occur at some point in time, with the possibility to shut it off. For now, the model suggests that very little formation is being produced, which is in line with observations.
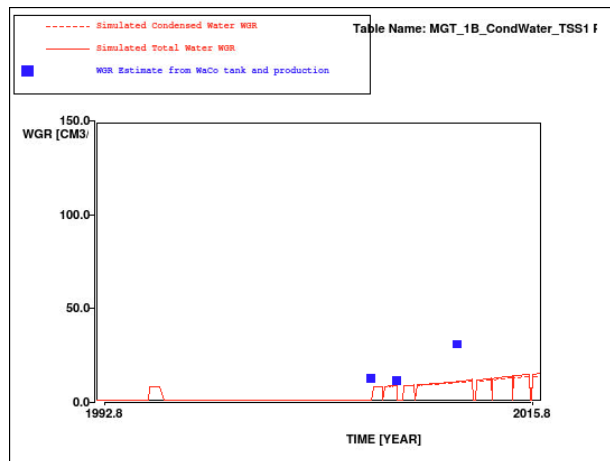


*Figure 54 Simulated total WGR (red solid line), simulated condensed WGR (red dashed line) and estimated WGR from production and WaCo tank observations (blue squares) for MGT-1B. Base case realisation.*

## 5.1.8   Nes

The Nes field (Figure 55) is located in the eastern Waddenzee part of the Noord Friesland Concession (NE-Netherlands). It was discovered by the well MGT-2 in April 1995. Wet gas is evacuated to the Anjum plant facilities as of February 2007. Its P/z plot can be found in Figure 56.

The Nes field is contained in the Upper Slochteren Sandstone Member (ROSLU) of the Rotliegend formation. It consists of aeolian and fluvial/lacustrine sediments deposited in a desert environment. The thickness of the ROSLU in MGT-2 is 112 m, of which approximately 60 mTV (gross) is gas bearing. The Nes gas field is a low-relief fault-closed structure.

In 2012, large amounts of water were being produced from MGT-2. PLT results showed water influx from the bottom perforations (Ref 7). A bridge plug was set on the shale layer between units 1 and 3 in October 2012, after which water production stopped. In 2012 MGT-3 was also drilled. Its top came in 22 m TV deeper than prognosis, and therefore only unit 1 was gas bearing. RFT results showed a pressure lag between unit 1 and unit 3 of around 100 bar (Ref 8). Units below unit 3 were also depleted, showing only minor pressure differentials compared to unit 3. This indicates that the shale layer (unit 2) between unit 1 and 3 is at least partially sealing and that the water bearing layers are relatively well connected. Currently, only unit 1 is being produced from.

In Q4 2015, an infill well was drilled, MGT-4A, which targeted the units 3-6 in the west of the field. However, it found the reservoir 32 metres deeper than prognosis and only found unit 1 gas-bearing. This resulted in the decision to drill a second well, MGT-5, in the south of the field. The reservoir model used for subsidence calculations was that of pre MGT-4 and MGT-5 drill results. The reservoir model will be updated in 2016 following MGT-5 drilling and hook-up of either or both new wells. Subsequent documentation in this section ignores MGT-4 and MGT-5 wells.
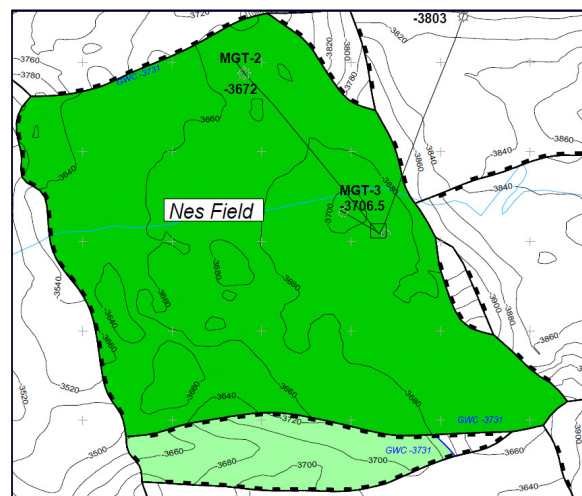


*Figure 55 NES ARPR top ROSL map*
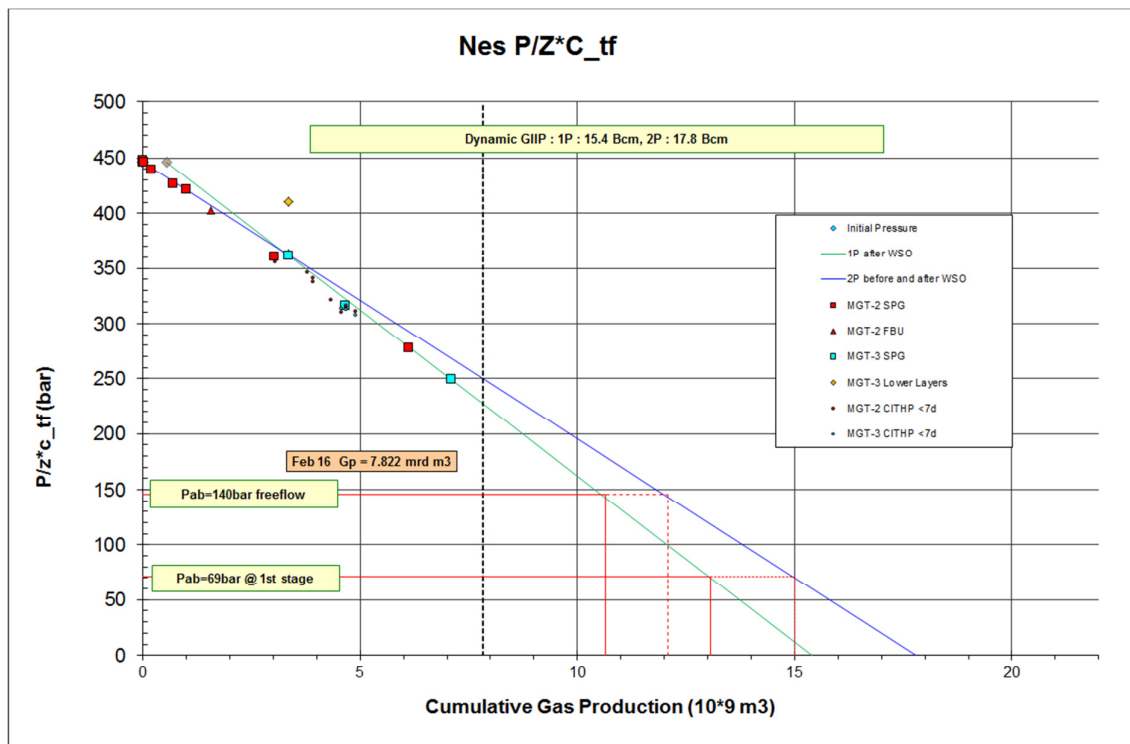
*Figure 56 P/z plot for MGT-2 and MGT-3. Due to the high initial pressures, P/z has been corrected for rock compressibility ($c_{tf}$).*
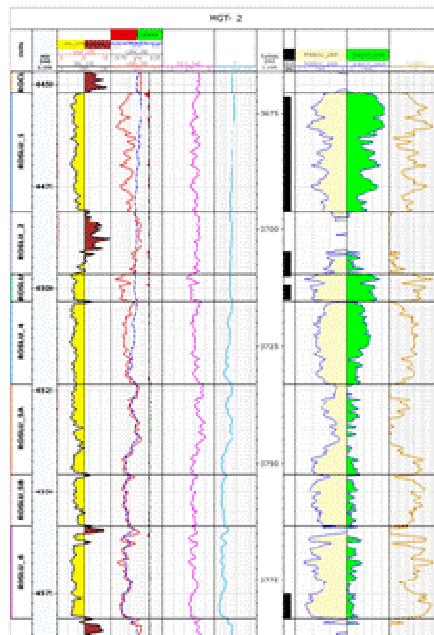


*Figure 57 Petrophysical log of MGT-2*

### 5.1.8.1   Reservoir model

The reservoir model for Nes is approached from a slightly different angle to that of the other fields. Nes has a second well drilled into the reservoir, MGT-3, where an RFT was performed after part of the field was depleted by MGT-2. It found gas pressures at ~420 bara in unit1 and water pressures at ~520 bara in unit 3. Virgin pressure is 564 bara. With the GWC in the

unit 2 shale, the RFT results are somewhat ambiguous: the pressure differential can be caused by (1) the phase difference, by (2) the baffling/sealing unit 2 or (3) a combination of the two.

To match the RFT on water pressures, the aquifer mobility has to be non-zero, ruling out a completely immobile aquifer. This results in a different approach to defining the low, base and high case subsidence realisations. With the aquifer pressure anchored at a certain pressure at a certain point in time, its mobility is no longer the key subsurface uncertainty.

### 5.1.8.2   Meet & Regel cycle 2014 vs 2015 model comparison

In M&R2014 this had resulted in the construction of two models: (1) aquifer depletion due to residual gas below FWL (resulting in less future pressure drop) and (2) a semi-mobile aquifer realisation (resulting in more future pressure drop). Both models are matched to the RFT of MGT-3 in both gas and water leg.

The uncertainty not taken into account in 2014 was the transmissibility of the unit 2 shale. If this is transmissible, gas produced from unit 1 may have originated from unit 3. If this is the case, the GIIP may be significantly smaller than originally thought. This thought was backed by MGT-4A well results that came in 33 metres deeper than prognosis. The M&R2014 models contained 21.7 and 22.1 BNCM for realisation (1) and (2) respectively[25]. However, a decent history match could be made with a GIIP as low as 17.2 BNCM. This results in a larger average pressure drop over the field. This gave reason to re-define the realisation for the Nes field as shown in Table 19.

*Table 19 Overview of dynamic realizations Nes M&R 2014 vs 2015.*

|  | Base structure | Residual gas below FWL | Semi-Mobile aquifer | GIIP [BNCM] above FWL | Unit 2 shale transmissibility |
|---|---|---|---|---|---|
| M&R2014 | | | | | |
| 1 – Base | x | x |  | 21.7 | sealing |
| 2 – High | x |  | x | 22.1 | sealing |
| M&R2015 | | | | | |
| 1 – Low | x | x |  | 21.7 | sealing |
| 2 – Base | x | x |  | 19.4 | large baffle |
| 3 – High | x | x |  | 17.2 | small baffle |

The old high case has been eliminated, since a 22.1 BNCM GIIP no longer made sense based on newly acquired data (MGT-4A). The new realisations (base and high) were constructed with a transmissible unit 2 shale.

Table 20 shows the parameters used for each realisation. The horizontal and vertical permeability multipliers have been split per unit (Top Unit 1, Bottom Unit 1, Unit 2 and Unit3-6) to be able to match on the PLTs and RFTs.

---

[25] GIIP is mainly varied by imposing a GBV multiplier on the entire model.

*Table 20 History matching parameters used for the Meet & Regel cycle for Nes*

| Parameter | Static | Low M&R2015 [26] | Base M&R2015 [26] | High M&R2015 [26] | Gas below FWL M&R 2014[27] | Semi-mobile aquifer M&R 2014[28] |
|---|---|---|---|---|---|---|
| Residual gas sat. below FWL | 0.16 | **0.15** | **0.15** | **0.15** | 0.15 | 0 |
| Connected GIIP (Bcm) | 17.7 | **21.7** | **19.4** | **17.2** | 21.7 | 22.1 |
| GBV multiplier | 1 | **1.20** | **1.05** | **0.93** | 1.20 | 1.22 |
| $k_h$ multiplier (TU1/BU1/U2/ U3-6) | 1 | **1.5 / 1.5 / 1.5 / 3.2** | **1.1 / 2.2 / 1 / 2.2** | **1 / 2.8 / 1 / 0.5** | 1.5 / 1.5 / 1.5 / 3.2 | 1.4 / 1.4 / 1.4 / 1.3 |
| $k_v$ multiplier (TU1/BU1/U2/ U3-6) | N/A | **0.01 / 0.01 / 1.9 $10^{-4}$ / 0.01** | **1 / 1 / 0.03 / 0.02** | **1 / 1 / 3.2 / 0.02** | 0.01 / 0.01 / 1.9 $10^{-4}$ / 0.01 | 0.10 |
| GWC (m TVNAP) | 3731 | **3731** | **3731** | **3731** | 3731 | 3731 |
| $k_h$ multiplier aquifer | N/A | **0.70** | **0.32** | **1** | 0.70 | 0.023 |
| $k_v$ multiplier aquifer | N/A | **1** | **1** | **1** | 1 | 0.023 |
| Residual gas | 0.3 | **0.34** | **0.28** | **0.28** | 0.34 | 0.34 |
| $k_w@S_{rg}$ | 0.1 | **0.1** | **0.1** | **0.1** | 0.1 | 0.10 |

The GIIPs are now more in line with the base case GIIP. This has come at expense of somewhat higher $k_v$ multipliers, which typically do not exceed 0.1.

The high (shallow) structure cases for Nes constructed in M&R2014 were also discarded, based on updated well results and dynamic data. These realisations had GIIPs exceeding 30 BNCM, which is deemed no longer possible.

Figure 58 shows the RFT match of the three M&R2015 models.

---

[26] Input deck: Wadden_2015_NES_MRN_v7.INP
[27] Input deck: Wadden_2015_NES_MRN_v2.inp. HM run: NES_BS_Immobaq_v3p
[28] Input deck: Wadden_2015_NES_MRN_v3.inp. HM run: NES_BS_Immobaq_v1
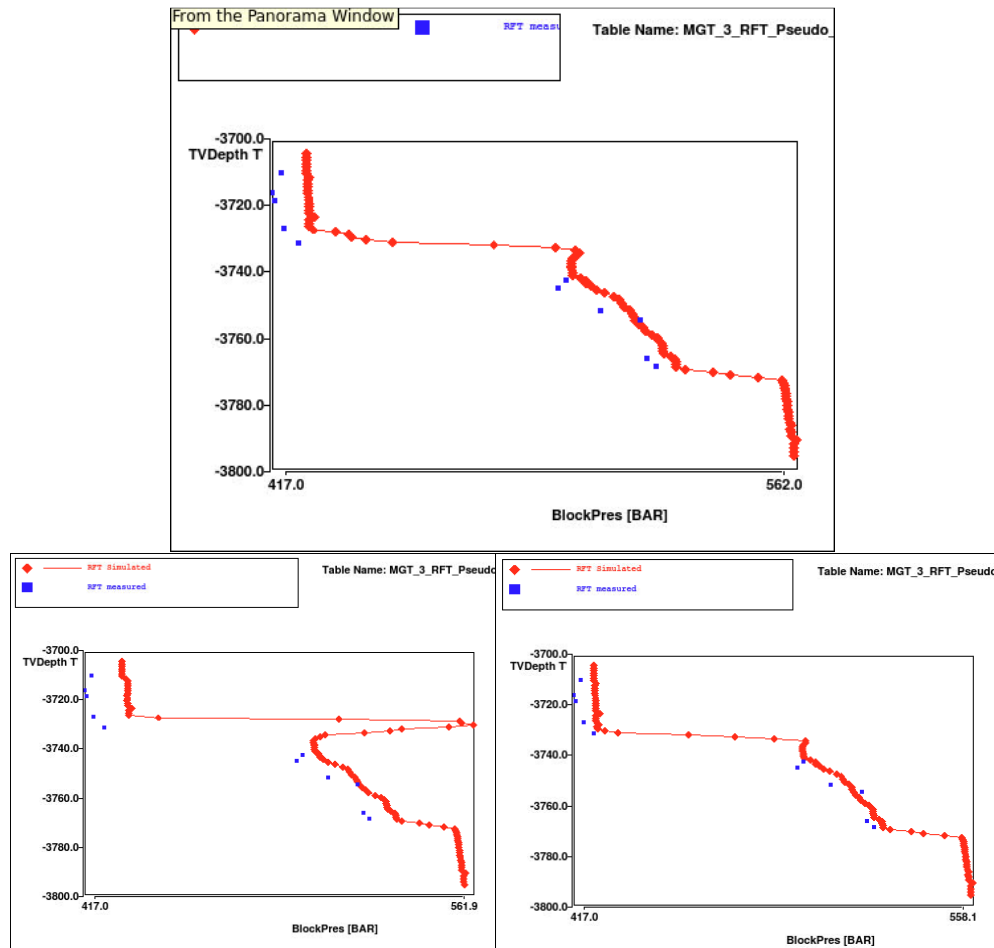
*Figure 58 Simulated (red line and squares) and measured RFT pressure data (blue squares) for MGT-3. Top: base case. Left: low case. Right: high case.*

Figure 59 and Figure 60 show the downhole pressure match of MGT-2 and MGT-3 respectively. Figure 61 and Figure 62 show trhe tubing head pressure match for MGt-2 and MGT-3 respectively.
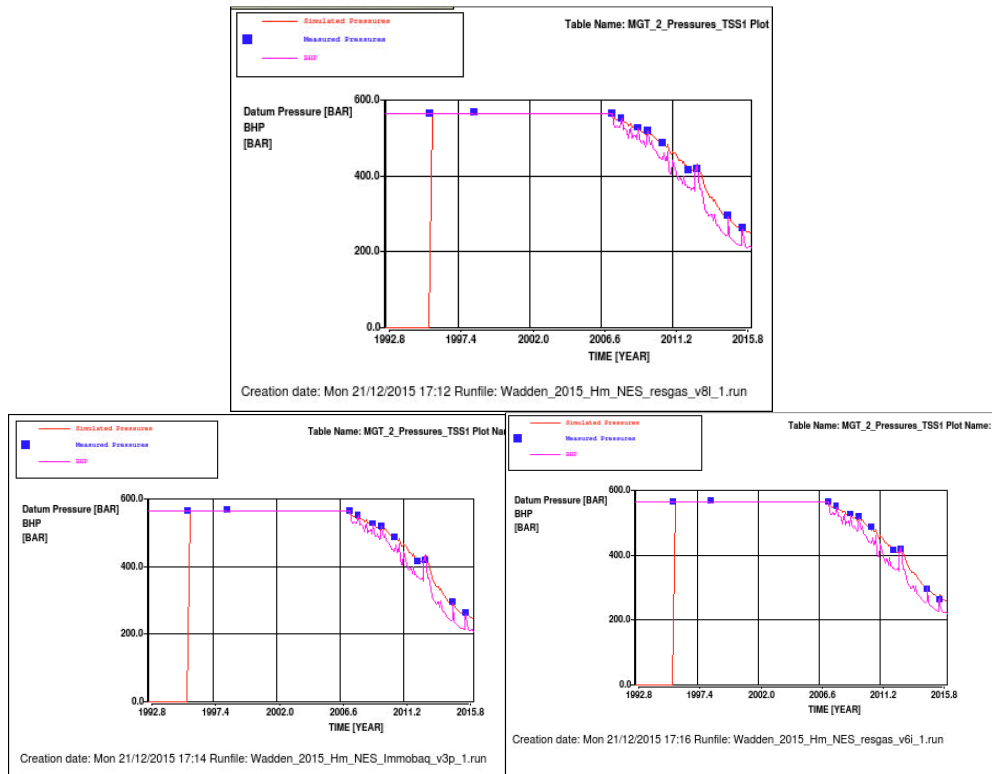
*Figure 59 Simulated reservoir pressure (red line), BHP (violet line) and measured (blue squares) downhole pressure data in MGT-2. Top: Base case. Left: low case. Right: high case.*
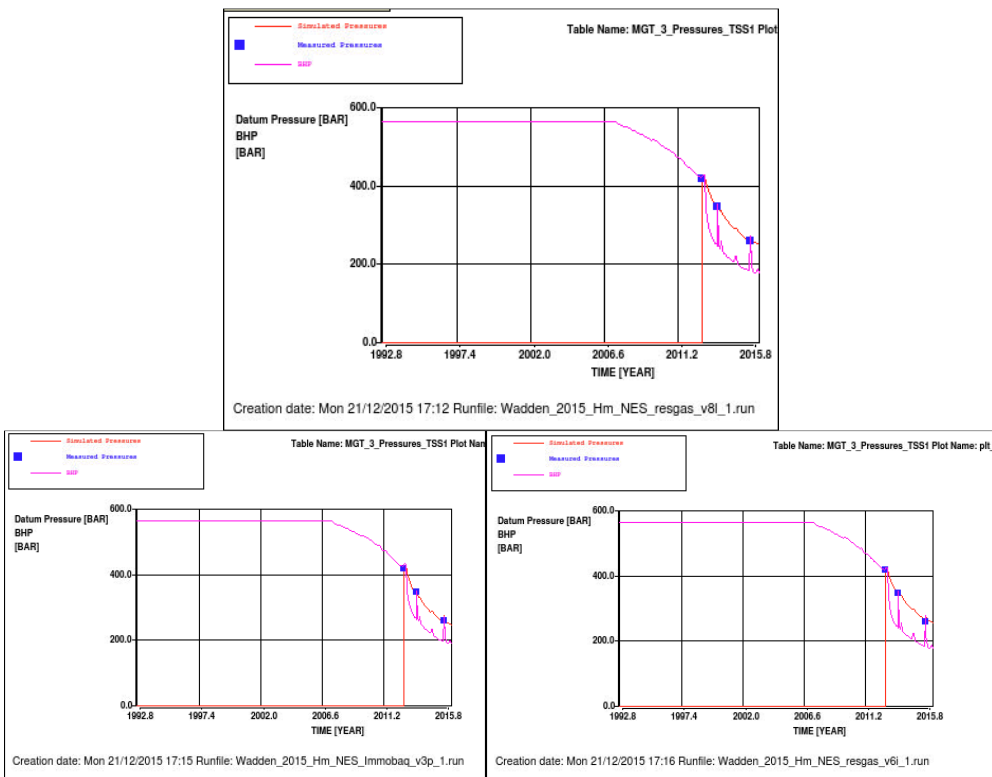


*Figure 60 Simulated reservoir pressure (red line), BHP (violet line) and measured (blue squares) downhole pressure data in MGT-3. Top: Base case. Left: low case. Right: high case.*
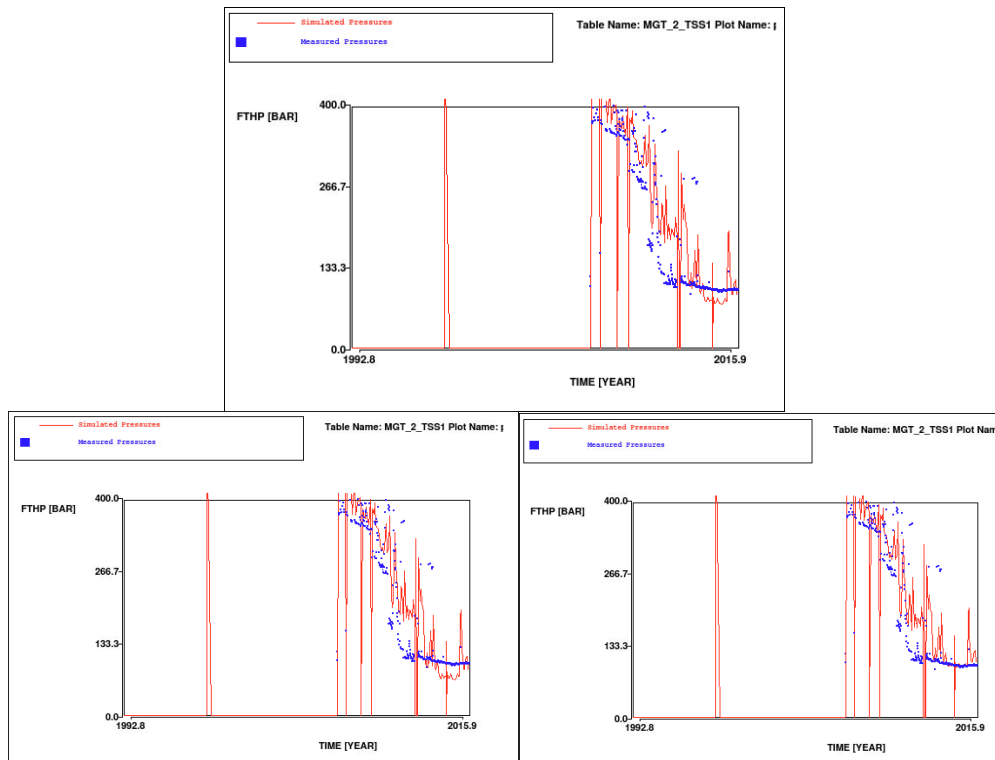
*Figure 61 Simulated (red line) and measured (blue squares) flowing tubing head pressures in MGT-2. Top: Bes case. Left: low case. Right: high case.*
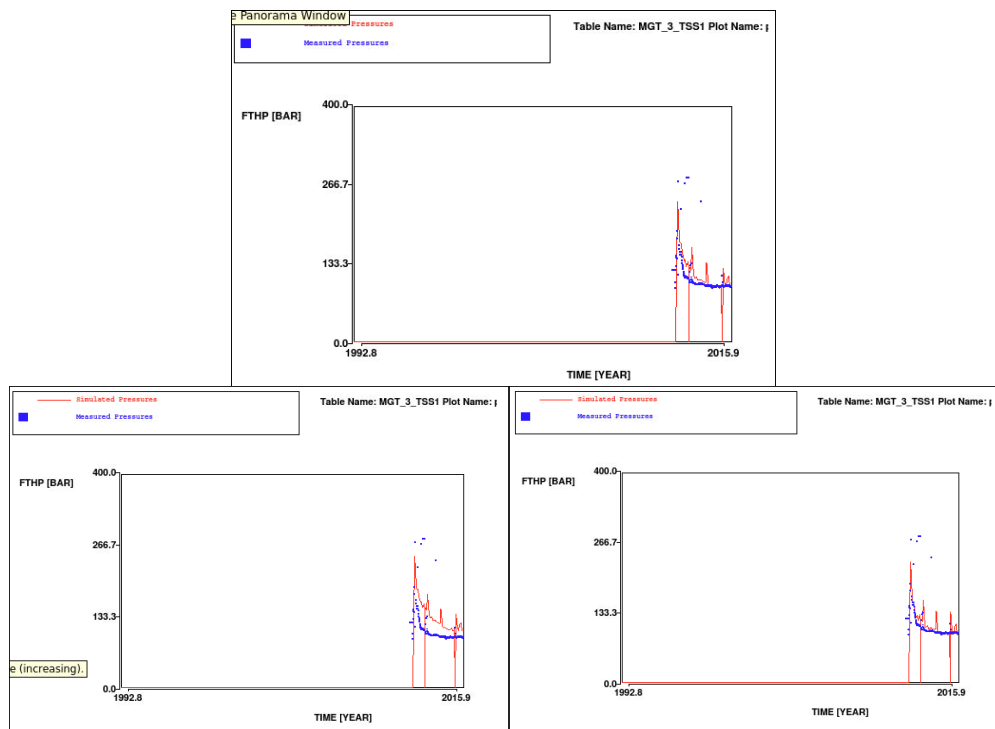


*Figure 62 Simulated (red line) and measured (blue squares) flowing tubing head pressures in MGT-2. Top: Bes case. Left: low case. Right: high case.*

### 5.1.8.3   **Water production**

Well MGT-2 experienced water breakthrough in 2012. This has been observed in increase in water production Figure 63 and PLT (Ref 7). The PLT showed that the lowest perforations were producing water. These were shut off with a plug. It is uncertain whether the water encroached vertically or horizontally. The lowest perforations are relatively close to the GWC, which makes vertical encroachment possible. The exact water encroachment behaviour can be poorly modelled.
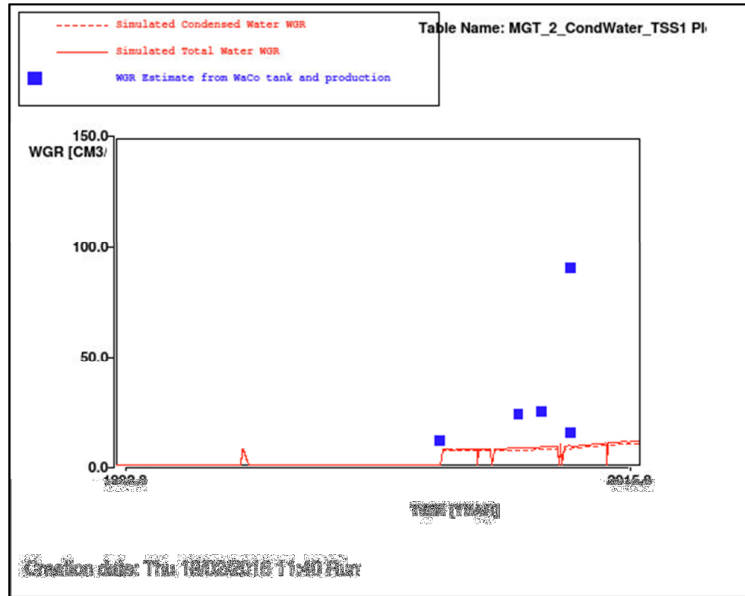


*Figure 63 Simulated total WGR (red solid line), simulated condensed WGR (red dashed line) and estimated WGR from production and WaCo tank observations (blue squares) for MGT-2*
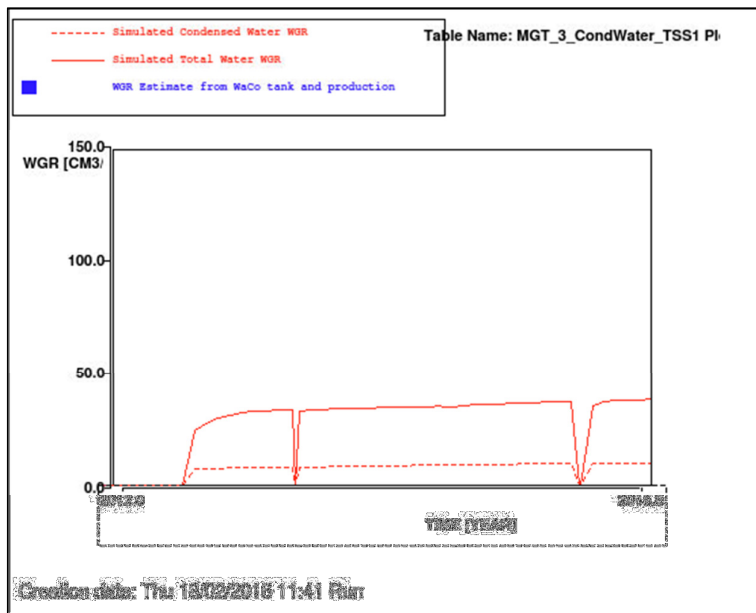


*Figure 64 Simulated total WGR (red solid line), simulated condensed WGR (red dashed line) and estimated WGR from production and WaCo tank observations (blue squares) for MGT-3*

### 5.1.9  Vierhuizen

The Vierhuizen field (Figure 65) is located approximately 5 km to the north of the
Munnekezijl field. The field was discovered by VHN-1 in 1994, which confirmed economic
gas productivity from the Upper Slochteren formation. The western lobe of the field
(discovered by VHN-3 well, but economic development has not been proven) is almost
completely contained in the Noord Friesland concession (and reported in the Vierhuizen West
entry). The South Block in the eastern lobe of the field (discovered by VHN-1) lies almost
fully in the Groningen concession. The area between the western and eastern lobe lies in the
De Marne concession. As GIIP in the De Marne concession is minor it is reported together
with the North Friesland volumes. The eastern lobe is bounded to the North by an East-West
running fault.
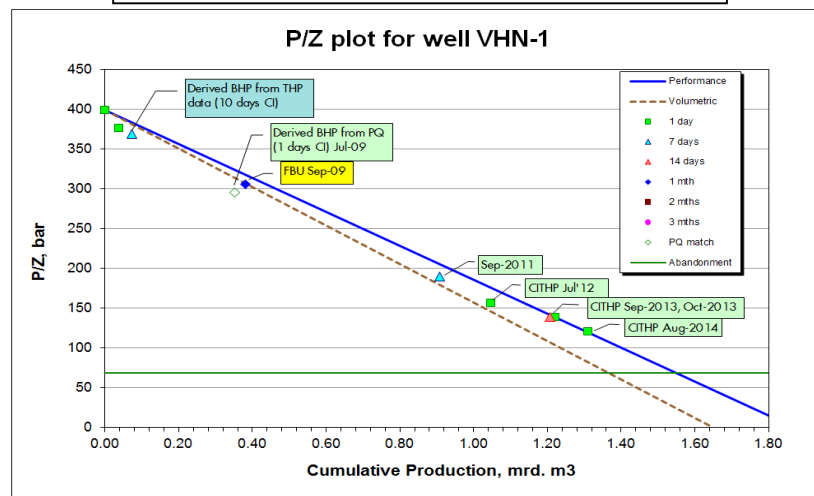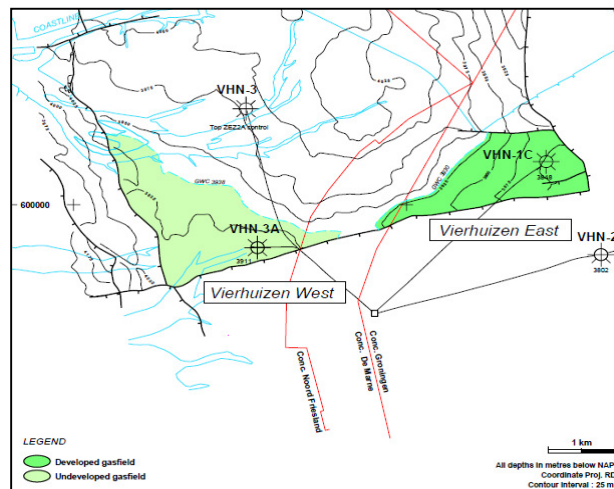


*Figure 65 ARPR Top ROSLU map for Vierhuizen-East and P/z plot for VHN-1C.*

#### 5.1.9.1  Reservoir model
The Vierhuizen reservoir is connected to a relatively large aquifer compared to the size of the
gas field. Because of this, the model expects strong water influx from the aquifer if this is
assumed fully mobile. The P/z plot in Figure 65 shows some extra pressure support in late
field-life. Due to the small size of the field and large aquifer behind it, it is suspected that
aquifer support plays a role here. Also the reservoir model supports this view.

The gas below FWL realisation indeed generates pressure support. But at the same time, aquifer pressures stay very high – almost virgin. At the same time, an immobile aquifer realisation cannot mimic the pressure behaviour described, without modifying certain parameters to unrealistic values. Because of this, it is decided to define a single realisation for both low and base case:  the gas below FWL realisation. The mobile aquifer realisation has also been constructed. An overview of the realisations is given in Table 21.

*Table 21. Overview of dynamic realizations during M&R 2015 for Vierhuizen*

|  | *Base structure* | *Immobile aquifer* | *Paleo-residual gas below FWL* | *Mobile aquifer* | *Base dynamic GIIP* |
|---|---|---|---|---|---|
| *1 – Low/ Base* | x |  | x |  | x |
| *2 – High* | x |  |  | x | x |

The downhole pressures matches are shown in Figure 66. The base case model shows a good match with the data. The mobile aquifer model is poorly matchable, since the model expects water encroachment, reducing the effective permeability around the well, or increasing drawdown. Nevertheless, the model is used as a high case subsidence sensitivity.
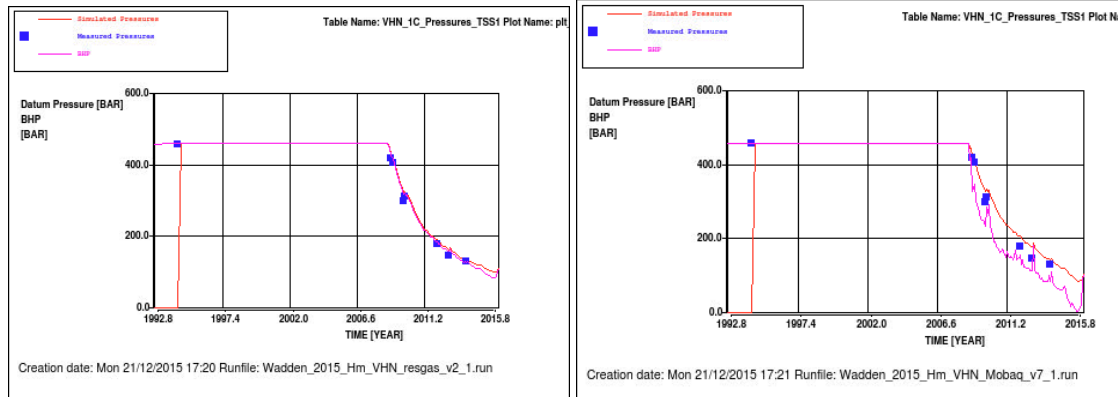


*Figure 66 Simulated reservoir pressure (red line), BHP (violet line) and measured (blue squares) downhole pressure data in MGT-3. Left: low/base case. Right: high case.*

Figure 67 shows the FTHP match. This match is poor. But in any case, the subsidence window is believed to be sufficiently captured by the two deterministic models, that the THP match is not of great importance.
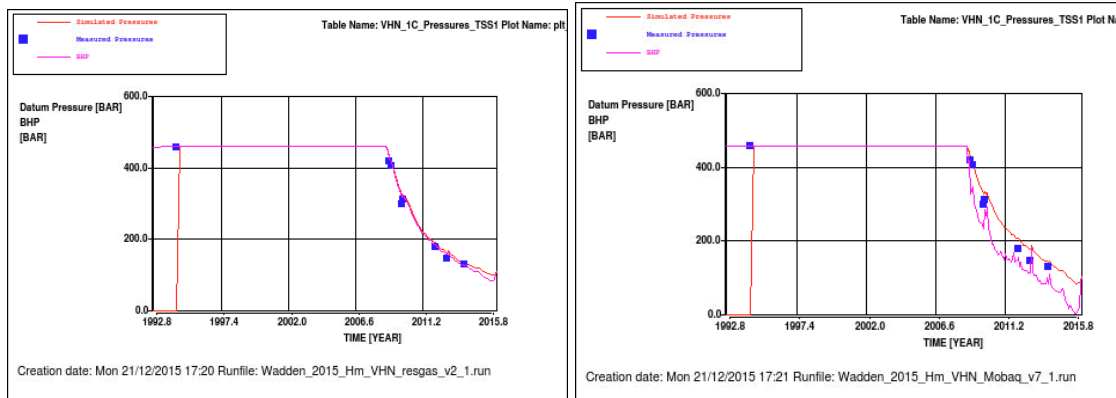


*Figure 66 Simulated reservoir pressure (red line), BHP (violet line) and measured (blue squares) downhole pressure data in MGT-3. Left: low/base case. Right: high case.*

Figure 67 shows the FTHP match. This match is poor. But in any case, the subsidence window is believed to be sufficiently captured by the two deterministic models, that the THP match is not of great importance.
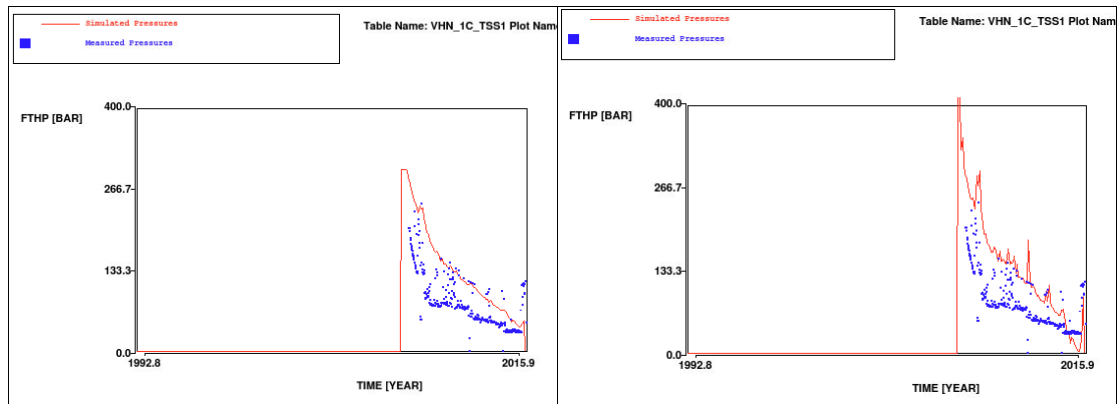
*Figure 67 Simulated (red line) and measured (blue squares) flowing tubing head pressures in VHN-1C. Left: low/base case. Right: high case.*

*Table 22 History matching parameters used for the Meet & Regel cycle for Vierhuizen.*

| Parameter | Static | Low/Base M&R2015 [29] | High M&R2015 | Immob M&R2014 [30] | Mob M&R2014 |
|---|---|---|---|---|---|
| Residual gas sat. below FWL | 0.16 | **0.16** | **0** | 0 | 0 |
| GBV multiplier | 2.3 | **1.0** | **1.05** | 0.99 | 1.05 |
| $k_h$ multiplier | 1 | **2.3** | **0.058** | 98 | 0.058 |
| $k_v$ multiplier | N/A | **0.058** | **0.99** | 0.14 | 0.99 |
| GWC (m TVNAP) | 3930 | **3930** | **3937** | 3930 | 3937 |
| $k_h$ multiplier aquifer | N/A | **0.32** | **1** | $1.0 \times 10^{-4}$ | 1 |
| $k_v$ multiplier aquifer | N/A | **0.32** | **1** | $1.0 \times 10^{-4}$ | 1 |
| Residual gas | 0.3 | **0.18** | **0.10** | 0.1 | 0.1 |
| $k_w @ S_{rg}$ | 0.1 | **0.16** | **0.1** | 0.1 | 0.1 |

### 5.1.9.2   Meet & Regel cycle 2014 vs 2015 model comparison

The immobile aquifer model has been discarded, since the high permeability multiplier of 98 was seen as an unlikely scenario. This high perm was required to gain extra pressure support from the shallow layers. The replacement, the low/base case model, has a much more realistic permability multiplier. Also the GBV equals one supporting this as a base case situation.

The mobile (high case) realisation has remained unchanged.

### 5.1.9.3   Water production

The Grijpskerk system to which Vierhuizen is flowing connects over 20 wells and the WGR allocation uncertainty is very high. Therefore, no WGR matching was performed for this field.

---

[29] Input deck: Wadden_2015_VHN_MRN_v2.INP
[30] Input deck: Wadden_2015_VHN_MRN_v1.inp.

## 5.2 Forecasting

### 5.2.1 Forecasting Assumptions

The forecasting method has changed, as described in Section 3.7 . Only a single forecast is run for each realisation, this being the forecast as reported in Business Plan 2015. This most closely resembles reality, as it was based on the latest production and pressure figures. The figures deviate from the Winningsplan 2011 figures, that are by now so outdated, that imposing models to this forecast gives a result that does not resemble reality. Also, with the uncertainty in aquifer depletion being so large, uncertainties in ultimate recovery and production rates are less of an issue.

An overview of all production figures is given in Appendix A (see also Ref 9).

### 5.2.2 Forecasting results

This section discusses the outcome of the forecasting and the impact it has had on the subsidence prognosis.
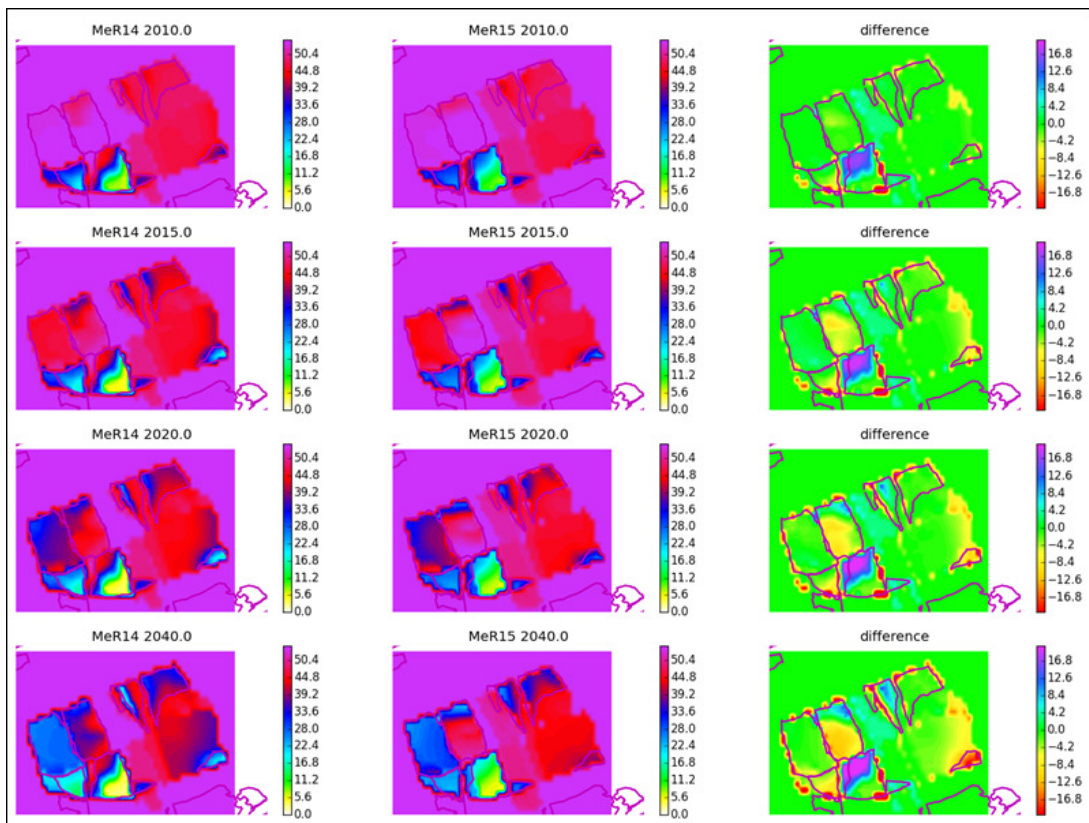


*Figure 68 Modelled average reservoir pressure (MPa) of Wadden area (base case). Left column: M&R2014. Middle column: M&R2015. Right column: difference plot. Top to bottom: 2010, 2015, 2020, 2050.*
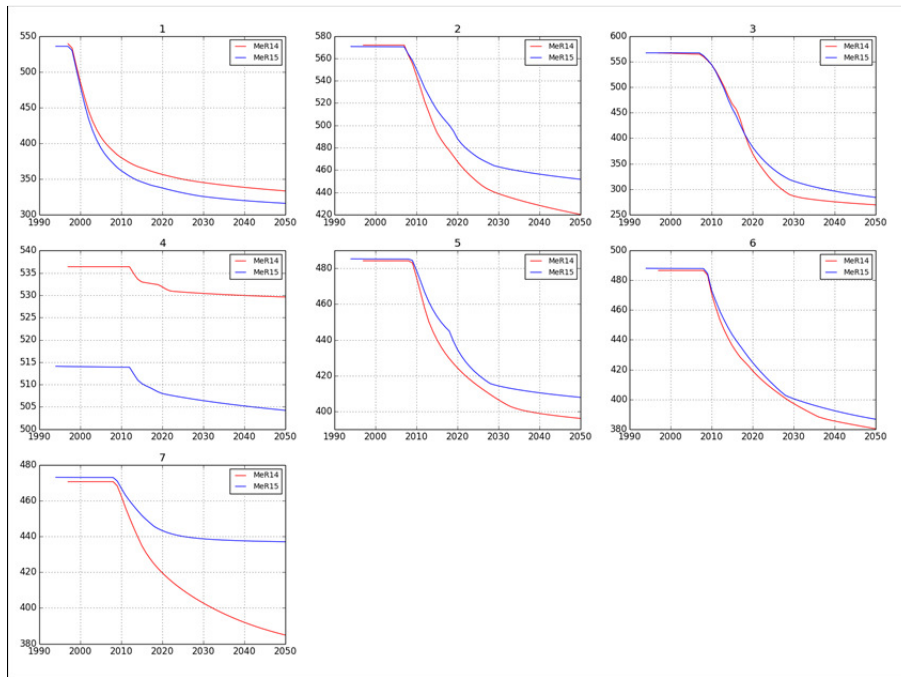
*Figure 69 Average reservoir pressures per (set of) field(s), base case. Red: M&R2014, blue: M&R2015.*
*1 = Anjum, Ezumazijl, Metslawier, 2 = Moddergat, 3 = Nes, 4 = Lauwersoog Central (initial pressure modified*
*due to gridding redefinition.), 5 = Lauwersoog East, 6 = Lauwersoog West, 7 = Vierhuizen East.*
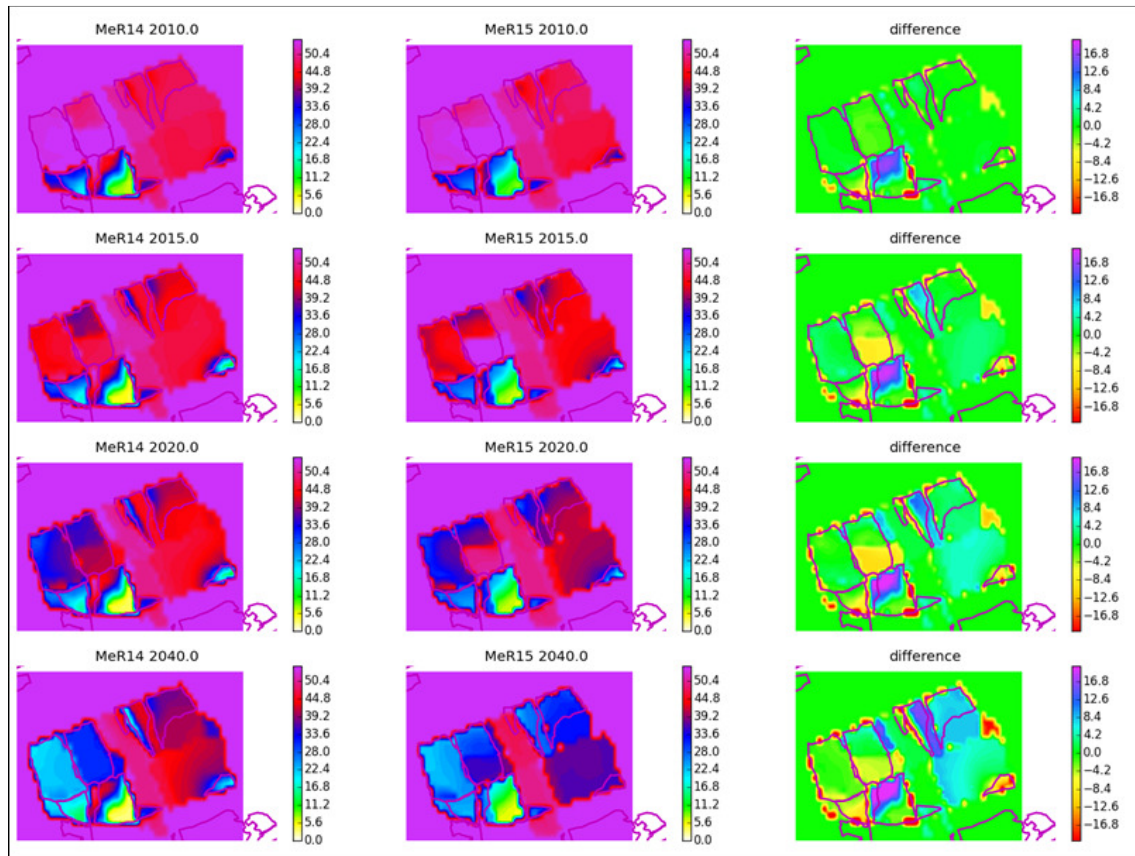
*Figure 70 Modelled average reservoir pressure (MPa) Wadden area (high case). Left column: M&R2014. Middle column: M&R2015. Right column: difference plot. Top to bottom: 2010, 2015, 2020, 2050.*
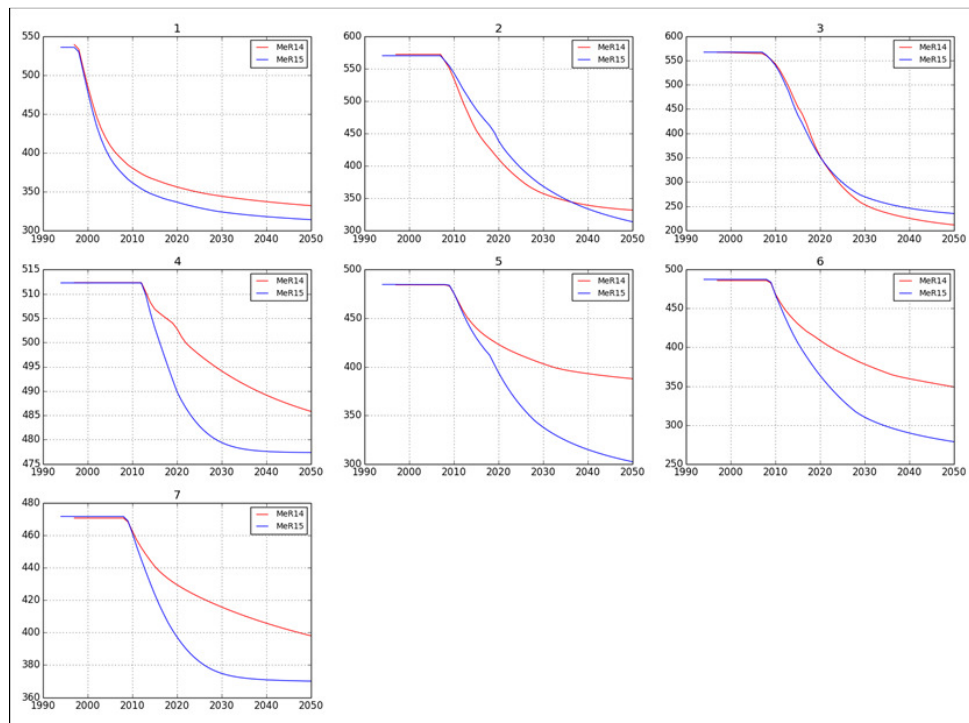


*Figure 71 Average reservoir pressures per (set of) field(s), high case. Red: M&R2014, blue: M&R2015. 1 = Anjum, Ezumazijl, Metslawier, 2 = Moddergat, 3 = Nes, 4 = Lauwersoog Central, 5 = Lauwersoog East, 6 = Lauwersoog West, 7 = Vierhuizen East*

### 5.2.2.1  Anjum, Ezumazijl, Metslawier

Since Anjum, Ezumazijl and Metslawier (non-Wadden fields) are the fields that act as a calibration for the subsidence prognosis for the other fields, these fields are analysed together. Therefore, the depletion is depicted in terms of today (2015) and not in the future.

Anjum is the most important 'calibration field' of the area. Figure 72 shows that the updated base case model has significantly more aquifer depletion for the base case (red) than the old immobile aquifer realisation. This has an effect on the compressibility of the rock used for subsidence forecasting. The high case subsidence model for Anjum has increased too, due to a modelling update of the aquifer permeability multiplier (modified from 0.1 to 1.0).

In the other two fields, the change from an immobile aquifer to a residual gas below FWL model has less impact on the aquifer pressure. The modification of the Metslawier immobile aquifer perm multiplier from $10^{-3}$ to $10^{-4}$ has caused a lower aquifer depletion for the low case.
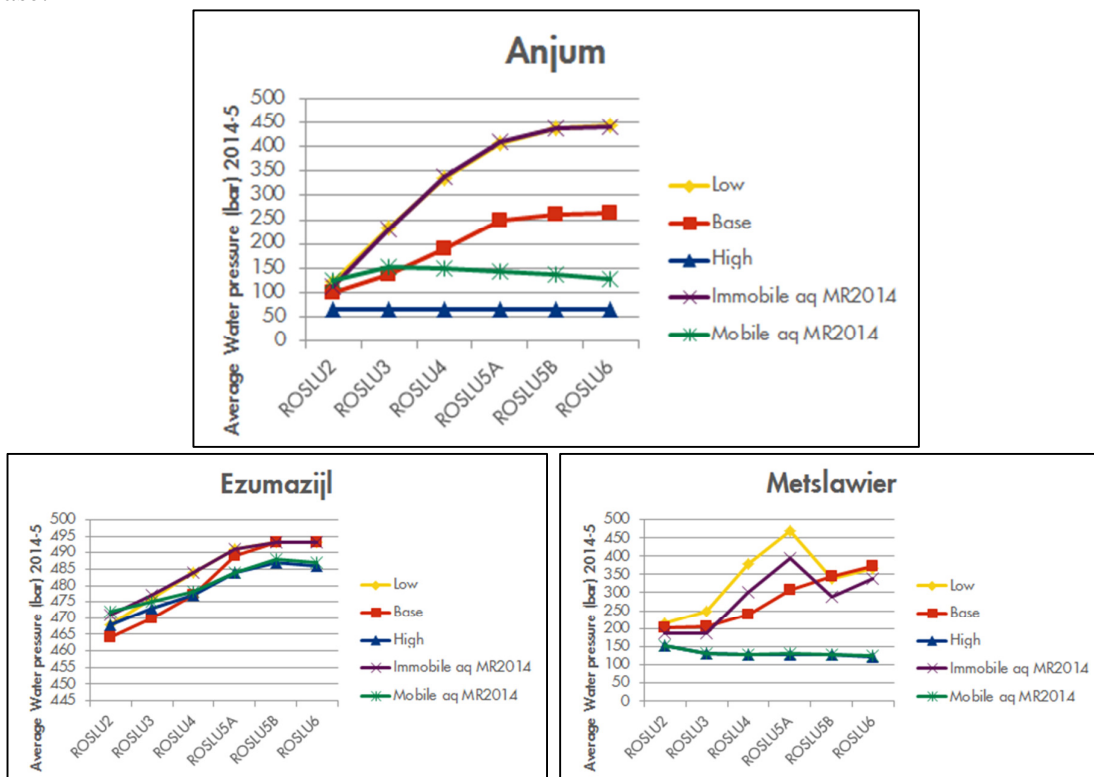


*Figure 72 Water pressures in 2015, per zone for fields Anjum, Ezumazijl and Metslawier.*

### 5.2.2.2  Lauwersoog Central

The modifications of modelling strategy have had marginal impact to the 2050 pressure of the base case of Lauwersoog C (Figure 73). For the high case, similar to the update described for Anjum, the pressure drop has increased. The aquifer permeability multiplier was modified to 1.0 from 0.1. But the depletion in any case, is very small.
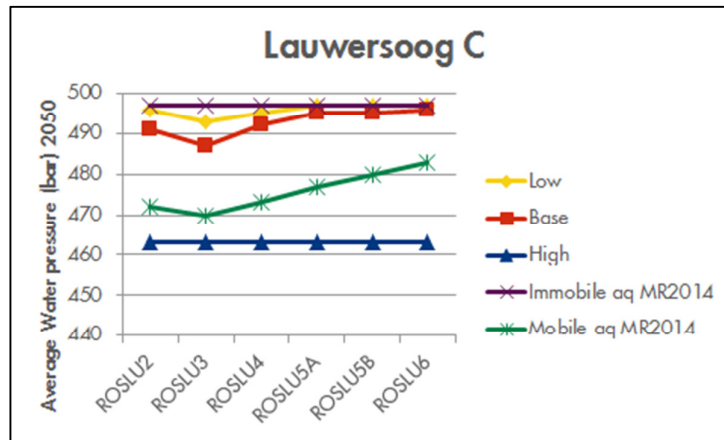
*Figure 73 Water pressures in 2050, per zone for Lauwersoog C.*

### 5.2.2.3 Lauwersoog East

For Lauwersoog East, the main change to the pressure forecasting is the inclusion of the infill opportunity to the production forecast. This infill opportunity explicitly targets the lower units and hence has a significant impact on the gas and aquifer pressures in the east side of the field. For the low and the base case, this effect is not so large (~30 bar in ROSLU3), but for the high case, depletion increased by ~150 bar in some cases (see Figure 74).
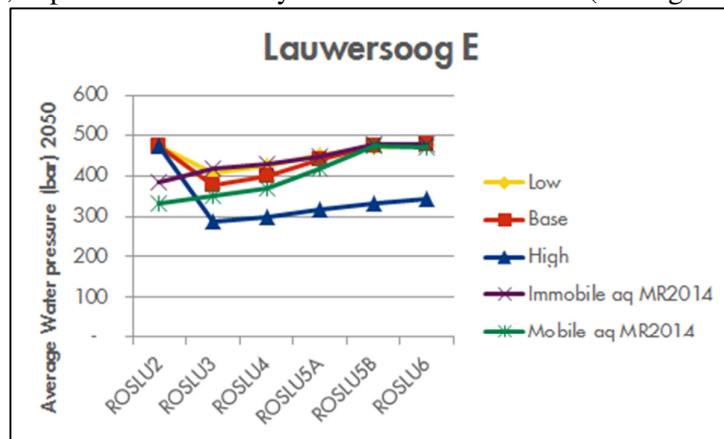


*Figure 74 Water pressures in 2050, per zone for Lauwersoog East.*

### 5.2.2.4 Lauwersoog West

For Lauwersoog West, the aquifer pressure drops for base and high case have significantly increased (Figure 75). This is the result of two effects. One effect is precisely the same as discussed for Anjum and Lauwersoog C: the aquifer permeability for the high case has been rectified from a factor 0.1 to 1. The second effect comes from the baffling of the intra-field fault being taken out of the model. This has resulted in significant pressure drop in the east side of the field.
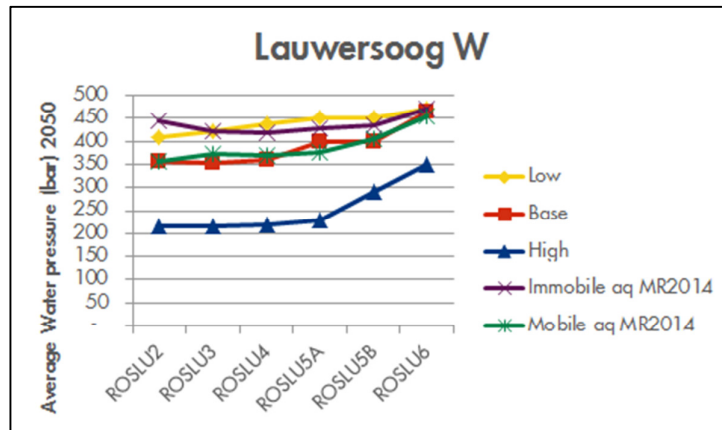
*Figure 75 Water pressures in 2050, per zone for Lauwersoog West*

### 5.2.2.5  **Moddergat**

The Moddergat field has had a significant reshaping, where especially the permeability model has been redone (see Section 3.2.3).  This has caused a significant decrease in the connectivity of the entire field, reducing the aquifer depletion for the base case (Figure 76). For the low case, the permeability multiplier was tightended from $10^{-3}$ to $10^{-4}$, decreasing the aquifer depletion for this realisation. The high case model has a similar result to M&R2014.

Another change incorporated in this model is the inclusion of the production forecast of the Moddergat (South) infill well. This however has been compensated by the lower no-further-activity (NFA) forecast for this new model, more or less cancelling each other out.
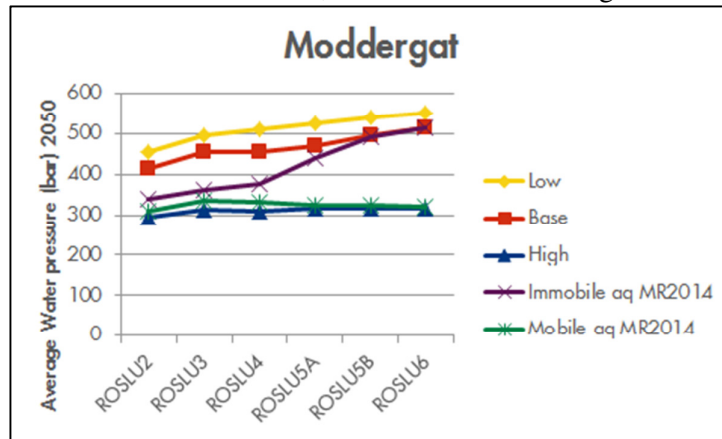


*Figure 76 Water pressures in 2050, per zone for Moddergat.*

### 5.2.2.6  **Nes**

The definitions of the low, base and high forecast for Nes have been changed, with the GIIP and connectivity through the Unit 2 shale as key uncertainties (see Section 5.1.8.2) . The yellow, red and blue lines (Figure 77) indeed indicate that this has a substantial effect on the average aquifer pressure drop.

A second change to the Nes forecasting has been the inclusion of MGT-4 and MGT-5 to forecasting. With MGT-4 at the time of forecasting already known to have seen the unit 1 only, forecasts were adapted to this, decreasing the amount of ROSLU3 production and hence aquifer depletion. The orange line compared to the green line shows this forecasting effect for the old high case slightly, and this effect is larger for the low and base case where aquifer mobility is poorer.

The remodelling has caused a decrease of the high case pressure drop. The old high case (semi-mobile aquifer)  model, containing GIIP far exceeding the base case, is seen as outdated and hence unusable. And the latest water measurements found in MGT-4 (450 to 475 bar) support the higher water pressures given, also in the high case.
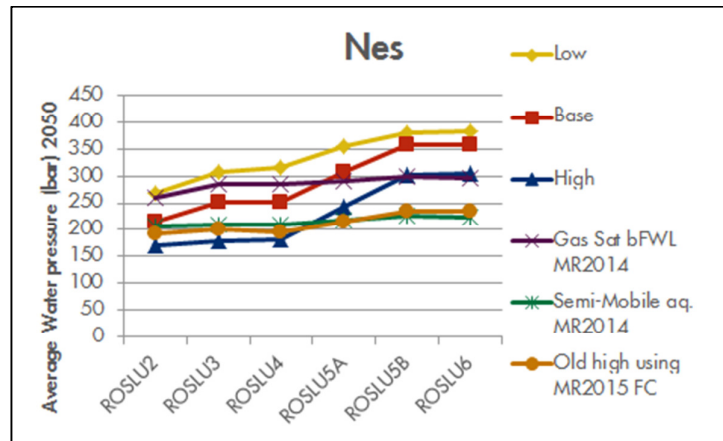


*Figure 77 Water pressures in 2050, per zone for Nes*

### 5.2.2.7  Vierhuizen

For Vierhuizen, the high subsidence case of MR2015 depletion exceeds that of MR2014 due to the same update as applied to Anjum, Lauwersoog C and W. Furthermore, the M&R2014 immobile aquifer case has been discarded, because it is seen as an unlikely case (with a permeability multiplier of 98). Therefore the new low and base case are chosen to be identical: residual gas below FWL. This has significantly decreased the expected pressure drop for the field. An attempt was made to increase the absolute and aquifer perm for the high case, but this had little effect on the high case pressure drop – hence it was chosen not to change.
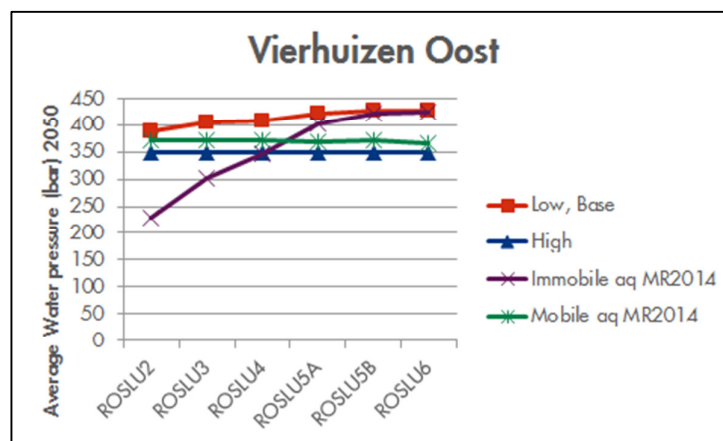


*Figure 78 Water pressures in 2050, per zone for Vierhuizen.*

## 5.2.3  Subsidence scenarios

The subsidence calculation method is beyond the scope of this report and is described thoroughly in Ref 10. However it is worth noting here in what way the different realisations have been used for subsidence calculations.

Subsidence is calculated by combining the pressure drop in the reservoir model with overburden compaction characteristics. A probabilistic method has been used to determine a realistic low-base-high subsidence scenario. Geomechanical parameters as well as the subsurface realisations presented in this document were used as input uncertainties to these calculations.

Deterministic subsidence scenarios have subsequently been defined to align with the P90, P50 and P10 subsidence outcomes. This was done by combining multiple realisations of different fields.

*Table 23 Subsidence scenarios.*

|  | Low case subsidence scenario | Base case subsidence scenario | High case subsidence scenario |
|---|---|---|---|
| **Anjum Fields** |  |  |  |
| Anjum | *High realisation* | *Base realisation* | *Base realisation* |
| Ezumazijl | *High realisation* | *Base realisation* | *Base realisation* |
| Metslawier | *High realisation* | *Base realisation* | *Base realisation* |
| **Wadden Fields** |  |  |  |
| Lauwersoog Central | *Low realisation* | *Base realisation* | *High realisation* |
| Lauwersoog East | *Low realisation* | *Base realisation* | *High realisation* |
| Lauwersoog West | *Low realisation* | *Base realisation* | *High realisation* |
| Moddergat | *Low realisation* | *Base realisation* | *High realisation* |
| Nes | *Low realisation* | *Base realisation* | *High realisation* |
| Vierhuizen East | *Low/Base realisation* | *Low/Base realisation* | *High realisation* |

Table 23 shows which subsurface realisation is used for which subsidence scenario. The table may read a little difficult and is illustrated by an example in the paragraph below.

*The high case subsidence scenario for the entire Wadden area is created by calibrating the base pressure-drop realisations of the Anjum fields to the existing subsidence measurements above these fields. The overburden compaction properties that are required to match the measured subsidence are then used in combination with the high pressure-drop realisations of the Wadden fields to determine the subsidence for the Waddenzee.*

Since Anjum, Ezumazijl and Metslawier have a calibration function, combining their high depletion realisation with the low realisation of the Wadden Fields will result in a low subsidence scenario and vice versa. However, the combination of a low depletion realisation of the Anjum fields with the high depletion realisation of the Wadden fields could not be matched with subsidence measurements. Hence the base realisation was used for the Anjum fields in the high subsidence scenario. Thus effectively, the low realisation of Anjum, Ezumazijl and Metslawier are not used in any subsidence scenario.

### 5.2.4  General forecasting conclusion

Generally, the base case average pressure drop of the Waddenzee fields have increased due to moving from an immobile aquifer to an aquifer modelled with residual gas below FWL. This was of course as expected. The RFT measurements in the Nes water leg and the subsidence above the Ameland southern aquifer have indicated that aquifers deplete more than previously thought. At the same time, we know that aquifers are not fully mobile, since that assumption greatly *over*estimated subsidence in the past. This in-between solution now represents the new base case of all fields.

In general, the high case models have an increased pressure-drop forecast. In four fields (Anjum, Lauwersoog C, West and Vierhuizen) this is due to the updated aquifer permeability multiplier and for Lauwersoog West it is also due to the elimination of an intra-field fault baffling.

The inclusion of potential infill wells (Lauwersoog East infill well, Moddergat-South infill well) to the forecast have mainly caused changes in Lauwersoog East. The Nes and Moddergat fields, where subsidence is most critical, the pressure drop forecasts have decreased. In the former due to the permeability update, in the latter due to increased information on the aquifer.

# REFERENCES

*Ref 1 J. Seubring & R.G. Hakvoort, Petrophysical evaluation of the Rotliegend in the North-Friesland Waddenzee area, 2004, EP200412271228*

*Ref 2 F.C. Seeberger, Methodology of predicting gas- and aquifer pressures in the proposed Waddenzee development area. EP200512206995*

*Ref 3 Ron Peterson. DEPLETION OF ROTLIEGEND GAS AQUIFERS- PART2 (draft18). \\europe.shell.com\tcs\ams\ui.nam\field\epe_re_02\wadden\mores_2013\Reports\11_MR2015\...*

*Ref 4 A.M. Tichler, SCAL inventory Land North 29-12-2015. EP201512253848*

*Ref 5 R. Gray, Advanced rock properties study for NAM BV; Well: Anjum-1, 1994,NAM 26.914*

*Ref 6 Ezumazijl North Development Well ANJ-5B, Summary of the ANJ-5B well, 2003, NAM200302001936*

*Ref 7 J. Seubring, MGT-2 PLT results (September, 2012), 2012, EP201209216710*

*Ref 8 M. Schenkel, Petrophysical Evaluation of MGT-3, June 2012, EP201205214774*

*Ref 9 Winningsplan Profiles. \\europe.shell.com\tcs\ams\ui.nam\field\epe_re_02\wadden\mores_2013\99_Include\10_Forecast\MR2015_Forecasts\Winningsplan+Actual_BP15.xlsx, tab Base_Forecasts_MR2015*

*Ref 10 Gaswinning vanaf de locaties Moddergat, Lauwersoog en Vierhuizen. Resultaten uitvoering Meet- en regelcyclus 2015*

# FIGURES

# TABLES

# APPENDIX A: IMPOSED FORECASTS BY WELL.

*Table 24 Historical production (italic) + M&R 2014 Forecast volumes (E6Nm3/y) – Normal profile*

| | ANJ-1 | ANJ-4 | ANJ-2 | ANJ-3 | LWO-1 | LWOO Infill | LWO-2 | LWO-3 | MGT-1 | MGT Infill | MGT-2 | MGT-3 | MGT-4 (Nes West) | MGT-5 (Nes South) | VHN-1 |
|---|---|---|---|---|---|---|---|---|---|---|---|---|---|---|---|
| | Anjum | | Mets-lawier | Ezu-mazijl | Lauwersoog-East | | Lauwers-oog-C | Lauwers-oog-West | Moddergat | | Nes | | | | Vier-huizen-East |
| 1997 | 352 | 293 | 18 | 0 | 0 | 0 | 0 | 0 | 0 | 0 | 0 | 0 | 0 | 0 | *0* |
| 1998 | 332 | 1769 | 532 | 0 | 0 | 0 | 0 | 0 | 0 | 0 | 0 | 0 | 0 | 0 | *0* |
| 1999 | 722 | 1223 | 577 | 76 | 0 | 0 | 0 | 0 | 0 | 0 | 0 | 0 | 0 | 0 | *0* |
| 2000 | 720 | 948 | 751 | 104 | 0 | 0 | 0 | 0 | 0 | 0 | 0 | 0 | 0 | 0 | *0* |
| 2001 | 784 | 862 | 664 | 154 | 0 | 0 | 0 | 0 | 0 | 0 | 0 | 0 | 0 | 0 | *0* |
| 2002 | 583 | 813 | 493 | 70 | 0 | 0 | 0 | 0 | 0 | 0 | 0 | 0 | 0 | 0 | *0* |
| 2003 | 480 | 651 | 366 | 65 | 0 | 0 | 0 | 0 | 0 | 0 | 0 | 0 | 0 | 0 | *0* |
| 2004 | 370 | 512 | 277 | 60 | 0 | 0 | 0 | 0 | 0 | 0 | 0 | 0 | 0 | 0 | *0* |
| 2005 | 272 | 395 | 209 | 32 | 0 | 0 | 0 | 0 | 0 | 0 | 0 | 0 | 0 | 0 | *0* |
| 2006 | 196 | 285 | 124 | 42 | 0 | 0 | 0 | 0 | 0 | 0 | 0 | 0 | 0 | 0 | *0* |
| 2007 | 168 | 218 | 130 | 53 | 0 | 0 | 0 | 0 | 382 | 0 | 340 | 0 | 0 | 0 | *168* |
| 2008 | 147 | 264 | 125 | 29 | 42 | 0 | 0 | 85 | 312 | 0 | 485 | 0 | 0 | 0 | *309* |
| 2009 | 89 | 188 | 18 | 40 | 271 | 0 | 0 | 300 | 453 | 0 | 540 | 0 | 0 | 0 | *292* |
| 2010 | 96 | 169 | 0 | 11 | 295 | 0 | 0 | 185 | 479 | 0 | 768 | 0 | 0 | 0 | *190* |
| 2011 | 111 | 137 | 0 | 44 | 315 | 0 | 0 | 187 | 518 | 0 | 983 | 0 | 0 | 0 | *154* |
| 2012 | 52 | 113 | 0 | 39 | 261 | 0 | 40 | 135 | 392 | 0 | 718 | 333 | 0 | 0 | *132* |
| 2013 | 0 | 117 | 0 | 31 | 215 | 0 | 37 | 122 | 406 | 0 | 813 | 614 | 0 | 0 | *114* |
| 2014 | 0 | 57 | 0 | 0 | 185 | 0 | 20 | 109 | 354 | 0 | 708 | 513 | 0 | 0 | 83 |
| 2015 | 0 | 65 | 0 | 16 | 146 | 0 | 10 | 89 | 275 | 0 | 526 | 385 | 0 | 0 | 55 |
| 2016 | 0 | 70 | 0 | 26 | 128 | 0 | 8 | 82 | 243 | 0 | 463 | 331 | 184 | 184 | 61 |
| 2017 | 0 | 30 | 0 | 0 | 104 | 0 | 11 | 87 | 230 | 0 | 403 | 285 | 236 | 236 | 0 |
| 2018 | 0 | 0 | 0 | 0 | 114 | 216 | 11 | 84 | 227 | 75 | 360 | 249 | 202 | 202 | 0 |
| 2019 | 0 | 48 | 0 | 0 | 100 | 161 | 6 | 77 | 208 | 216 | 300 | 203 | 160 | 160 | 0 |
| 2020 | 0 | 80 | 0 | 0 | 86 | 107 | 0 | 71 | 163 | 84 | 243 | 162 | 124 | 124 | 0 |
| 2021 | 0 | 75 | 0 | 0 | 79 | 81 | 0 | 67 | 148 | 43 | 222 | 143 | 104 | 104 | 0 |
| 2022 | 0 | 70 | 0 | 0 | 70 | 61 | 0 | 63 | 126 | 28 | 193 | 125 | 84 | 84 | 0 |
| 2023 | 0 | 64 | 0 | 0 | 63 | 48 | 0 | 59 | 120 | 23 | 167 | 107 | 68 | 68 | 0 |
| 2024 | 0 | 59 | 0 | 0 | 56 | 36 | 0 | 56 | 116 | 18 | 147 | 91 | 53 | 53 | 0 |
| 2025 | 0 | 55 | 0 | 0 | 53 | 31 | 0 | 54 | 30 | 48 | 136 | 82 | 40 | 40 | 0 |
| 2026 | 0 | 50 | 0 | 0 | 47 | 27 | 0 | 49 | 77 | 0 | 122 | 71 | 23 | 23 | 0 |
| 2027 | 0 | 45 | 0 | 0 | 41 | 22 | 0 | 43 | 75 | 0 | 106 | 58 | 16 | 16 | 0 |
| 2028 | 0 | 40 | 0 | 0 | 0 | 0 | 0 | 0 | 73 | 0 | 93 | 47 | 6 | 6 | 0 |
| 2029 | 0 | 0 | 0 | 0 | 0 | 0 | 0 | 0 | 0 | 0 | 0 | 0 | 0 | 0 | 0 |
| 2030 | 0 | 0 | 0 | 0 | 0 | 0 | 0 | 0 | 0 | 0 | 0 | 0 | 0 | 0 | 0 |
| **Total** | **5472** | **9765** | **4284** | **891** | **2670** | **790** | **143** | **2005** | **5407** | **536** | **8835** | **3798** | **1299** | **1299** | **1558** |